

Effects of different ventilation strategies on the microclimate and transpiration of a rose crop in a greenhouse

By

Juwawa Chayangira

A thesis submitted in partial fulfillment of the requirements for the Master of Science Degree in Agricultural Meteorology

Department of Physics

Faculty of Science

University of Zimbabwe

MAY 2010

ABSTRACT

In this study, the water vapour balance method was used to evaluate the ventilation rate to calibrate and validate the ventilation sub-model of the Gembloux Dynamic Greenhouse Climate Model (GDGCM) in a naturally ventilated three span Azrom type greenhouse in Zimbabwe. Two ventilation strategies were considered to investigate their effects on the microclimate and transpiration of the rose crop: the configuration with roof vents only (while the side vents were closed) and the configuration with both roof vents and side vents. Crop transpiration was evaluated using the Penman-Monteith method. This allowed continuous and automatic determination of the ventilation rate and leakage rate using the water vapour balance method. The model was fitted to experimental data for ventilation rates, and the parameters for the model, the discharge and wind effect coefficient were determined using statistical analysis. The results showed that there was a good fit between measured and predicted values ($R^2 = 0.702$ and 0.729 for the model of ventilation for the greenhouse operating respectively with both roof and side vents and with roof vents only for the summer period considered), although there was a general overestimation of the air renewal rates, particularly during the night. The air renewal rate was found to be influenced by the ventilation regime in practice. The greenhouse was found to have higher air renewal rates for the configuration with both roof and side vents. On a typical hot day, the maximum simulated air renewal rate was 15.6 hr⁻¹ for the configuration with roof and side vents at 1600hrs, while it was only 6.5 hr⁻¹ for the configuration with roof vents at the same time. The difference between the air renewal rates for the different regimes resulted in different microclimates, since the ventilation affects both the energy balance and mass balance of a greenhouse. The greenhouse inside air temperature was reduced significantly for the configuration with both roof and side vents as it had lower simulated air temperatures than the configuration with roof vents only. On a typical hot day the maximum simulated air temperature for the configuration with roof and side vents was 29.7 °C, while it was 31.5 °C for roof vents configuration at 1400 hrs. On typical selected days the maximum differences between the inside air temperature and the external air temperature were 3.7 °C and 4.6 °C for the configuration with both roof and side vents and the configuration with roof vents only, respectively. Thus during summer periods it is necessary to have a greenhouse with both roof and side vents so that plants

will have a better physiological and morphological development, as the air renewal rates influence crop behaviour largely through their effects on gas exchanges, particularly transpiration and photosynthesis. The transpiration of the rose crop was found to be influenced by the ventilation strategy. The simulated maximum canopy transpiration flux density was 166.5 W m⁻² for the configuration with both roof and side vents, while it was 152.9 Wm⁻² for the roof vents only on a selected hot day. The simulated night-time relative humidities were higher for the configuration with roof vents only. The simulated relative humidity was above 90 % for the configuration with roof vents only, while it was 84 % for the configuration with both roof and side vents. To prevent excessive humidity build up, the ventilation strategy with both roof and side vents needs to be employed in order to prevent condensation in the greenhouse.

ACKNOWLEDGEMENTS

Firstly I would to thank my supervisor Mr E Mashonjowa for his guidance and advice throughout the project. I would also want to thank Floraline Pvt Ltd management and staff for granting me permission to use their greenhouse and equipment to carry out this research. The friendly environment they provided is greatly appreciated.

I would also want to offer my profound gratitude to all staff members in MAGM programme; particularly Mr B Chipindu for his assistance throughout the programme. To my colleagues; particularly Ms Niclah Nyamutata and Mr Farai Simba I would like to thank them for helping in setting up the automatic weather station and some of the field work. I would also want to appreciate my family for their moral support and patience.

Lastly I am also grateful to Miss Sophia Mubango for her encouragement and moral support when times were hard and for advising me to move forward.

TABLE OF CONTENTS

ABSTRACT	ii
ACKNOWLEDGEMENTS	iv
TABLE OF CONTENTS	v
LISTS OF TABLES	ix
LIST OF FIGURES	xi
CHAPTER 1 INTRODUCTION	1
1.0 Introduction	1
1.1 Greenhouse Ventilation	2
1.2 Problem Statement	2
1.3 Background and Justification	3
1.4 Aims and Objectives	4
1.5 Expected Benefits	4
1.6 Project Layout	4
CHAPTER 2 LITERATURE REVIEW	6
2.1 Introduction	6
2.1.2 Transport mechanisms which affect the microclimate of the greenhouse	7
2.1.2.1 Radiation	7
2.1.2.2 Conduction	8
2.1.2.3 Convection	9
2.2.0 Mass and Energy balance in the greenhouse	13
2.2.1 Greenhouse Energy Balance	13
2.2.2 Greenhouse Vapour Balance	15
2.3 Ventilation	16
2.3.1 Vertical Ventilation Flux	16
	••

2.3.2 Horizontal ventilation flux due to side wall and turbulent effects	18
2.4 Methods of determining the ventilation rate	21
2.4.1 Tracer gas technique	21
2.4.1.1 Static method	21
2.4.1.2 Dynamic method	22
2.4.2 The water vapour balance method	23
2.5 Determination of Transpiration Rate	25
2.5.1 Penman-Monteith Method for determining transpiration	25
2.5.2 Sap flow gauge method of determining transpiration rates	27
2.5.2.1Stem heat balance basics	27
2.5.3 Sap flow Thermodynamics	31
CHAPTER 3 MATERIALS AND METHODS	33
3.0 Experimental Sites and Location	33
3.1 Description of the greenhouse	33
3.2 Climatic and Physiological measurements	35
3.2.1 Climatic measurements outside the greenhouse	35
3.2.1.1 Air Movement Sensors	36
3.2.1.2 CM3 pyranometer	37
3.2.2.1 Air temperature and relative humidity sensors	39
3.2.2.1.1 Vaisala HMP45C Temperature and Relative Humidity Probe	40
3.2.2.1.2 RHT2nl Temperature and Relative Humidity Probe	40
3.2.2.2 Net Radiometer	40
3.2.2.3 Tube Solarimeter	41
3.2.2.4.1 Leaf temperature thermocouples	42

3.2.2.5 Soil temperature probe	43
3.3 Instrument calibration	43
3.3.1 Introduction	43
3.3.2 Calibration of temperature humidity sensors	43
3.3.3 Calibration of radiation sensors	45
3.4 Model Description	45
3.4.1 Ventilation sub-model	50
3.4.2 Ventilation Rate Determination	53
3.5 Modeling the transpiration	54
3.6 Simulation of the GDGCM using TRNSYS	56
3.6.1 Structure of a TRNSYS Simulation Program	58
3.6.2 Calibration of the ventilation sub model	60
3.6.3 Validation of the greenhouse Ventilation Sub model	62
3.7 Measurements of Leaf Area Index (LAI)	64
CHAPTER 4: RESULTS AND DISCUSSIONS	66
4.1 Greenhouse microclimate	66
4.2 Validation of Penman Monteith Method	75
4.3 Determination of stomatal resistance	77
4.4.1 Calibration and Validation of Ventilation Sub-model	84
4.4.2 Calibration and Validation of the Roof vents only model	86
4.5 Model Results	89
4.5.1 Introduction	89
4.5.2 Influence of Ventilation Strategy on Air renewal rates	89
4.5.3 Effects of ventilation on the microclimate of the greenhouse	94

4.5.3.1 Influence of Ventilation on inside air Temperature	94
4.5.3.2 Effects of ventilation strategy on relative humidity	100
4.5.4 Effects of ventilation regimes on the transpiration	103
4.5.5 Effects of ventilation strategy on canopy temperature	107
CHAPTER5 Conclusions and Recommendations	111
5.1 Conclusions	111
5.2 Recommendations	113
REFERENCES	114
APPENDIX A	118
APPENDIX B	121
APPENDIX C	122

LISTS OF TABLES

Table 3.1 Calibration multipliers for temperature sensors	44
Table 3.2: Calibration results for relative humidity sensors	44
Table 3.3: Calibration multipliers for the radiation sensors	45
Table 3.4: Parameters of the ventilation system. T _{set} represents the set ventilation temperature	per
period , Y represents the humidity dependent decrease (+) or increase (-) in ventilation	
temperature at a humidity level, X.	53
Table 3.5: Values for the Gembloux Dynamic Greenhouse Climate Model parameters (after	
Pieters, 1996; Pieters and Deltour, 1997; Pollet and Pieters, 2000)	61
Table 4.1: Summary of greenhouse air temperature and relative homogeneity test resu	ılts,
measured at five positions during a 4-day period (27-31 October 2009)	70
Table 4.2: Model specific parameters obtained in this study compared to those foun0d by Bail	le
et al (1994c) and Kittas et al (1999) for two cultivars of roses (Rosa x Hybrida)	81
Table 4.3:Results of significance test using t-test at 5% level of significance for the observed a	and
predicted stomatal resistance for calibration and validation, including the Root Mean Squ	ıare
Error(RSME)	83
Table 4.4: Discharge (C _D) and wind effect (C _w) coefficients obtained in this study	84
Table 4.5:. Discharge and wind effect coefficients found by other researchers	85
Table 4.6: Coefficients (C_1) and coefficients (C_2) obtained in this study	86
Table 4.7: Coefficients (C_1) and Coefficients (C_2) obtained by Fernandez and Bailey (1992)	86
Table 4.8: Results of regression analysis between the predicted and observed air renewal rates	,
including the 95% confidence intervals and the slope and intercept for the equation $R_{a(obs)}$	₅₎ =
$m R_{a(pred)} + c$	88

Table 4.9: Simulated maximum temperatures and average temperature difference for the two	
ventilation regimes on selected days in summer	99
Table 4.10: Maximum transpiration for the two ventilation configurations	106

LIST OF FIGURES

Figure 2.1: Heat exchanges between the various components of a greenhouse (Adapted from	
Chou 2004)	20
Figure 2. 2: showing the schematic of Dynagage for measuring Sap flow (adapted from Van	
Bavel, 1999)	28
Figure 2.3: The diagram showing the connection of Dynagage for determination of transpiration	on
(Van Bavel,1999)	30
Figure 3. 1: showing (a) a schematic representation showing dimensions of the greenhouse (b))
the commercial greenhouse at Floraline Pvt Ltd where the inside automatic weather station	on
was installed	34
Figure 3. 4: The positions of air temperature and relative humidity sensors within the	
greenhouse	39
Figure 3. 5: The picture showing thermocouples attached to the underside of the leaf for	
measuring leaf temperature	42
Table 3. 1 Calibration multipliers for temperature sensors	44
Table 3. 2: Calibration results for relative humidity sensors	44
Table 3. 3: Calibration multipliers for the radiation sensors	45
Figure 3.6: The schematic diagram showing the heat and mass exchanges between the	
greenhouse layers (after Pieters and Deltour, 1997)	46
Table 3. 4: Parameters of the ventilation system. T_{set} represents the set ventilation temperature	3
per period , Y represents the humidity dependent decrease (+) or increase (-) in ventilation	on
temperature at a humidity level, X.	53
Figure 3.7: The GDGCM running in TRNSYS program	59
Table 3.5: Values for the Gembloux Dynamic Greenhouse Climate Model parameters (after	
Pieters, 1996; Pieters and Deltour, 1997; Pollet and Pieters, 2000)	61
Figure 3. 8:(a) The AP4 Diffusion porometer for measuring stomatal resistance and (b)the	
radiation thermometer measuring leaf temperature	63
Figure 3. 9: Showing the set up for the sunscan ceptometer for measuring the leaf area index.	65

Figure 4.1: Diurnal variation of (a) air temperature and (b) relative humidity on 14 December	•
2009	66
Figure 4.2: The vertical variation of (a) air temperature and (b) relative humidity in the	
greenhouse on 28 October 2009. The temperature and relative humidity were measured	at
heights of 0.4 m, 0.8m, 1.5m (crop height) and 2 m at the position of the internal AWS (as
shown Figure 3.3).	68
Figure 4.3: Variation of air temperature and relative humidity at five positions in the greenhouse	ouse
during a single day 28 October 2009.	69
Table 4.1: Summary of greenhouse air temperature and relative homogeneity test results,	
measured at five positions during a 4-day period (27-31 October 2009)	70
Figure 4.4: Diurnal variation of (a) vertical profile of temperature (b)vertical profiles of rela	tive
humidity on 21 January 2010	72
Figure 4. 5: The diurnal variation of (a) of average leaf temperature and solar radiation on 13	3
December 2009	74
Figure 4.6: correlation between transpiration obtained from sap flow and transpiration obtain	ed
from Penman-Monteith method on days 1-31 December 2007	76
Figure 4.7: Variation of measured stomatal resistance and solar radiation on 28 February 201	0 -
14 March 2010	78
Figure 4. 8: Variation of measured stomatal resistance with vapour pressure deficit (VPD) or	ı 28
February 2010-14 March 2010	79
Figure 4.9: stomatal resistance of four different cultivars (a) Upendo, (b) Betsy, (c) Symphon	ica
Rosso and (d)King Arthur on 28 February 2010	80
Table 4.2: Model specific parameters obtained in this study compared to those found by Baill	le et
al (1994c) and Kittas et al (1999) for two cultivars of roses (Rosa x Hybrida)	81
Figure 4.10: Showing (a) the daytime variation of stomatal resistance and (b) the correlation	
between observed stomatal resistance and predicted stomatal resistance on 16 March 20	10
	82
Table 4.3: Results of significance test using t-test at 5 % level of significance for the observe	d
and predicted stomatal resistance for calibration and validation, including the Root Mea	n
Square Error(RSME)	83

Tab	ble 4. 4: Discharge (C _D) and wind effect (C _w) coefficients obtained in this study	84
Tab	ole 4. 5: Discharge and wind effect coefficients found by other researchers	85
Tab	ble 4.6: Coefficients (C_1) and coefficients (C_2) obtained in this study	86
Tal	ble 4. 7: Coefficients (C ₁) and Coefficients (C ₂) obtained by Fernandez and Bailey (1992)	86
Fig	ure 4.11: Regression between the experimentally observed and predicted air renewal rates	for
	(a) calibration 1-31 December 2007 and (b) validation for the period 1-25January and	1-
	23 February 2008 using model for both roof and side vents	87
Tab	ble 4. 8: Results of regression analysis between the predicted and observed air renewal rate	es,
	including the 95% confidence intervals and the slope and intercept for the equation $R_{a(ob)}$	$p_{s)} =$
	$m R_{a(pred)} + c$	88
(b)	90	
Fig	ure 4.12: The simulated air renewal rate (a) for the period from 11-13 September 2007 and	d
	(b) for the period from 16-17 October 2007.	90
Fig	ure 4.13: Simulated air renewal rate for (a) 1-5 December 2007 and (b) 15-21 January 200)8.
		93
Fig	ure 4.14: The simulated diurnal variation of internal air temperature for the two	
	configurations on (a) 18 October 2007 and (b) on 18 November 2007	95
Fig	ure 4.15: Simulated inside air temperature of the greenhouse of the two ventilation regime	S
	on (a) 2 December 2007 and (b) 16 January 2008.	97
Fig	ure 4.16: Simulated temperature on (a) 1 February 2008 and (b) on 8 March 2008 for the t	wo
	ventilation regimes	98
Tab	ole 4.9: Simulated maximum temperatures and average temperature difference for the two	
	ventilation regimes on selected days in summer	99
Fig	ure 4.17: The simulated diurnal variation of relative humidity on (a) 18 November 2007 at	nd
	b) 2 December 2007	101
Fig	ure 4.18: The simulated relative humidity on (a) 16 January 2010 and (b) 1 February 2010	102
Fig	ure 4.19(i): Simulated canopy transpiration on (a) 18 October 2007 and (b) 18 November	
	2007 for the two ventilation regimes	104
Tal	ble 4. 10: Maximum transpiration for the two ventilation configurations	106

Figure 4. 20: Simulated canopy temperature on 16 January 2008 for roof vents only an	d for both
roof and side vents	107
Figure 4.21: The simulated canopy temperature on (a) 2 December 2007 and (b) 1 Feb	ruary 2008
	109
Figure 4. 22: Simulated diurnal variation of canopy temperature on (a) 18 November 2	.007 and
(b) 18 October 2007	110
Figure B- 1: (a) Program for outside automatic weather station Delta-T datalogger and	(b) the
program for inside weather Delta-T dalogger	121

CHAPTER 1 INTRODUCTION

1.0 Introduction

The greenhouse is a cultivation environment that is partly separated from its surroundings. The roof's transparency establishes a link between the internal microclimate and outdoor atmospheric conditions (Fuchs, 1996). The air exchange between the inside and outside of a greenhouse influences the environmental conditions, such as temperature, humidity and carbon dioxide concentration that affect the development and production crop.

The major challenge faced by many greenhouse users is cooling the greenhouse during periods of high solar irradiance. The most practiced ventilation method is natural ventilation because it is cheaper the forced ventilation method which requires fans to drive ventilation. Natural ventilation is a result of air exchange between the exterior and interior of a greenhouse through openings designed to cater for that purpose. Most greenhouse designs have both roof and side vents.

Ventilation affects both the energy and mass balance in a greenhouse. The effects of energy balance are manifested by change in the inside air temperature of the greenhouse, where as the mass balance affects the concentrations of air components such as water vapour which affects the humidity inside the greenhouse, which directly affect crop transpiration and also the carbon dioxide concentration that affect the photosynthesis process in crops, (Bot, 1983, Bakker et al, 1995, Pieters and Deltour, 1997; Hanan, 1998) In Zimbabwe high solar radiation occurs during summer. The greenhouse and crop form a complex system of sources and sinks for mass and energy which are usually unevenly distributed. The ventilation plays a vital role of controlling environmental factors such as temperature, humidity and carbon dioxide concentration. In this study, the effect of different ventilation strategies was investigated. Thus in order to grow crops

throughout the year it is necessary to practice good ventilation strategy that is optimum for crop growth.

1.1 Greenhouse Ventilation

As ventilation is one of the criteria of controlling the greenhouse microclimate, the air exchange between the inside and outside of a greenhouse influences environmental parameters such as temperature, humidity, crop transpiration and carbon dioxide concentration that affect the development and production of crops.

There are two types of ventilation which are the natural ventilation and the forced ventilation. Natural ventilation is the most commonly practiced ventilation strategy in Zimbabwe's greenhouses because of its cost effectiveness. Natural ventilation systems rely on pressure differences between the inside and outside of greenhouse for air to be exchanged. Air move from a high pressure to where there is low pressure. Pressure difference arises from wind or the buoyancy effect created by temperature differences or differences in humidity. In either case, the amount of ventilation will depend critically on the size and placement of openings in the greenhouse.

Forced ventilation is achieved through use of mechanical devices such as exhaust fans. This will cause air to be circulated within the greenhouse. The disadvantage of this method is that it is expensive and many growers are not financial sound to have that ventilation strategy in their greenhouses.

1.2 Problem Statement

As Zimbabwe experiences high ambient daytime temperatures as a result of high solar irradiance associated with summer, the major challenge of most horticulturalists in the country is to try to maintain temperature at safer level that would allow good crop production and development in the greenhouse. Thus there is need of finding the most efficient way of reducing the difference

between inside and outside temperature which is cost effective. Thus the use of vents which is termed passive or natural ventilation uses less energy as opposed to mechanical or forced ventilation driven by fans which requires more energy but it requires proper management in order to obtain favourable crop response and yields.

Many attempts have been made to predict the microclimate and in particular the air exchange or ventilation for commercial greenhouses (Boulard et al 1997, Boulard et al 1995, Wang 1998). Thus it is imperative to use modeling in the prediction of the microclimate, before the model is applied it needs to be validated in the particular area it is going to be used.

1.3 Background and Justification

Greenhouses provides a controlled and favorable environment for the crops to grow and give yield in all seasons. The greenhouse enables growers to grow crops throughout the year. As there is climate control in greenhouse there is higher yield per unit area. For there to be proper control of environment in the greenhouse, growers should be able to practice good ventilation. With good ventilation the prevalence of pests and diseases associated with high humidity are reduced.

Despite the fact that ventilation is an important physical process influencing, the indoor greenhouse microclimate, it has been poorly investigated especially in Zimbabwe. Thus as horticulture industry helps the country with foreign currency which is realized from exports of roses, it is therefore necessary to investigate the effects of ventilation in crop production in a greenhouse in order to come out with recommendations that would benefit greenhouse users.

Most greenhouse growers in Zimbabwe employ natural ventilation because it is cheaper than forced ventilation systems. Thus in most greenhouses in the country, natural ventilation is usually the only air renewal process in protected cultivation. Natural ventilation systems, however, offer a limited control over the airflow through the greenhouse. As a result, there are difficulties in controlling the indoor temperature, the relative humidity and CO₂ concentration.

Hence, a deeper analysis of mechanisms of natural ventilation is necessary in order to understand the dependence of the ventilation rate on the greenhouse design and improve its efficiency.

1.4 Aims and Objectives

The main aim of this study was to measure the air exchange rates resulting from natural ventilation in a greenhouse equipped with continuous roof and side vents and to investigate the effect of different natural ventilation regimes on the microclimate and transpiration of several cultivars of a well- watered rose canopy in Zimbabwe by measurement and modeling.

The specific objectives of project are:

- 1) To evaluate the ventilation rates for different ventilation strategies
- 2) To investigate the effects of these different strategies on the greenhouse microclimate and transpiration rate by measurement and through the use of dynamic greenhouse climate model.

1.5 Expected Benefits

As ventilation plays a major role in the control of the microclimate of the greenhouse, therefore this study will help greenhouse growers to practice good ventilation for them to get products of high quality and minimize operation cost. The recommendations from this study would help farmers with effective way of mitigating the prevalence of disease and pests and increase plant growth.

1.6 Project Layout

This project was made up of five chapters. The first chapter describes the thesis title, and outlines the problem statement and objective of the study. Chapter 2 includes the Literature review relevant to the study and aims and objective of the study. Chapter 2 outlines the possible method for determining ventilation rates. The materials and methods used in the study are outlined in chapter 3, including the overview of the Gembloux Dynamic Greenhouse Climate Model

(GDGCM). Chapter 4 presents the results obtained in the research and the discussions on these findings. Chapter 5 summarizes the results and gives conclusions and recommendations basing on the findings from the research.

CHAPTER 2 LITERATURE REVIEW

2.1 Introduction

A microclimate is the local modification of the general climate that is imposed by the special configuration of a small area. It is influenced by topography, the ground surface and plant cover and man made forms such as greenhouse, houses and wind breaks (Jones, 1992). The basic goal of greenhouse users is to strive to provide environmental conditions which allow photosynthesis and respiration to occur so that plants grow, and that the quality is good and are marketable. Air exchange rate is one of the most important parameters of ventilation systems in a greenhouse. The ventilation systems serves the purpose of optimum control of greenhouse climatic conditions for plant growth through supply of sufficient and uniform air exchange rate, between the inside and the outside of greenhouse environments. A better air exchange rate helps reduce the greenhouse air temperature and improves the evapo-transpiration processes for crops. Ventilation and leakage rates are influenced by environmental factors such as wind speed, wind direction, temperature difference between inside and outside and ventilator aperture (Baptista, et al., 1998).

2.1.1 Greenhouse Microclimate

The thermal environment of the greenhouse arises from the complicated mass and heat exchanges between the various components of the greenhouse and the fluctuating weather conditions which present a dynamically changing greenhouse microclimate. The conditions which define the microclimate of the greenhouse are the inflows and outflows and production of energy and mass as result of interactions between the external and internal of the greenhouse.

The greenhouse structures are used to overcome low temperatures in winter and high temperatures in summer. Thus it is necessary for modifying the temperature not only for crop protection, but also to provide comfortable working conditions. In Zimbabwe growers overcome the effects of high summer temperatures by practicing good ventilation, shading and evaporative cooling.

2.1.2 Transport mechanisms which affect the microclimate of the greenhouse

2.1.2.1 Radiation

Radiation refers to the continual emission of energy from the surface of all bodies of a given temperature. This emitted radiation is of electromagnetic in nature. The radiant energy emitted by a body depends on the nature of the surface of that body and its temperature. At low temperature the rate of radiant energy is low. At higher temperatures total radiant energy increases rapidly.

The greenhouse through the cladding covering allows solar radiation to be trapped and absorbed depending on the transmissivity of the cover. The solar radiation which is in the form of shortwave radiation may be absorbed directly from the sun or it may be diffuse short wave radiation scattered by surrounding objects. The greenhouse structures are used to overcome low temperatures in winter and high temperatures in summer caused by high solar irradiance. The radiation which is of interest to growers is the Photosynthetically active radiation (PAR) which is the visible light range of the electromagnetic spectrum. The wavelength of the PAR ranges from 400nm to 700nm and it is the radiation which is utilized during photosynthesis. The greenhouse roof is constructed with material which is Ultra-violet film which does not allow UV light to enter the greenhouse. The radiation which the greenhouse absorbs contributes to temperature and humidity inside the greenhouse. The radiation transmitted into the greenhouse will be absorbed by crops, which will consequently cause the leaf temperature to increase, some of the radiation will be used in the photosynthesis process, while the other will be converted to heat and will contribute to latent heat flux and sensible heat flux. The latent and sensible heat is transported to the greenhouse atmosphere by convection. Some of the radiation will penetrate the crop canopy and can be absorbed by ground or soil. The crop canopy also radiates thermal radiation to the greenhouse atmosphere further contributing to the greenhouse heat load.

According to Stefan-Boltzmann's law the total emitted radiation emitted is proportional to the fourth power of absolute temperature.

$$R = \varepsilon \, \sigma T^{4} \tag{2.1}$$

Where R= radiant energy flux density (W m $^{-2}$)

ε: the emissivity of the surface

 σ : the Stefan-Boltzmann constant (5.67 x 10^{-8} W m⁻² K⁻⁴)

T: absolute temperature (K)

If radiation falls on a body, part of the radiation is absorbed, part is reflected and part is transmitted. From the conservation of energy the following equation can be deduced.

$$\alpha + \rho + \tau = 1 \tag{2.2}$$

Where α is the absorptivity of the body on which radiation is incident.

 ρ is the reflectivity of the body

 τ is the transmissivity of the body.

In a greenhouse there is exchange of thermal energy between the sky and the cover by radiation. Some of the radiation that is incident may be absorbed by the cover and some is reflected into the atmosphere and part of the radiation. Thus this solar radiation transmitted inside the greenhouse cause the inside temperature to rise. The inside air which has been heated by radiation also transmits the radiation to the vegetation inside the greenhouse.

2.1.2.2 Conduction

Conduction is a process where by heat is transmitted within an object by means of free electrons within a metal or by means of colliding molecules in a fluid or by means of intermolecular forces

in an insulator. Thus in a greenhouse conduction occurs in the soil and the roof and side walls of the greenhouse. The direction of flow depends on the temperature gradient. The heat is transferred from a region of higher temperature to a region of lower temperature.

$$C = -k\frac{dT}{dz} \tag{2.3}$$

Where *C* is the rate of conduction of heat per unit area

k is the thermal conductivity of the material.

z is the axial distance travelled by heat.

2.1.2.3 Convection

The transport of energy and mass by a flow from one place to the other in the direction of flow and transport from a surface to a flowing medium or vice-versa are transfer by convection. In a greenhouse the ventilative exchange of energy and mass (water vapour, CO_2) is the transfer by advection. The transfer of heat and mass between the greenhouse air and internal surfaces such as cover, crop canopy, heating pipes and soil surface or the exchange of energy and mass between the outer surface of the greenhouse and ambient air is achieved through convection. The driving for the transport mechanism of convection is temperature or concentration difference between surface and flowing medium and therefore for energy the heat flux Φ_h is given as:

$$\phi_h = k_h (T_s - T_a) \tag{2.4}$$

And for the mass transfer, the mass flux density Φ_m equals

$$\phi_m = E = k_m (c_{m,s} - c_{m,a}) \tag{2.5}$$

Where E= transpiration, k_h is the heat transfer coefficient (W m⁻² K⁻¹)

 k_m is the mass transfer coefficient (m s⁻¹)

 $T_{\rm s}$ and $T_{\rm a}$ is the surface and air temperature respectively.

The transfer coefficients for both energy and mass depend on many relevant factors including the properties of the flowing medium, the flow conditions and on the geometry of the flow field. The heat transfer coefficient k_h is given in terms of the Nusselt number (Nu). If the flow is driven by external factors the convection is called forced convection and the flow condition is characterized by the Reynolds- number. The relevant properties of the flowing medium for heat transfer are combined into Prandtl-number (Pr). The following relationship fit with experimental data for most forced convective heat transfer.

$$Nu = C_1 \operatorname{Re}^n \operatorname{Pr}^m \tag{2.6}$$

Where
$$Nu = \frac{k_h d}{\lambda}$$

$$Re = \frac{ud}{v}$$

$$\Pr = \frac{v}{a}$$

Where u is speed in the flow field (m s⁻¹), λ is thermal conductivity (W m⁻¹ K⁻¹), d is the characteristic length (m) of the surface considered, v is the kinematic of viscosity of the flowing medium(m³ s⁻¹) and a is the thermal diffusivity of the medium. In the greenhouse the coefficient C_1 and the powers n and m depend on the geometry of the surface and the flow conditions as determined by the range of Reynolds value.

For low Reynolds number

$$Nu = 0.664 \,\text{Re}^{\frac{1}{2}} \,\text{Pr}^{\frac{1}{3}} \tag{2.7}$$

With $2x10^2 < Re < 10^5$; Pr>0.7

For high Reynolds values or turbulent flow

$$Nu = 0.036 \text{Re}^{0.8} \text{ Pr}^{\frac{1}{3}}$$

With $10^5 < \text{Re} < 10^7$; $\text{Pr} \ge 0.7$

Similarly for mass transfer coefficient k_m is combined in a dimensionless number called the Sherwood number (Sh) and its dependency on the flow conditions and the properties of medium is expressed again on a relation between dimensionless numbers.

$$Sh = C_1 \operatorname{Re}^n Sc^m \tag{2.8}$$

With
$$Sh = \frac{k_m d}{D}$$

$$Sc = \frac{v}{d}$$

Where D is the diffusivity of gas component in the medium (m² s⁻¹) and Sc is the Schmidt number.

For the same flow field and field conditions and the same geometry the Nu, Re, Pr and the Sh, Re and Sc relation are similar, so the coefficients C_1 and powers n and m are equal

In order to investigate the effects of free or natural convection which is driven by the temperature and pressure difference in the flow –field. For natural ventilation, the Nusselt number is function of a dimensionless number characterizing the density (caused by temperature difference) as driving force, called the Grashof number (Gr), the Prandtl number characterises the properties of the medium

For air under normal conditions

 $Gr = \frac{g\Delta Td^3}{Tv^2}$, where g is the acceleration due to gravity(m s⁻²), ΔT is the temperature difference

between surface and medium

For low Grashof numbers

$$Nu = 0.55(Gr.Pr)^{\frac{1}{4}}$$
 (2.9)

With: $10^4 < Gr < 10^8$, 0.5 < Pr < 10

For high Grashof number

$$Nu = 0.13(Gr. Pr)^{\frac{1}{3}}$$
 (2.10)

With: $Gr > 10^8$, 0.5<Pr < 10

The greenhouse cover exchanges energy at the inner surface to the greenhouse air and to the outside air at the outer surface. Water vapour is transported from the greenhouse air to the cover and sometimes condenses there. The mechanism of these exchanges is that of convection. Inside natural convection is caused by low wind speed generated by prevailing temperature difference, and outside forced convection is due to wind speed generated by wind field. (Bakker, 1995). The convective heat exchange is defined as:

$$Q_V = k_h A_s \left(T_a - T_s \right) \tag{2.11}$$

 Q_{v} is the convective heat exchange (Wm⁻²)

 T_s and T_a are the cover surface and ambient air temperature (K)

 $A_{\rm s}$ the surface area (m²)

 K_h is the transfer coefficient (W m⁻² K⁻¹)

Sensible heat in the greenhouse is as result of solar radiation that is absorbed by the greenhouse cover, vegetation and soil which makes these surfaces warmer than the surrounding area and may release some of the energy by convection. This would increase air temperature during periods of high solar irradiance (Rosenberg, 1983)

2.2.0 Mass and Energy balance in the greenhouse

2.2.1 Greenhouse Energy Balance

Ventilation removes energy from a greenhouse and prevents high temperatures during periods of high insolation. For a greenhouse with no heating, the energy removed by the process of leakage and ventilation is equal to the solar energy collected in the greenhouse minus the thermal losses through the cover minus the energy stored. The energy lost by leakage and ventilation has two components, one component due to sensible heat, and the other component due to latent heat.

For the energy balance of a greenhouse, the energy inputs equal the sum of energy losses and the greenhouse transient energy content, the energy inputs result from the absorption of long and short wave radiation. The net radiometer can be estimated from the net radiometer installed between the top of the crop canopy and the cover. The net radiation is partly absorbed by the protected crop and the other part is transmitted through the crop canopy where it is absorbed by the greenhouse soil surface (Demrati, et al, 2001).

$$R_{net} = R_{a,v} + R_{a,s} (2.12)$$

Where $R_{a,v}$ represents part of radiation absorbed by the vegetation inside the greenhouse.

 $R_{a,s}$ represents part of net radiation absorbed by the greenhouse soil surface.

Thus this radiation absorbed by the crop and soil surface contributes to the inside air heating resulting from sensible heat from vegetation and soil which are given the following symbols $H_{v,i}$

in W m⁻² and $H_{s,i}$ in W m⁻² and subscript i denotes inside, and the also has the effect of increase of water vapour content through increase of latent energy from the crop and soil $\lambda E_{\nu,i}$ and $\lambda E_{s,i}$ and heat the thermal mass of the crop and soil.

The thermal balance of the crop inside the greenhouse is therefore given by the relation below

$$R_{a,v} = H_{v,i} + \lambda E_{v,i} + \rho_v c_v l_v \frac{dT_v}{dt}$$
 (2.13)

Where $H_{v,i}$ is the sensible flux exchanged between the vegetation and inside air in W m⁻², $\lambda E_{v,i}$ is the latent flux exchanged between the vegetation and inside air in W m⁻², ρ_v is the density of vegetation in kg m⁻³, c_v is the specific heat in J kg⁻¹ K⁻¹, l_v is the mean equivalent height of crop in m, T_v is the temperature of vegetation in $^{\circ}$ C and t is the time in s.

Similarly, the diurnal thermal balance of the soil surface is

$$R_{a,s} = H_{s,i} + \lambda E_{s,i} + F_s + \rho_s c_s l_s \frac{dT_s}{dt}$$
 (2.14)

Where $H_{s,i}$ is the sensible flux exchanged by convection between the soil and inside air in W m⁻², $\lambda E_{s,i}$ is the latent flux exchanged between the soil surface and inside air in W m⁻², ρ_s is the density of soil in kg m⁻³, l_s is the thickness of the soil layer in m, c_s is the specific heat of soil in J kg⁻¹ K⁻¹, T_s is the temperature of soil in $^{\circ}$ C and t is the time in s. F_s is the thermal flux in the soil in W m⁻² (positive when moving from air to the soil)

When neglecting the energy storage terms for long time steps and condensation during daytime and substituting equations (1) and equations (3), equation (1) becomes

$$R_{net} = H_{v,i} + H_{s,i} + \lambda E_{v,i} + \lambda E_{s,i} + F_s$$
 (2.15)

The term ($H_{s,i}+H_{v,i}$) represents the greenhouse sensible heat gain which is either evacuated by ventilation flux, or exchanged with the greenhouse roof and side walls. The term ($\lambda E_{v,i} + \lambda E_{s,i}$)

represents the greenhouse latent heat gain which is evacuated by ventilation flux, and increases the inside air latent heat content.

2.2.2 Greenhouse Vapour Balance

Evaporation of small droplets of water, evaporation from wet soil or surfaces, and transpiration are all influenced by the vapour content of nearby air. If the air is saturated evaporation will occur, if not evaporation can proceed (Rosenberg, 1983). Evaporation or evapotranspiration increases in response to an increasing difference between the vapour pressure at the evaporating surface and the vapour pressure of air (vapour pressure deficit). The humidity build up in the greenhouse are transferred to the outside by ventilation. The temperature of the air and or that of the evaporating surface exert a major influence on evapotranspiration. In general the higher the temperature, whether of air or evaporating surface, the greater will the rate of evaporation. Because of the strong dependence of evaporation on temperature and because temperature is good integrator of several environment variables, many models for predicting ET use temperature as a major unit. Temperature influences evapotranspiration in the following four ways. The amount of water vapour that air can hold increases exponentially with increasing temperature. As the surface temperature increases the vapour pressure at the evaporating surface increases as does the vapor pressure between the surface and nearby air. Because air can hold more vapour as its temperature increases the vapour pressure deficit between surface air and the evaporating surface becomes larger and evaporative demand is increased as air is warmed. Warm dry air may supply energy to an evaporating surface. The rate of evaporation is dependent on the amount of heat transferred, therefore the warmer the air the stronger the temperature gradient and the higher rate of evapotranspiration. If it is the evaporating surface that is warmed less, sensible will be extracted and evaporation will decrease.

2.3 Ventilation

The main driving forces of ventilation for a greenhouse with both roof and side vents are:

- 1. The chimney effect, due to thermal buoyancy forces (Bruce, 1982), aiming at a vertical distribution of pressures between the side and roof openings.
- 2. The static wind effect due to the mean component of the wind velocity, which induces a spatial distribution of pressures over the envelope of the greenhouse.
- 3. The turbulent effect of the wind, linked to the pressure fluctuations of the wind velocity along openings (Boulard and Baille, 1995), inducing an influx and out flux within the same opening.

The static wind effect give rise to a vertical distribution of pressures between the side and roof openings (1978) and to a horizontal distribution of pressures between the upwind and the downwind parts of the greenhouse (Hoxey and Maron, 1991; Boulard et al 1991) resulting in "side wall effect" already analyzed by several authors (De Jong, 1991; Fernandez and Bailey, 1992)

Two main air fluxes are generated by these effects:

- (a) A vertical ventilation flux due to chimney effect and the vertical static wind pressure distribution.
- (b) A horizontal ventilation flux due to side wall effect and the turbulent effect.

2.3.1 Vertical Ventilation Flux

Air flow through an opening is caused by a combination of pressure differences induced by the buoyancy forces (the chimney or the stack effect) and the wind forces.

Considering a greenhouse equipped with roof and side openings. If the wind is parallel to the ridge, then static wind pressure coefficients of the roof openings are identical (C_R), the same is valid for the side openings which are characterized by a common static wind pressure coefficient (C_S) (Baille, 1992: Gandemer and Bietry, 1989).

The vertical air flow exchanged between the side (S) and the roof(R) openings is composed of two parts, thermal buoyancy and wind effect.

$$G_{V} = C_{d} \frac{A_{R} A_{S}}{\sqrt{A_{R}^{2} + A_{S}^{2}}} \left[2g \frac{\Delta T}{T_{0}} + (C_{R} - C_{S})u^{2} \right]^{0.5}$$
(2.16)

Where G_v = vertical ventilation flow rate (m³s⁻¹) exchanged between the side and roof openings.

 $C_{\rm d}$ = discharge coefficient

 A_R = roof openings area (m²)

 $A_{\rm S}$ = side openings area (m²)

g = acceleration due to gravity (m s⁻²)

 ΔT = difference between inside and outside temperature (K)

 $T_o = outside temperature (K)$

h = vertical distance between the midpoint of the side and roof openings (m)

 C_R = static wind pressure coefficient at the level of roof openings

 $C_{\rm S}$ = static wind pressure coefficient at the level of side openings

 $u = \text{wind velocity (m s}^{-1})$ at 4.5 m above the ground

Assuming that C_R-C_S=k equation 1 becomes

$$G_{v} = C_{d} \frac{A_{R} A_{S}}{\sqrt{A_{R}^{2} + A_{S}^{2}}} \left[2g \frac{\Delta T}{T_{o}} h + ku^{2} \right]^{0.5}$$
(2.17)

2.3.2 Horizontal ventilation flux due to side wall and turbulent effects

A wind parallel to a continuous opening extended along a building gives rise to a static pressure field near the edges of the building, which induces a steady influx at the leeward and an out flux at the windward part (Boulard et al, 1995) This is known as the "side wall" effect and is linked to a pressure gradient along the opening. Its contribution to the total ventilation flux is important and varies inversely to the size of the greenhouse (Fernandez and Bailey, 1992).

Wind turbulence, in interaction with the structure or with immediate surrounding, create fluctuating pressures around the greenhouse, which induce two ways airflow through the same opening (Van der Moas, 1992). In a greenhouse equipped with only roof openings the air flow enters and leaves the building through the same opening so that inflow area is equal to outflow area over time (Bot, 1983; Boulard, 1993). In a case where both roof and side ventilators are open, the ventilation area is considered to be half of the total vents area. The global wind coefficient C_w can be defined as the coefficient which includes both the turbulent and side wall effects and thus horizontal wind driven flux G_h is equal to

$$G_h = \frac{A_T}{2} C_d \sqrt{C_w} u \tag{2.18}$$

Where

$$\frac{A_R + A_S}{2} = \frac{A_T}{2} \tag{2.19}$$

 G_h = horizontal ventilation flow rate (m³ s⁻¹)

 $A_{\rm T}$ = total area of vents (m²)

 $C_{\rm w}$ = global wind coefficient

This expression of horizontal ventilation flux is similar to that given by several authors (Boulard, 1993; Kittas et al 1995) for greenhouse with only roof vents

Combination of the Vertical and Horizontal Fluxes

We can combine these fluxes through either (Boulard& Baille, 1995)

The algebraic sum:

$$G = G_v + G_h \tag{2.20}$$

Where G is the total ventilation flow rate (m³ s⁻¹)

The vertical sum:

$$G = \sqrt{G_v^2 + G_h^2} \tag{2.21}$$

In this case, the flow is driven by the pressure field equal to the sum of two forces (stack and wind)

Local estimation of air flows and energy fluxes along a continuous roof opening, using eddy correlation techniques (Boulard et al, 1995), has shown that the 'side wall' effect was much greater than the turbulent effect

Hence the static pressure field linked to the wind effect can thus be combined with static pressure field linked to buoyancy forces through a vectorial sum of G_v and G_h

$$G = C_d \left[\left(\frac{A_R A_S}{\sqrt{A_R^2 + A_S^2}} \right)^2 \left(2g \frac{\Delta T}{T_o} h + ku^2 \right) + \left(\frac{A_T}{2} \right)^2 C_w u^2 \right]^{0.5}$$
 (2.22)

From studies of Kittas, Papadakis and Boulard it was revealed that the vertical air flow due to wind driven static pressure has the same direction as the airflow which is induced by the chimney effect, however, the k value was found to be small and statistically not significant and it means that wind flux generated by the vertical distribution of pressures is negligible, and a large part of the static wind effect is already explained by C_w neglecting K equation 2.22 becomes

$$G = C_d \left[\left(\frac{A_R A_S}{\sqrt{A_R^2 + A_S^2}} \right)^2 \left(2g \frac{\Delta T}{T_o} h \right) + \left(\frac{A_T}{2} \right)^2 C_w u^2 \right]^{\circ 0.5}$$
 (2.23)

Figure 2.1 shows the heat exchanges of the various components which are as a result of the transport mechanisms and this project focuses on ventilation and how it affects the microclimate and transpiration of the crops in the greenhouse.

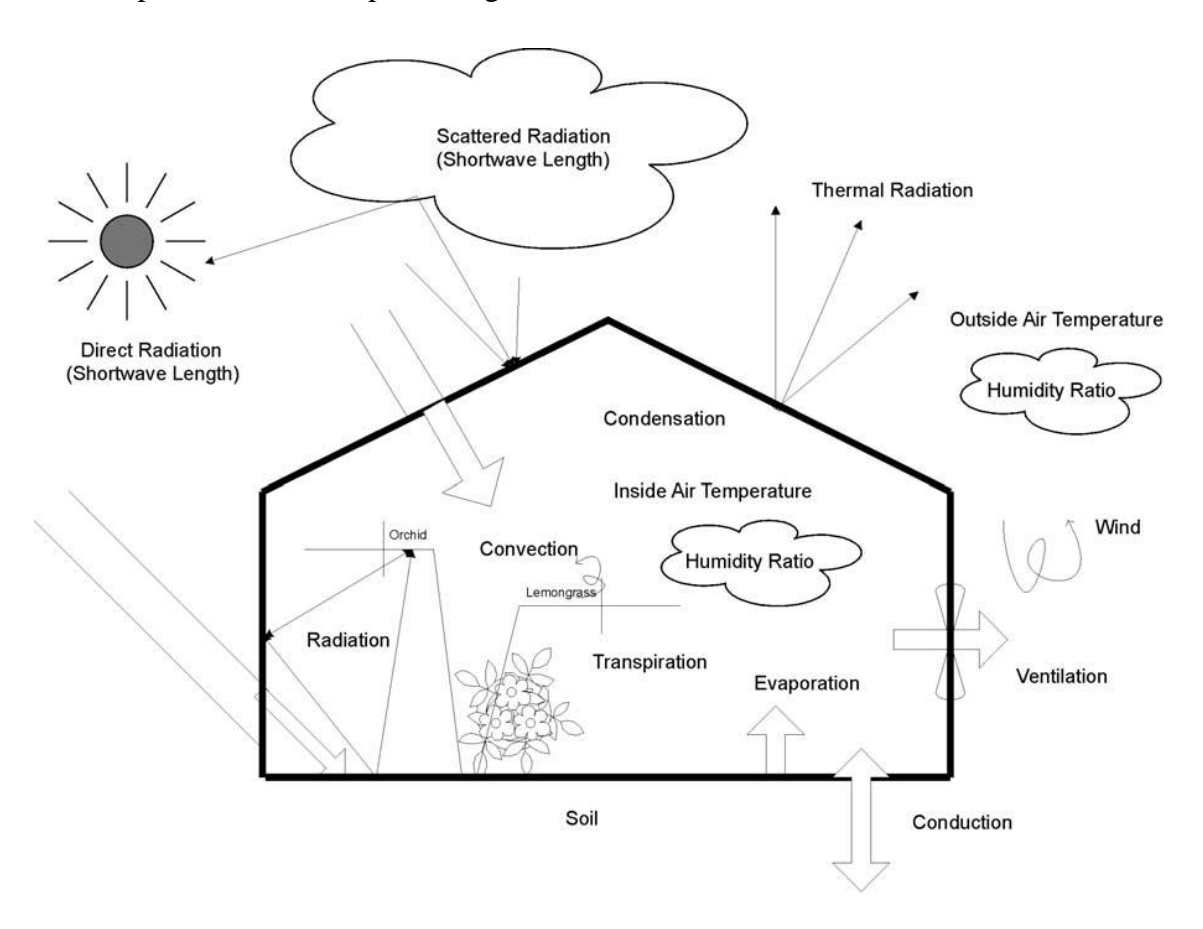


Figure 2.1: Heat exchanges between the various components of a greenhouse (Adapted from Chou 2004)

2.4 Methods of determining the ventilation rate

2.4.1 Tracer gas technique

The tracer gas technique is one of the most important techniques for measuring ventilation and leakage rates which has been used by (Bot (1983), Nederhoff et al 1985, De Jong 1990, Fernandez and Bailey (1993) and Boulard et al (1993). The tracer gas technique is based on a mass balance of a tracer gas in the greenhouse air.

There are two main methods of measuring ventilation and leakage rates which are

- 1. the continuous injection or static method.
- 2. the pulse injection or dynamic method

The characteristics of the tracer gas are based on the following, easy to measure at low concentrations, inert, non-toxic, non flammable, not a natural component of air and with a molecular weight close to the average weight of the air components. The gases which are used as tracer gases include sulphur hexafluoride (SF₆, methane (CH₄), carbon dioxide (CO₂), hydrogen (H₂), nitrous oxide (N₂O), argon 41 and krypton 85. The most commonly used gases are carbon dioxide and nitrous oxide. Nitrous oxide is the best because it meets all the above requirements, carbon dioxide can be used, but it is necessary to measure the concentration of CO_2 in the external air and rate of release from the soil. In a greenhouse with crops, N₂O is the better of the two because its concentration is not affected by the photosynthesis and respiration of the plants.

2.4.1.1 Static method

In this method, the injection rate of gas into the greenhouse is held at a constant value until an equilibrium concentration is reached. The gas supply and sampling system must be distributed around the greenhouse in order to obtain good dispersion of the gas and uniform sampling of the air. The ventilation rate is calculated from

$$G = \frac{M}{\left[C_{i(t1o)} - C_{0(t1)}\right]} - \frac{V}{t_2 - t_2} \times \ln \left[\frac{C_{i(t2)} - C_{o(t2)}}{C_{i(t1)} - C_{0(t1)}}\right]$$
(2.24)

Where *M* is the mass flow of gas entering the greenhouse

 C_i and C_o are the internal and external gas concentration

V is the volume of the greenhouse, and t_1 and t_2 are sequential measurements.

The advantage of this method is that it provides continuous information, and a range of wind speed and direction can be covered during one measurement. The disadvantage is the high consumption of tracer gas.

2.4.1.2 Dynamic method

In this method, the tracer gas is injected and distributed uniformly in the greenhouse until a certain pre-determined concentration is reached and then stopped. The decay in the concentration of the tracer gas is then measured. When the concentration has decreased to 80-90% of the initial value, another pulse of gas is injected, and decay is measured. It is possible to change the angle of ventilator opening on each decay but not during one period of decay.

The ventilation rate is calculated by the following procedure

the natural logarithm of (C_i-C_o) is plotted against time

A time period t is selected during which $\ln (C_i - C_0)$ decreases linearly.

A linear regression is fitted to the values of $ln(C_i-C_o)$ over this period

$$\ln(C_i - C_o) = a + R_a t \tag{2.25}$$

Where Ra is the ventilation rate in air changes per hour and a is a constant. The air renewal rate is negative because the concentration of the gas decreases during measurement. The ventilation rate G in m³/s is given by

$$G = \frac{R_a V}{3600} \tag{2.26}$$

Mean values are obtained for the wind speed, wind direction and internal and external temperature, over the time period selected.

The advantages of the decay method over the static method are that it uses less tracer gas and can be used to measure over a wide range of ventilation rates while the continuous injection method requires an appropriate flow meter to measure the injection rate. The disadvantages are the difficulty in obtaining a uniform concentration of the tracer gas throughout the greenhouse and for high ventilation rates, the concentration of the gas decreases rapidly and the data obtained for analysis can be insufficient.

2.4.2 The water vapour balance method

Assuming (i) Perfect mixing of water vapour in the volume of the greenhouse, and (ii) that evaporation from the soil and/ or other medium is negligible (justified by the presence of a plastic mulch on the soil surface and the cover offered by the crop); the greenhouse ventilation rate, G can be calculated from mass balance of water vapour of the greenhouse:

$$V\frac{dx_{i}}{dt} = G(t)[x_{e}(t) - x_{i}(t)] + T_{r}(t)$$
(2.27)

Where G (t) is the ventilation rate (m³ s⁻¹), V is the greenhouse volume (m³), x_i and x_e are the inside and outside air absolute humidity, respectively (kg m⁻³), and $T_r(t)$ is the greenhouse crop transpiration rate (kg s⁻¹)

For small time steps, Δt Equation (2) can also be expressed as:

$$V\frac{\Delta x_{i}}{\Delta t} = V\frac{x_{i}(t + \frac{\Delta t}{2}) - x_{i}(t - \frac{\Delta t}{2})}{\Delta t} = G(t) [x_{e}(t) - x_{i}(t)] + T_{r}(t)$$
(2.27)

So that:

$$G(t) = \frac{\left[V \frac{x_i \left(t + \frac{\Delta t}{2}\right) - x_i \left(t - \frac{\Delta t}{2}\right)}{\Delta t}\right] - T_r(t)}{\left[x_e(t) - x_i(t)\right]}$$

$$(2.29)$$

Measured values of air temperature and relative humidity outside and inside the greenhouse (at 30-minute time steps) will be used to calculate the values of outside and inside greenhouse air absolute humidity, respectively. These values and the crop transpiration rate, $T_r(t)$, obtained from measurements of sap flow, leaf area and the leaf area index will then be used to calculate the greenhouse ventilation rate, and hence the air renewal rate, using equation (2.29)

The absolute humidity in equation (2.29) is evaluated from the from relationship as given by Jones (1992)

$$x = \frac{2165}{T} * e \tag{2.30}$$

Where x is the absolute humidity in kg m⁻³, T is air temperature and e is the actual vapour pressure (kPa).

The areas of the vent openings will be calculated by using the control algorithm of the ventilation control system and compared to a few values measured on selected days and at selected times of the day.

Leakage rates will be calculated as the average value of the ventilation rates when the greenhouse is closed.

2.5 Determination of Transpiration Rate

The transpiration rate in a greenhouse can be determined by using many methods which include gravimetric analysis, heat pulse velocity, time domain reflectometry, single leaf and whole plant infra-red gas exchange measurements and combination or energy balance methods. Fuchs (1973) examined these methods and separated them as to energy balance, mass and heat transport, and turbulent mixing, aerodynamic and the Bowen ratio method. The Penman Monteith can be used to evaluate transpiration rate in a greenhouse and it is formulated from the following basic principles.

Penman in 1948 combined the energy balance with mass transfer method and derived an equation to compute the evaporation from an open water surface from standard climatological records of sunshine, temperature, humidity and wind speed. This is the combination method which was further developed by many researchers and extended to cropped surfaces by introducing resistance factors. The resistances are aerodynamic resistance and surface resistance. The surface resistance, r_s describes the resistance of vapour flow through the stomata openings, total leaf area and soil surface. The aerodynamic resistance, r_a , describes the resistance from vegetation upward and involves friction from air flowing over the vegetative surface.

2.5.1 Penman-Monteith Method for determining transpiration

The Penman-Monteith form of the combination equation is as follows:

$$\lambda T_r(t) = \frac{\Delta (R_A - G) + \rho_a c_p \frac{(e_s - e_a)}{r_a}}{\Delta + \gamma \left(1 + \frac{r_s}{r_a}\right)}$$
(2.31)

Where R_A is the net radiation, G is the soil heat flux, (e_s-e_a) represents the vapour pressure deficit of the air, ρ_a is the mean air density at constant pressure, c_p is the specific heat of air, Δ represents the slope of the saturation vapour pressure temperature relationship, γ is the psychometric constant, and r_s and r_a are the (bulk) surface and aerodynamic resistances respectively.

Transpiration in a greenhouse is generally from the understanding that the rate of transpiration depends on the amount of radiative energy absorbed by the canopy, R_A , and on the vapour pressure deficit, $D=e_s(T)-e$, $e_s(T)$ being the saturated pressure vapour deficit (mb) at temperature T. The transpiration is expressed by means of Penman-Monteith formula (Monteith 1973) extended to the whole canopy considered as a "big leaf".

$$T(t)_{r} = \frac{\Delta}{\Delta + \gamma^{*}} \bullet \frac{R_{A}}{\lambda} + \frac{\rho_{a}c_{p}}{\lambda} \bullet \frac{r_{a}D}{\Delta + \gamma^{*}}$$
(2.32)

For the greenhouse with A_g covered with a fraction of vegetation P_v equation 2.31 becomes

$$T_{r}(t) = P_{v} A_{g} \left\{ \frac{R_{A}}{\lambda} \bullet \frac{\Delta}{\Delta + \gamma^{*}} + \frac{\rho c_{p}}{\lambda} \bullet \frac{D}{r_{b}(\Delta + \gamma^{*})} \right\}$$
(2.33)

Where $T_r(t)$ = transpiration rate (kg s⁻¹)

 P_{ν} is the fraction of the greenhouse occupied by the greenhouse

 A_g is the greenhouse floor area in m²

 λ = latent heat of vaporization (J kg⁻¹)

 $\rho_a c_p$ =volumetric heat capacity of air (J m⁻³ °C⁻¹)

The psychometric constant (kPa K⁻¹) is depend on pressure and latent heat of vaporization

$$\gamma = \frac{Pc_p}{0.622 \,\lambda} \tag{2.34}$$

and λ in kJ kg⁻¹ is given by the relationship below, where P is the pressure (kPa)

$$\lambda = 10000 \left(2501 - 2.361T \right) \tag{2.35}$$

$$P = 101.3 \left\lceil \frac{293 - 0.0065E_L}{293} \right\rceil^{5.26} \tag{2.36}$$

Where P is the barometric pressure in kPa, calculated from elevation (E_L) in m above sea level (Jensen, Burman and Allen, 1990)

 Δ = slope of the water vapour saturation curve

$$\Delta = \frac{4098e_s}{(T + 273.3)^2} \tag{2.37}$$

in (kPa ${}^{\circ}\text{C}^{-1}$) and e_s in kPa and T in ${}^{\circ}\text{C}$, the saturation vapour pressure of the air when the number of water molecules condensing equals the number evaporating from a flat surface of water with both the air and water vapour at some temperature, T. An equation for the saturation vapour pressure (e_s) over water at temperature, T, (${}^{\circ}\text{C}$) was given by (Tetens, 1930) as

$$e_s = 0.6108 \exp\left(\frac{17.27T}{(T+237.3)^2}\right)$$
 (2.38)

In greenhouse conditions, $r_a = 200 \text{ s m}^{-1}$ was chosen as a representative value of leaf aerodynamic resistance(Seginer,1984, Stanghellini, 1987; Baille et al , 1994c; Kittas et al ,1999)

2.5.2 Sap flow gauge method of determining transpiration rates

2.5.2.1Stem heat balance basics

The stem heat balance (SHB) requires a steady state and constant energy input from the heater strip inside the gauge body. Therefore the stem section must be insulated from changes in the environment. For the same reason, the gauge time constant is limited from five minutes to an hour, depending on the flow rate and the stem size. The Dynamax loggers have a power down mode so that power is saved at night and the stem is preserved from overheating. During the power down mode and at the transitions to power on, sap flow is not computed to maintain the accumulated flow accurately the measurement.

Figure 3.2 shows a stem section and the possible components of heat flux, assuming no heat storage. The heater surrounds the stem under test and is powered by a DC supply with a fixed amount of heat, Qh.

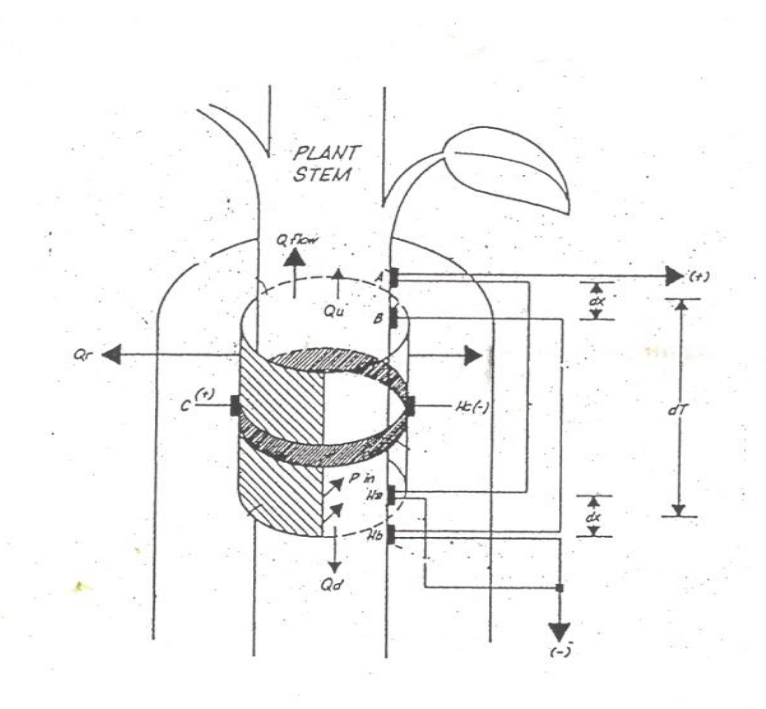


Figure 2. 2: showing the schematic of Dynagage for measuring Sap flow (adapted from Van Bavel, 1999)

Qh is equivalent to the power input to the stem from the heater, Pin, Qr is the radial heat conducted through the gauge to the ambient. Qv, is the vertical, or axial heat conduction through the stem and has two components, Qu and Qd. The heat convection carried by sap Qf, is determined by the measurement of Pin, Qu, Qd and Qr. Dividing the result by the specific heat of water and the sapflow temperature increase, the heat flux is converted directly to mass flow rate.

Energy Balance Equations

The energy balance is expressed as:

$$Pin = Qr + Qv + Qf \tag{2.39}$$

$$Pin = \frac{V^2}{R} \tag{2.40}$$

(From ohm's law)

Fourier's law describes the vertical conduction components as:

Where Qv = Qu + Qd

$$Qu = KstA \frac{dTu}{dx}$$

$$Qd = KstA \frac{dTd}{dx}$$
(2.41)

Where Kst is the thermal conductivity of the stem (W m⁻¹ K⁻¹), A is the stem cross-sectional area (m²), the temperature gradients are dTu/dx and dTd/dx (K m⁻¹), dx is the spacing between thermocouple junctions (m). One pair of the thermocouple is above the heater and one pair is below the heater as shown in Figure 2.3

There are two differentially wired thermocouples both measuring the rise in sap temperature. Channel AH measures the difference in temperature A-Ha (mV). Channel Hb measures the difference in temperature B-Hb (mV). Subtraction of these two signals we obtain

$$BH - AH = (B - Hb) - (A - Ha) = (B - A) + (Ha - Hb)$$
 (2.42)

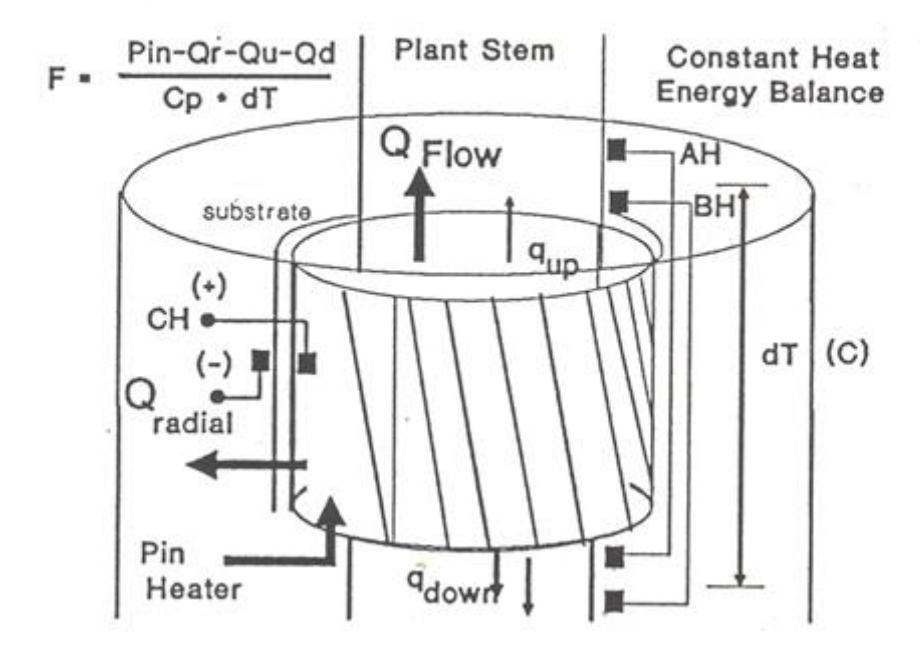


Figure 2.3: The diagram showing the connection of Dynagage for determination of transpiration (Van Bavel,1999)

The result gives the two components of axial heat conduction out of the stem section, Qu and Qd.

Since the distances, dx, separating the upper thermocouples pair and lower thermocouples pair are fixed by design for each particular gauge to the same value, the components of Qv are combined with a common denominator.

$$Qv = KstA \frac{BH - AH}{dx * 0.04mv / {}^{\circ}C}$$
 (2.43)

The factor 0.04 mV / $^{\circ}\text{C}$ convert the thermocouple differential signals to degrees Celsius. *Kst* values are given for varying stem conductivity, $0.42 \text{ W m}^{-1} \text{ K}^{-1}$ (woody stem), 0.54 (herbaceous) and 0.28 (hollow).

2.5.3 Sap flow Thermodynamics

After solving equation (1) for *Qf*, the flow rate per unit is calculated from equation for sap flow as described by Sakuratani (1981) and Baker- Van Bavel (1987). This equation takes the residual of the energy balance in watts, and converts it to a flow rate by dividing by the temperature increase of the sap and the heat capacity of water. Water is 99 % of the sap content and it is safe to assume the heat capacity, cp is constant to all stems.

$$F = \frac{Pin - Qv - Qr}{Cp * dT} (g / s)$$
(2.44)

In equation (2.39) the radial heat loss is computed in as:

$$Qr = Ksh * CH (2.45)$$

Ksh is the thermal conductance constant for particular gauge installation, Cp is the specific heat of water (4.186 J/g °C), and dT is the temperature increase of the sap.

The Ksh is determined using conditions when sap flow is zero, substituting into equation (2.45) we obtain

$$Qr = Ksh(CH) = Pin - Qv (2.46)$$

$$Ksh = \frac{Pin - Qv}{CH}(W/mV) \tag{2.47}$$

From measurements *Ksh* is obtained from zero flow, this is usually observed in pre dawn conditions between 0200 hrs and 0400 hrs.

The temperature increase of the sap, dT, is measured in mV by averaging the AH and BH signals, and then converted to degrees Celcius by dividing by the thermocouple temperature conversion constant as follows:

$$dT = \frac{(AH + BH)/2(mV)}{0.040mV/C}$$
 (2.48)

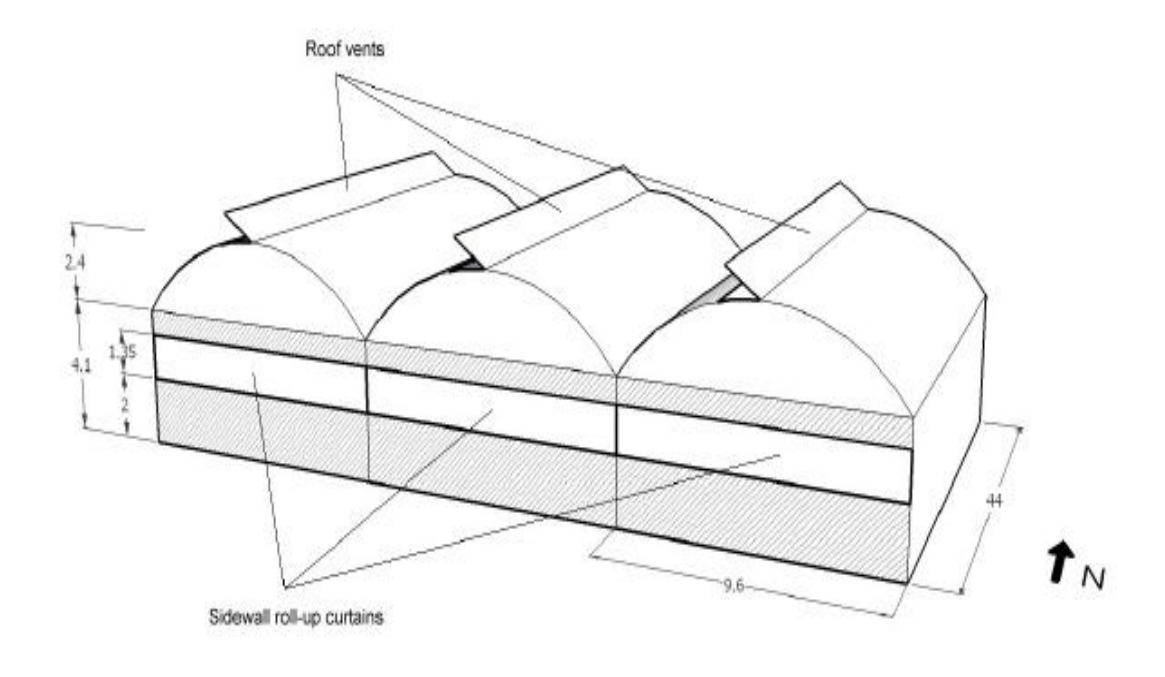
CHAPTER 3 MATERIALS AND METHODS

3.0 Experimental Sites and Location

The experiments were done in two phases in Harare, Zimbabwe at approximately 17,8 °S, 31.1 °E and at an altitude of approximately 1483 m. The first phase was instruments calibration that was done at the University of Zimbabwe in the Agricultural Meteorology laboratory, Physics Department. The second phase where two automatic weather stations were installed to measure weather parameters for the determination of ventilation rates and determining the microclimate and transpiration of crops inside the greenhouse were done at Floraline (Pvt) Ltd, that is about 5 km from the University of Zimbabwe.

3.1 Description of the greenhouse

All experiments were carried out in a 3-span commercial Azrom type greenhouse (Figure 3.1) at Floraline (Pvt) Ltd in Zimbabwe (17.8 °S, 31.1 °E, altitude 1500 m) between September 2009 and April 2010. Each span of the greenhouse measured 9.6 m wide and 44 m long, with ridge and gutter heights of 6.5 m and 4.1 m, respectively. The ridges were oriented north- south, the greenhouse total floor area was 1267 m² and the roof sloped at about 26° to the horizontal. The cladding material was 200 µm polyethylene film with terrestrial infrared and UV absorbing additives (Ganeiger Co, Israel). The roof vents (one in each span on the west side of the roof) were located along the whole length of the ridge and were 1.4 m, wide, with maximum opening angle of 34° with the roof. The polyethylene side could be rolled up from the 2 m above the floor to 3.35 m on the south wall and to 3.45 m on the north wall. The side and roof vents positions were controlled by an automated climate control system (NETAFIM NETAGROW Version 718.3 Priva, Israel) in response to ventilation temperatures (temperature at which ventilation begin) which are calculated on the basis of set ventilation temperatures and a number of influences, such as the measured inside air temperature and relative humidity and outside conditions.



(a)

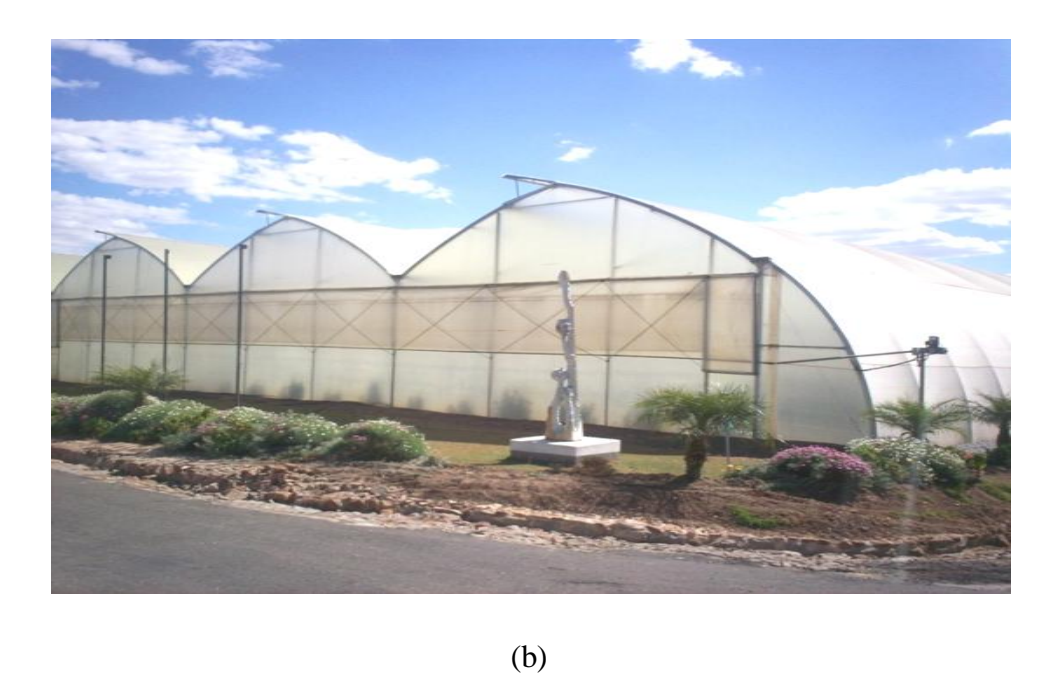


Figure 3. 1: showing (a) a schematic representation showing dimensions of the greenhouse (b) the commercial greenhouse at Floraline Pvt Ltd where the inside automatic weather station was installed

Two circulation fans, 0.75 m in diameter with a rated outflow of 16 00 m³/hr at zero static pressure (blowing N-S) were installed under each gutter at a height 3.5m and 12m from the north and south wall respectively. The plants were planted in the greenhouse included several cultivars of roses, grown in vermiculite medium in slightly raised 20 m x 0.45 m x 0.2 m containers which were watered through an automated drip system. The total area of the vegetation cover represented about 40 % of the total greenhouse floor. The containers were laid parallel to the gutters in twelve 20 m rows in each span. The greenhouse roses were a variety of cultivars which included commercial ones line Nectarine, Betsy, King Arthur, Upendo and Symphonica Rosso.

3.2 Climatic and Physiological measurements

Climatic data were measured by two Automatic weather stations (AWS), one inside the greenhouse and other outside. The external station was sited in an open space, which was clear of buildings and obstacles. The external AWS provided climatic data of air temperatures and humidity, incoming solar radiation, wind speed and direction, PAR (Photosynthetically active radiation) and diffuse radiation. The atmospheric conditions inside the greenhouse were continuously monitored by the AWS included air temperature and relative humidity, net radiation, incoming solar radiation and PAR above the canopy, leaf temperature and soil temperature.

3.2.1 Climatic measurements outside the greenhouse

The external automatic weather station Figure 3.2 was installed at an open space which was free from obstacles and buildings and was used to measure the following weather parameters:

The outside ambient air temperature and relative humidity were measured at 1.5 m above ground by means of temperature and humidity probe with serial number RHT 261 equipped with a capacitative relative humidity chip and a platinum resistance thermistor (model RH2nl,Delta T Devices, Cambridge,UK). The incoming solar radiation, PAR, wind speed and direction were measured at 2 m above ground.



Figure 3.2: The external weather station at Floraline Pvt Ltd

The solar radiation was measured by a pyranometer CM3 637 (model CM3, Kipp and Zonen, Delft, Netherlands). Wind speed was measured by a cup anemometer, with serial number 5525 (model A100L2, Delta T Devices, Cambridge, UK). The wind direction was measured by a wind vane serial number 7879 (model WD1, Delta T Devices, and Cambridge, UK). The diffuse radiation was measured using a pyranometer CM3 638 (model CM3, Kipp and Zonen, Delft, Netherlands) mounted on the shade ring. All outside measurements were automatically recorded on DL2e data logger (Delta T Devices, Cambridge, UK) every 5 seconds and averaged over 30 minutes.

3.2.1.1 Air Movement Sensors

A wind vane of type WD1 serial number 7879 was used to measure wind direction outside the greenhouse. A cup anemometer type AL1002 serial number 5525 was used to measure wind speed outside the greenhouse at Floraline Pvt Ltd and its measurement range is 0 to 300 m s⁻¹

3.2.1.2 CM3 pyranometer

The pyranometer CM3 is an instrument for measuring solar irradiance, it measures the solar radiation it receives from the whole hemisphere (180 degrees field of view), the energy flux is expressed in Watts per meter square, and the specified spectral density was given from the manufacturer as 0.3 to 3 microns.

3.2.2 Climatic measurements inside the greenhouse

The internal automatic weather station (AWS), Figure 3.3, was installed approximately at the centre of the greenhouse. The climatic parameters which were measured by the AWS included temperature and relative humidity at above soil heights of 0.4 m and 0.8 m (within the canopy) and on top of the canopy at 1.5 m and 2 m (just below the roof of the greenhouse) in order to investigate possible vertical gradients of air temperature and relative humidity. To test the homogeneity within the greenhouse, the relative humidity and temperature were measured at the centre of the greenhouse and at four other positions at 1.5 m above soil surface (see Figure 3.4) by temperature humidity probes (model HMP45C, Vaisala Inc,Boston,USA). The greenhouse internal air temperature and humidity were taken as the average of the five sensor positions. The net radiation, PAR, the incoming solar radiation were measured above the canopy and the soil temperature measured at two positions in the vermiculite medium. Leaf temperature was measured at six positions.

The leaf temperature was measured at six positions with fine chromel-alumel thermocouples, type K, 0.2 mm in diameter, attached to the lower side of leaf by paper clips.

The leaf temperature was taken as the average of six leaf temperatures. The vermiculite temperature at two positions were measured with by soil temperature probes (type STI, Delta T Devices, Cambridge, UK), and the average of the two readings was taken as vermiculite temperature.



Figure 3.3: The Automatic weather station (AWS) inside the greenhouse at Floraline Pvt Ltd.

The incoming solar radiation was measured with a tube solarimeter TSL29 (model TSL, Delta T Devices, Cambridge, UK). The net radiation was measured by the net radiometer equipped with coated Teflon coated sensor surfaces with serial number Q03194 (model Q7, Radiation and Energy Systems, Seattle, Washington, USA). The relative humidity and temperature were measured using the temperature humidity probes equipped with capacitive relative humidity chip and a platinum resistance thermistor (model RHT2nl, Delta T Devices, Cambridge, UK and HMP45C, Vaisala Inc., Boston, USA). The photo synthetically active radiation (400-70 µm) was measured using a quantum sensor with serial number PAR 639 (model PAR-LITE, Kipp and Zonen, Delft, Netherlands).

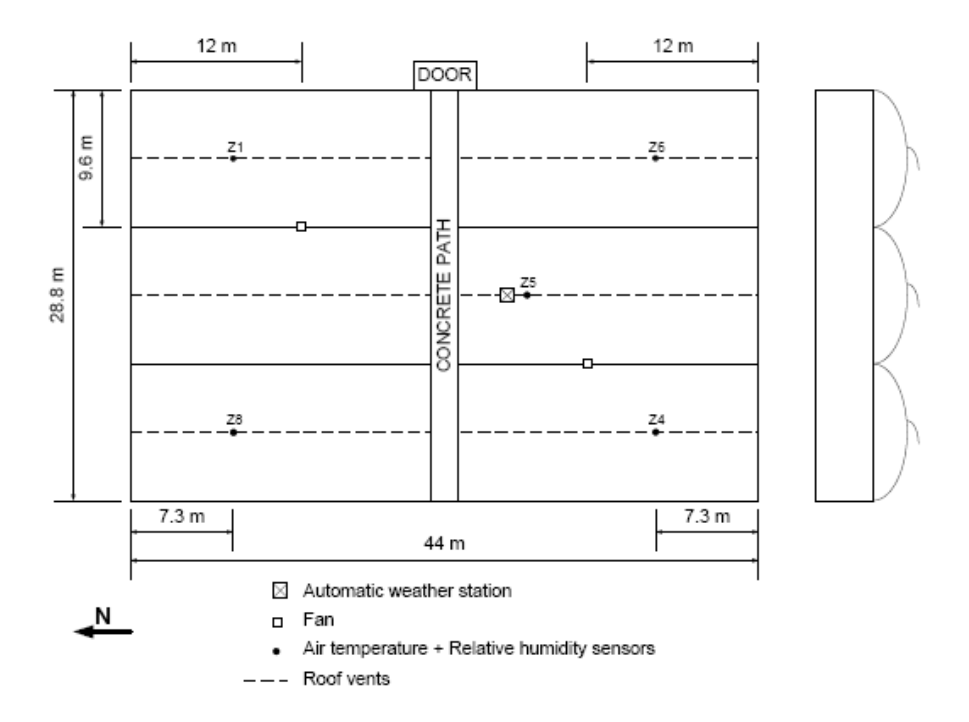


Figure 3. 4: The positions of air temperature and relative humidity sensors within the greenhouse

All measurements were automatically recorded by the two data loggers, one that was Campbell Scientific data logger CR23X (Campbell Scientific Ltd, Shepshed, UK) that recorded measurements every 5second and averaged over , and DL2e data logger (Delta T Devices, Cambridge, UK) which recorded every 5 seconds and averaged over 30 minutes.

3.2.2.1 Air temperature and relative humidity sensors

There were two types of temperature and humidity sensors which were used for field measurements, as already mentioned in section 3.2 for measuring air temperature and relative humidity and are described below.

3.2.2.1.1 Vaisala HMP45C Temperature and Relative Humidity Probe

The HMP45C Temperature and Relative Humidity Probe contain a Platinum Resistance Temperature detector (PRT) and a Vaisala HUMICAP[®] 180 capacitive relative humidity sensor. To prevent direct exposure from the solar radiation the probe was placed in a louvered radiation shield. The temperature sensor had manufacturer's specifications with a range stated as -40°C to 60 °C and its accuracy (± 0.2 %) at 20 °C and (± 0.4 °C) at -40 °C. The HUMICAP[®] 180's measurement range stated as 0 to 100 %, accuracy stated as ± 2 % in the range of 0 to 90 % relative humidity and ± 5 % in the range of 90 to 100 %. The temperature dependence of relative humidity is ± 0.05 % relative humidity per degree Celsius

3.2.2.1.2 RHT2nl Temperature and Relative Humidity Probe

The internal and outside air temperatures were measured using Delta T temperature humidity probes. The sensor head has a capacitance which is used for measuring the relative humidity. The head consist of a permeable 'cracked chromium oxide top plate evaporated onto a dielectric which is supported by a metal. The dielectric absorbs water according to the relative humidity of its environment. The sensor uses a 2 kohm hermetically sealed thermistor to measure temperature. The sensor is fitted inside a cylindrical louvred radiation screen, to shield the sensor from solar radiation and rain. The measurement range for relative humidity is 0-100 %, and operating temperature range -30 °C to 70 °C and accuracy of 2.5 % between 10 and 90 % relative humidity. In the range 90-100 % the error of the sensor is ± 5 %, the measurement range for the temperature sensor is -30 °C to 70°C, and its accuracy is ± 0.1 °C over a temperature range of 0-80 °C, ± 0.13 °C at -20 °C and additional error ± 0.17 °C from Delta-T Logger.

3.2.2.2 Net Radiometer

The REBS Net Radiometer was used measure only net radiation and it is sensitive to wavelength from 0.25 to $60 \mu m$. The net radiometer contains a high output 60 junction thermopile with a nominal resistance of 4 ohms and linear calibration. It generates an mV signal proportional to the net radiation level. The thermopile was mounted in a glass reinforced plastic frame with a built-

in level. Thermopile surfaces (or surfaces) and surrounding surfaces are flat black and the frame is black to reduce internal reflections within the instrument thus providing more uniform performance over reflective and non reflective surfaces. Sensor surfaces are protected from excessive convective cooling by hemispherical polyethylene windshields. Polyethylene is used for the windshield material because it is transparent to both long and short wave energy. The sensitivity of the Net Radiometer was stated from the manufacturer was given for positive values as 9.3W m⁻² mV⁻¹ and 11.6 W m⁻² for negative values and the standard cable required is the shielded 7.6 m long.

3.2.2.3 Tube Solarimeter

The tube solarimeter was used to measure average irradiance in (W m⁻²) falling above the canopy. The tube solarimeter is used where the distribution of radiant energy is not uniform particularly greenhouses. The tube solarimeter consists of an element which is painted black and white alternatively, the incident energy flux results in a small temperature difference between the black and white areas, and this is turned into a voltage output by a copper-constantan thermopile. The arrangement of the black and white areas which are alternated makes the radiation heats one side of the tube more than the other; the mean temperature difference between black and white surfaces is not affected. The element is protected by a Pyrex glass envelope which limits the response to visible and infra-red radiation in the waveband. The operating temperature range for tube solarimeter was given as -30 to 60 °C. The sensitivity of tube solarimeter was obtained from calibration using an in house radiation sensor CM11 pyranometer

3.2.2.4 Leaf temperature sensors

Two types of leaf temperature sensors were used, leaf temperature thermocouples and radiation thermometer



Figure 3. 5: The picture showing thermocouples attached to the underside of the leaf for measuring leaf temperature

3.2.2.4.1 Leaf temperature thermocouples

The thermocouples used were type K (chromel-alumel) with 200 μ m diameter. These were clipped onto the underside of the leaves by plastic paper clips as shown in Figure 3.5. The sensitivity curves for each type of thermocouple are pre-recorded in the data logger so that the thermocouple outputs were displayed in $^{\circ}$ C.

3.2.2.4.2 Radiation Thermometer

To check the reliability of thermocouples an infrared radiation thermometer was used on selected days. An infrared radiation thermometer utilizes the principle that: above absolute zero, all bodies emit electromagnetic radiation with wavelength and density which depends on temperature. The radiation emitted by a body also depends on its emissivity which is less than 1 for real bodies. The emissivity depends on the nature of the surface of the material, on the material itself and on the wavelength. If the emissivity is known, the temperature of the object can be determined by measuring the infrared radiation emitted by the object. Radiation thermometers are used to measure this kind of radiation, which includes a reflected component from the surrounding emitters. As the measurement is taken without the radiation thermometer

contact with the object, so there no distortion of the temperature field. Most radiation thermometers allow for the emissivity setting on the sensor to be set to a correct value applicable to the surface to be measured.

3.2.2.5 Soil temperature probe

The soil temperature was measured using the soil temperature probe (type STI, Delta T Devices, Cambridge, UK). The thermistor is designed for measuring temperatures in the range -40 °C to 56 °C. The major error component is the tolerance specification of the thermistor, which is ± 0.32 °C from -20 °C to 60 °C.

3.3 Instrument calibration

3.3.1 Introduction

All meteorological and agro-meteorological sensors lose accuracy with time after they have been manufactured. It is essential that before these sensors are taken for field use they are calibrated against standard ones and the accuracy limits should be within those stipulated by the manufacturer. Several experiments were carried out in the laboratory and on the roof top of Physics department at the University of Zimbabwe to obtain readings from the temperature-humidity sensors and radiation sensors. A considerable set of readings was obtained and analyzed in the computer excel spreadsheets to check on the accuracy of the sensors.

3.3.2 Calibration of temperature humidity sensors

The temperature humidity sensors calibrated were the Vaisala HMP45AC type and the Delta-T type, RHT2nl and were compared against the Walz system (Dew point system TS-2, Mess-unit and GegelTechnik). The temperature sensor were calibrated against the platinum resistance thermometer incorporated in the Walz system, the relative humidity sensor were calibrated

against the dew point generator. The calibrations were done on 7 to 8 September 2009. The results of the calibration of temperature sensors are shown in table 3.1

Table 3. 1 Calibration multipliers for temperature sensors

Sensor type	Reference number	Multiplier	$R^2(\%)$			
Vaisala HM45C	225	0.9616	99.56			
Vaisala HM45C	393	0.8430	94.16			
Vaisala HM45C	603	0.8461	97.57			
RHT2nl	261	1.0746	99.93			
RHT2nl	636	1.0869	99.62			

Table 3. 2: Calibration results for relative humidity sensors

Sensor type	Reference number	Multiplier	$R^2(\%)$	
Vaisala HM45C	225	0.8958	91.09	
Vaisala HM45C	393	0.8212	93.29	
Vaisala HM45C	603	0.843	94.16	
RHT2nl	261	1.277	99.32	
RHT2nl	636	1.643	98.95	

3.3.3 Calibration of radiation sensors

The radiation sensors were calibrated against CM11 pyranometer that has been designated as an in house standard. The calibration process was done from 20 August to 24 August 2009. The sensors were exposed and the mean output over consecutive 15 minute period was recorded for four consecutive days on the data logger. The ratio of the outputs in (W m⁻²) was evaluated. If the mean ratio (test sensor/standard sensor) at the highest values of solar radiation deviated from 1 by more than 5 % a new calibration was obtained as follows:

The output of the sensor in mV is plotted against the output of the standard (in W m⁻²). The gradient of the graph was used to correct the drift in the multiplier given by the manufacturer.

Table 3. 3: Calibration multipliers for the radiation sensors

Sensor type	Reference number	Multiplier
Tube solarimeter	TSL29	0.73637
PAR	380	1.1953
PAR	639	0.96084
Pyranometer	CM3-637	0.72253
Pyranometer	CM3-638	0.68183

3.4 Model Description

In order to evaluate the ventilation rates and the microclimate for different ventilation strategies a model GDGCM was used. The Gembloux Dynamic Greenhouse Climate Model (GDGCM), previously validated for a tomato crop in European greenhouses by Deltour et al. (1985), and Wang and Boulard (2000), was adapted, calibrated and validated to simulate the microclimate for a naturally ventilated Zimbabwean greenhouse containing a rose crop by Mashonjowa et al

(2008). The GDGCM is a multiple component semi- one dimensional dynamic greenhouse climate model which calculates eight heat balances for the following greenhouse layers which are the cover, air, vegetation, soil surface and four soil layers as shown in Figure 3.6 (Pieters, 1995; Pieters and Deltour, 1997). The model also takes into account a mass balance for the simulation of the relative humidity of the greenhouse air. The greenhouse microclimate is the result of heat and mass exchanges between these layers.

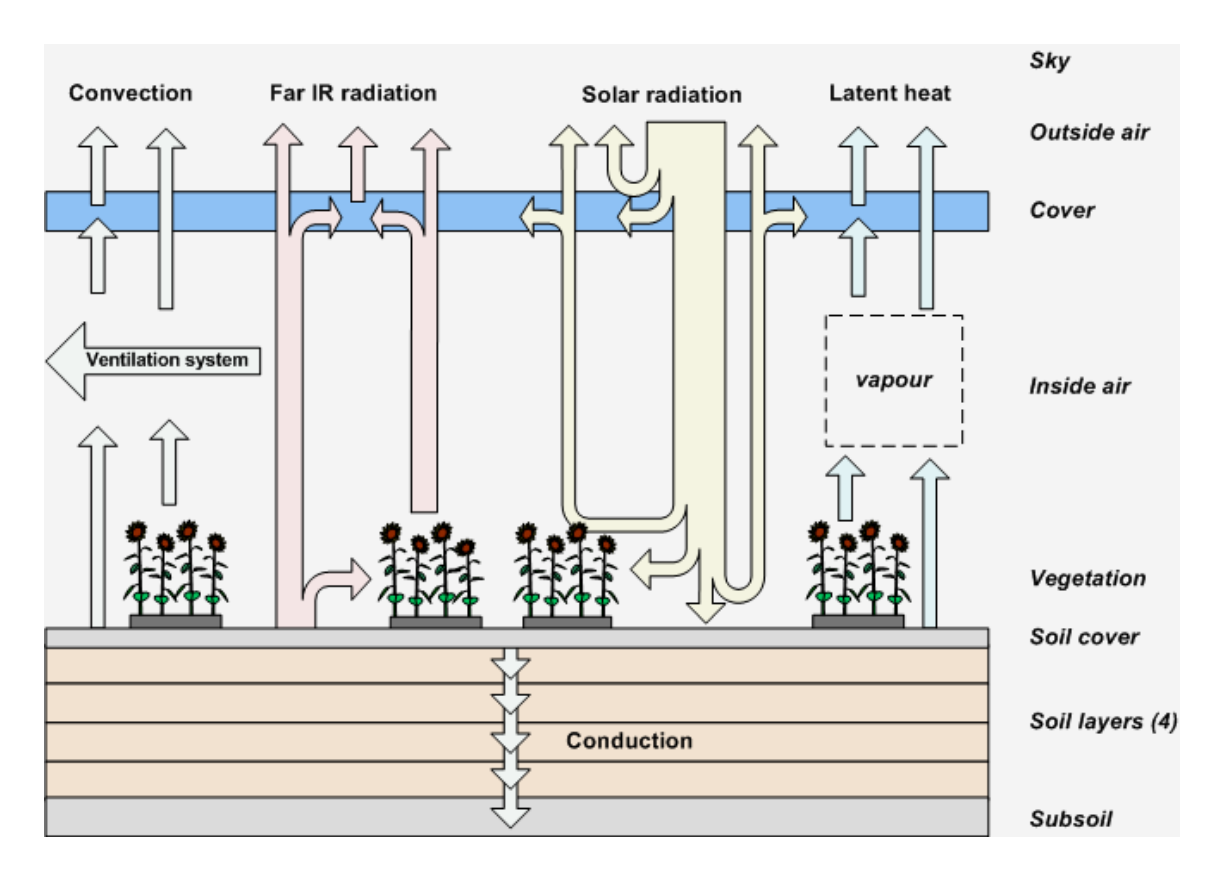


Figure 3.6: The schematic diagram showing the heat and mass exchanges between the greenhouse layers (after Pieters and Deltour, 1997)

The model assumes that the greenhouse layers are homogeneous and that all fluxes are vertical. Considering that the solar radiation absorptance of some layers depends on the angle of incidence, and thus on the sun's position in the sky, the model is not strictly one-dimensional, hence it is said to be semi-one dimensional. The interactions between these layers include heat transfers by conduction, convection, solar radiation and thermal radiation, as well as the latent

heat exchanges. The greenhouse cover forms a barrier between the interior and external climate and consequently its outer surface exchanges heat with the sky and outside air, while its inner surface exchanges heat with inside air, the vegetation and the soil surface. The greenhouse surfaces also exchanges mass with the inside and outside air through condensation of water vapour and latent heat is released in the process. The greenhouse air exchanges heat by convection with the cover, the vegetation, the soil and the heating system (if any) and through exchange with the outside air by advection and ventilation. The crop inside the greenhouse absorbs solar radiation; there is also the radiative exchange with the cover, soil and heating system, convective heat exchange with the greenhouse air and latent heat linked with the transpiration from crops and evaporation from the soil surface.

The soil gains and losses energy through the absorption of solar radiation, radiative exchange with the cover, the crop and heating system, convective exchange with the greenhouse air and conductive exchange with the underlying soil surfaces.

To allow the simulation of the effect of control procedures for regulating the inside air, several possibilities of heating and ventilating strategies, among which the user can choose, are built into the model (Bakker, et al, 1995; Pieters and Deltour, 1997; Hanan, 1998; Wang and Boulard, 2000).

$$c_c^1 \frac{dT_c}{dt} = \frac{A_{gr}}{A_c} \left(Q_{V(i,c)} - Q_{V(c,e)} + Q_{L(i,c)} + Q_{R(s,c)} + Q_{R(v,c)} - Q_{R(c,sky)} + Q_{S(c)} \right)$$
(3.1)

$$\rho_a.c_i.\frac{V}{A_{or}}\frac{dT_i}{dt} = Q_{V(s,i)} + Q_{V(v,i)} - Q_{V(i,c)} - Q_{V(i,e)} + Q_{HS}$$
(3.2)

$$c_{v}.m_{v}\frac{dT_{v}}{dt} = -Q_{V(v,i)} - Q_{L(v,i)} - Q_{R(v,c)} - Q_{R(v,sky)} + Q_{R(s,v)} + Q_{S(v)}$$
(3.3)

$$\rho_s c_s l_s \frac{dT_s}{dt} = -Q_{V(s,i)} - Q_{L(s,i)} - Q_{R(s,c)} - Q_{R(s,sky)} - Q_{R(s,v)} + Q_{S(s)} - Q_{D(sl)} = 0 \quad (3.4)$$

$$\rho_{s12}.c_{s12}.l_{s12}.\frac{dT_{s12}}{dt} = Q_{D(s1)} - Q_{D(s2)}$$
(3.5)

$$\rho_{s23}.c_{s23}.l_{s23}.\frac{dT_{s23}}{dt} = Q_{D(s2)} - Q_{D(s3)}$$
(3.6)

$$\rho_{s34}.c_{s34}.l_{34}.\frac{dT_{s34}}{dt} = Q_{D(s3)} - Q_{D(s4)}$$
(3.7)

$$\rho_{s4s}.c_{s4s}.l_{s4s}.\frac{dT_{s4s}}{dt} = Q_{D(s4)} - Q_{D(ss)}$$
(3.8)

$$h_{fg} \cdot \frac{V}{A_{gr}} \frac{dx_i}{dt} = Q_{L(s,i)} + Q_{L(v,i)} - Q_{L(i,c)} - Q_{L(i,e)}$$
(3.9)

Where all fluxes (in W m^{-2}) are expressed per unit horizontally projected greenhouse surface area and with:

A: surface area (m²)

c: specific heat capacity ($J kg^{-1} K^{-1}$)

 c_c^1 : specific heat capacity per unit area of the cover (J m⁻² K⁻¹)

 x_i : water vapour concentration of the greenhouse air (kg m⁻³)

 h_{fg} : latent neat of condensation of water (kJ kg⁻¹)

l: Thickness of layer (m)

 m_{ν} : vegetation mass per unit greenhouse surface area (kg m⁻²)

 $Q_{Z(x,y)}$: density of the net heat flux transferred from layer x to y in the way described by subscript $Z(W m^{-2})$

```
Q_{D(x)}: conductive heat flux through layer x (W m<sup>-2</sup>)
Q_{s(x)}: density of the solar flux absorbed by layer x (W m<sup>-2</sup>)
t: time
T: temperature (K or ^{\circ}C)
V : greenhouse volume (m<sup>3</sup>)
\rho: density (kg m<sup>-3</sup>)
And where the subscripts stand for:
V: convective
D: conductive
R : far infrared radiation
L: (phase change) latent heat
c: cover
e: external air
i: internal (greenhouse) air
s: soil surface
v: vegetation
gr: greenhouse
sky: sky (treated as a full radiator or blackbody)
HS: heating system
```

s1, s2, s3, s4, ss four soil layers and subsoil

s12, s23, s34, s4s: the four soil layer interfaces.

The detailed descriptions are given in Pieters and Deltour (1997). The energy and mass balance equations are solved for given input parameters (external air temperature and relative humidity, global solar radiant flux density, wind speed, cover transmittances and the climate control system settings for ventilation and heating) and boundary conditions (the subsoil) using an iterative procedure to obtain the temperatures of the different layers and humidity of the inside air

3.4.1 Ventilation sub-model

Ventilation is a very important tool for greenhouse climate control. Ventilation is mainly used for control of temperature, humidity and concentration of gases, such as CO_2 , in the greenhouse. An efficient ventilation performance is a crucial feature of a greenhouse in hot summer conditions. Besides cooling the greenhouse in summer, ventilation is important for transport of heat and mass in form of water vapour and other gases through replacement of inside air by outside air. Ventilation is characterized by the air renewal rate R_a , which expresses the ratio of the total volume of fresh air supplied in one hour to greenhouse volume. In the GDGCM the equations for convective heat flux density and latent heat flux density are written as:

$$Q_{V(ie)} = \frac{R_a}{3600} \cdot \frac{V}{A_{gr}} \rho_a \cdot c_{ha} \cdot (T_i - T_e)$$
(3.10)

$$Q_{L(ie)} = \frac{R_a}{3600} \cdot \frac{V}{A_{gr}} \cdot \rho_a \cdot h_{fg} \cdot (x_i - x_e)$$
(3.11)

Where R_a is the air renewal rate (hr⁻¹)

cha is the specific heat capacity of humid air,

 x_i and x_e are the absolute humidity of inside and outside air (kg m⁻³)

 T_i - T_e is the temperature difference between inside and outside air (K or $^{\circ}$ C) and all other terms are as defined in equation (Pieters and Deltour, 1997)

The air renewal rate for a greenhouse with continuous roof and side vents was described by an equation proposed by Kittas et al (1997) and also used by (Sbita et al., 1996; Demratti et al., 2001; Roy et al., 2002; Fatnassi et al., 2003):

$$R_{a} = \left(\frac{3600}{V}\right) C_{D} \left[\left(\frac{A_{r} A_{s}}{\sqrt{\left(A_{r}^{2} + A_{s}^{2}\right)}}\right)^{2} 2g \cdot h_{c} \cdot \left(\frac{T_{i-} T_{e}}{T_{e}}\right) + \left(\frac{A_{T}}{2}\right)^{2} C_{w} u_{e}^{2} \right]^{0.5}$$
(3.12)

Where V is the greenhouse volume (m^3)

 $C_{\rm D}$ is referred to as the discharge coefficient for the openings

 $T_{\rm i}$ and $T_{\rm e}$ are the internal air and the external air temperature (K), respectively

 A_r is the total opening area of the roof vents (m²)

 A_s is the total opening of side vents (m²)

 $A_{\rm T}$ is the total opening area of all vents (= $A_{\rm r} + A_{\rm s}$) (m²)

g is the acceleration due to gravity (= 9.81 m s^{-1})

 $C_{\rm w}$ is the global wind coefficient

 $u_{\rm e}$ is the external wind speed at height of 2 m (m s⁻¹)

This equation applies when $T_i > T_e$, if $T_i < T_e$, T_i in the denominator is replaced by T_e and $(T_i - T_e)$ in the numerator is replaced by $(T_e - T_i)$ (ASHRAE, 2005).

If the greenhouse is closed (so that $A_T\!=\!0$) or if the temperature difference between interior and exterior air is zero and wind speed is zero (as may the case at night or under an overcast sky) the ventilation rate is replaced by the leakage rate, R_{a0} , so that

$$R_a = R_{a0}$$

For the determination of the ventilation set point temperature of the inside air, four periods were considered which are to the sunrise and sunset periods. These periods are defined as:

$$H_{p1} = H_{srise} + \Delta t_{p1} \tag{3.13}$$

$$H_{p2} = H_{srise} + \Delta t_{p2} \tag{3.14}$$

$$H_{p3} = H_{srise} + \Delta t_{p3} \tag{3.15}$$

$$H_{p4} = H_{sset} + \Delta t_{p4} \tag{3.16}$$

$$H_{p5} = H_{sset} + \Delta t_{p5} \tag{3.17}$$

$$H_{p6} = H_{sset} + \Delta t_{p6} \tag{3.18}$$

With *H* representing hour of day (hr)

 Δt is the time interval between the beginning of the period and the moment of sunrise or sunset (hr) and the subscripts p1,p2,p3,p4,p5 and p6 stand for the six ventilation periods and where srise and sset stand for sunrise and sunset respectively. The table 3.4 gives parameters of the ventilation.

Table 3. 4: Parameters of the ventilation system. T_{set} represents the set ventilation temperature per period , Y represents the humidity dependent decrease (+) or increase (-) in ventilation temperature at a humidity level, X.

Period		1			2			3			4			5			6	
Summe -April)	er (Sept	ember																
Start (hr:mir	time	5:12			7:11			16:00			16:27			19:37			3:30	
Tsctv (°C)	10			23			20			15			12				
	X		Y	X		Y	X		Y	X		Y	X		Y	X		Y
1	30		5	40		4	30		3	30		4	30		5	30		4
2	40		0	50		3	40		0	40		3	40		0	40		3
3	50		-6	60		-5	50		-5	50		-6	50		-4	50		-5
4	60		-6	90		-6	70		-6	70		-8	60		-6	70		-6

3.4.2 Ventilation Rate Determination

The ventilation rates were determined for the two different ventilation strategies which were:

- 1. roof vents only
- 2. both roof and side vents

The ventilation rates determined using the water vapour balance which uses water vapour as the tracer (Boulard and Draoui, 1995, Mashonjowa et al 2008, Kittas et al., 2002., Harmanto et al, 2006 and Teitel., 2008) during the period of 1 September 2007- 30 March 2008, summer period

Mashonjowa et al.(2007b). Assuming perfect mixing of water vapour in the volume of the greenhouse and that evaporation from the soil and other medium is negligible justified by the presence of a plastic mulch on the soil surface and the cover by the vegetation, the greenhouse ventilation rate, G can be calculated from the mass balance of water vapour of the greenhouse equation 2.29.

Measured values of air temperature and relative humidity outside and inside the greenhouse (at 30 minute time steps) were used to calculate the outside and inside greenhouse air absolute humidity, respectively. These values and crop transpiration rate, T(t), obtained from Penman Monteith method equation (2.31) up scaled to the whole crop canopy, leaf area and the leaf area index were then used to calculate the greenhouse ventilation rate, using equation (2.29), and hence the air renewal rate from the relationship in equation 2.26.

The transpiration from the crop canopy is obtained by multiplying equation (2.32) with the fraction occupied by vegetation and green house floor area

3.5 Modeling the transpiration

Crop transpiration rate is the main component of the greenhouse air water balance; hence its estimation is critical for climate control. The model of the transpiration rate in the GDGCM was modified by considering the climatic dependence of leaf stomatal resistance (r_1) and rose canopy surface resistance (r_s) to water vapour transfer. In the GDGCM, the transpiration flux density, $Q_{L(vi)}$, is given by:

$$Q_{L(vi)} = h_{fg} . h_{Tr} . (x_s (T_V) - x_i)$$
(3.19)

Where h_{fg} is the latent heat of condensation of water (Jkg⁻¹), $x_s(T_v)$ is the saturation water vapour concentration at the temperature of the vegetation, T_v (kg m⁻³), x_i is the water vapour concentration of the surrounding air (kg m⁻³), and h_{Tr} is the mass transfer coefficient (m s⁻¹) defined for hypostomatal leaves as (Pieters and Deltour, 1997):

$$h_{Tr}' = \frac{LAI_g}{h_{fg}} \cdot \left(h_{P1} + h_{fg} \cdot \frac{1}{\frac{h_{fg}}{h_{P2}} + r_s} \right)$$
(3.20)

Where LAI_g is the leaf area index expressed per unit greenhouse floor area, obtained as the product of the crop leaf area index, LAI (expressed per unit cultivated greenhouse floor area) and the cultivated fraction of the greenhouse floor area, r_s is the canopy resistance to water vapour transfer and h_{PI} and h_{P2} are the phase change heat transfer coefficients for the upper and lower faces of the leaves, respectively, as defined as:

$$h_P = h_{fg}.Sh.\frac{D}{d} \tag{3.21}$$

Where Sh is the Sherwood number (a non-dimensional parameter whose value depends on the flow conditions and the properties of the air), D is the molecular diffusion coefficient of water vapour in air (m² s⁻¹) and d is the characteristic dimension (m).

The results of several researchers (Baille et al., 1994a; Baille et al., 1994b; Baille et al., 1994c; Papadakis et al., 1994; Kittas et al., 1999) suggest that the climatic dependence of the crop stomatal resistance to water vapour transfer can be described by a "reduced" Jarvis type model. The leaf stomatal resistance, r_l (sm⁻¹) can thus be predicted as a function of the solar irradiance incident on the crop, QS_{int} (W m⁻²), the leaf-air vapour pressure deficit, VPD (kPa), the air temperature, T_a (°C), and CO_2 concentration:

$$r_l = r_l \cdot f_1(QS_{int}) \cdot f_2 \cdot (VPD) \cdot f_3 \cdot (T_a) \cdot f_4(CO_2)$$
 (3.22)

 f_1, f_2, f_3 and f_4 are dimensionless functions, quantifying the relative increase of stomatal resistance whenever one of the parameters is limiting the exchange rate (Jarvis, 1985). For ambient CO₂, and well watered plants, the effect of temperature on r_l may be assumed to be very small (Pasian and Lieth, 1989), so that r_l may be considered as dependent on global radiation above canopy and vapour pressure deficit (Baille et., 1994a; Baille et al.,1994b; Baille et al., 1994c; Papadakis et al. 1994; Kittas et al., 1999). If we consider that the surface or canopy

resistance includes most of the characteristics of the leaf stomatal behaviour, we can normalize equation 3.20 by the leaf area index, LAI_g (expressed per unit greenhouse floor area), to obtain the canopy resistance, $r_{s:}$

$$r_s = \frac{r_l}{LAI_g} = r_{s,\text{min}}.f_1(QS_{\text{int}}).f_2(VPD)$$
 (3. 23)

Where $r_{s,\min} \left(= \frac{r_{l\min}}{LAI_g} \right)$ is the minimum possible value for r_s in conditions of optimal water supply and environment.

In this study the relationship for greenhouse roses suggested by Baille et al (1994c) was used:

$$r_{s} = \frac{r_{l \min}}{LAI_{g}} \left(\frac{a + QS_{\text{int}}}{b + QS_{\text{int}}} \right) \left\{ 1 + \exp[c(VPD - VPD_{m})] \right\}$$
(3.24)

Where $VPD_{\rm m}$ is the vapour pressure deficit of the air at which the resistance is minimal and was considered to be 2.5 kPa and $r_{l,\rm min}$ was chosen to be 100 s m⁻¹ (Baille et al., 1994c; Kittas et al., 1999). The parameters a, b and c were determined through the calibration process using Sigma plot by substituting all weather parameters in the stomatal model and comparing it with measured stomatal resistance from several cultivars using dynamic diffusion porometer (model AP4, Delta T Devices, Cambridge, UK). The stomatal resistance measured for the purposes of calibration and validation of stomatal sub model required the leaf area index measurements. The leaf area index was measured using the non destructive method using sun scan ceptometer on selected days.

3.6 Simulation of the GDGCM using TRNSYS

The TRNSYS was used for the running of the GDGCM. The TRNSYS is a transient system simulation program which was developed at the Solar Energy of the University of Wisconsin-Madison. The simulation program is designed for the simulation and analysis of time dependent

phenomena, particularly for the domain of heat and mass transfer. The advantage of using this program is because of its modularity and it is also flexible and user friendly and user defined modules can easily be added using FORTRAN language as was the case in this study. The user defined module which was manipulated was Type 72 the ventilation Flux density, the ventilation mode which was selected for the greenhouse with both roof and side vents was ventilation mode 11 which was used by Kittas (1997) also applied by Ashrae (2005). Simulation for the greenhouse with roof vents only was ventilation mode5, the ventilation model proposed by Fernandez and Bailey (1992) for greenhouse equipped with roof vents only and validated for European climates, the model was calibrated and validated before use. The description of the model for the roof vents only configuration is outlined below:

$$Ra = 3600 * Ue * Pwin * \left(\frac{A_{t}}{V}\right) * \left(C_{1}Alfwin + C_{2}\right)$$
(3.25)

Where Ra is the air renewal rate (hr⁻¹), Ue is the external wind speed.

Pwin area of the ventilation window, expressed as fraction of the total cover area [-], Alfwin the ventilation window opening angle [°].

In this case where the only the roof vents are considered, the total area of the vent opening is Ar (the roof vents area) as the area of side vent opening As = 0.

$$Pwin = \frac{Ar}{Ac} \tag{3.26}$$

Where Ac is the total cover area [m], which is evaluated from the following relationship:

$$Ac = 2 * NRSPANS * dc * GRLEN$$
(3.27)

Where NRSPANS represents number of spans the greenhouse has, dc is the characteristic length of the greenhouse [m], and GRLEN is the greenhouse length of the greenhouse [m].

The characteristic length was determined from the following relationship:

$$dc = \sqrt{\frac{GRRWID}{2*NRSPANS}}^2 + (EAVES - RIDGE)^2$$
 (3.28)

GRWID is the greenhouse width [m]

EAVES is the height to the eaves [m]

RIDGE is the height to the ridge [m]

The coefficients were determined by sigma plot by fitting experimental data.

3.6.1 Structure of a TRNSYS Simulation Program

The body of the program consist of several modules, which are all described in separate units referring to one component of the system to be simulated. Since the behaviours of two components or units may be described by the same mathematical expressions and thus by the same FORTRAN subroutine, a distinction must be made between the units (referring to one component of the model) and the types. A type refers to a subroutine, which can be used for the description of several units, thus a type can be used more than once in a given simulation,

In the main body of the program, there are still many other subroutines and also the main program. A detailed description of how these subroutines and the main program can be found in Klein et al.(1998). In TRNSYS system there are 73 Types of Subroutines. Each of the types needs inputs and generates outputs. Since the output of one unit can be output of another unit, the information flow between the several units must be specified. The file with the information flow is called a deck file; a deck file has a DEK extension. The deck file governs the whole simulation. The TRNSYS requires time dependent input data for time- dependent simulations. TRNSYS output simulations results in output types, the simulation results can be converted to excel for data analysis. The output from the simulation was obtained from files with .out

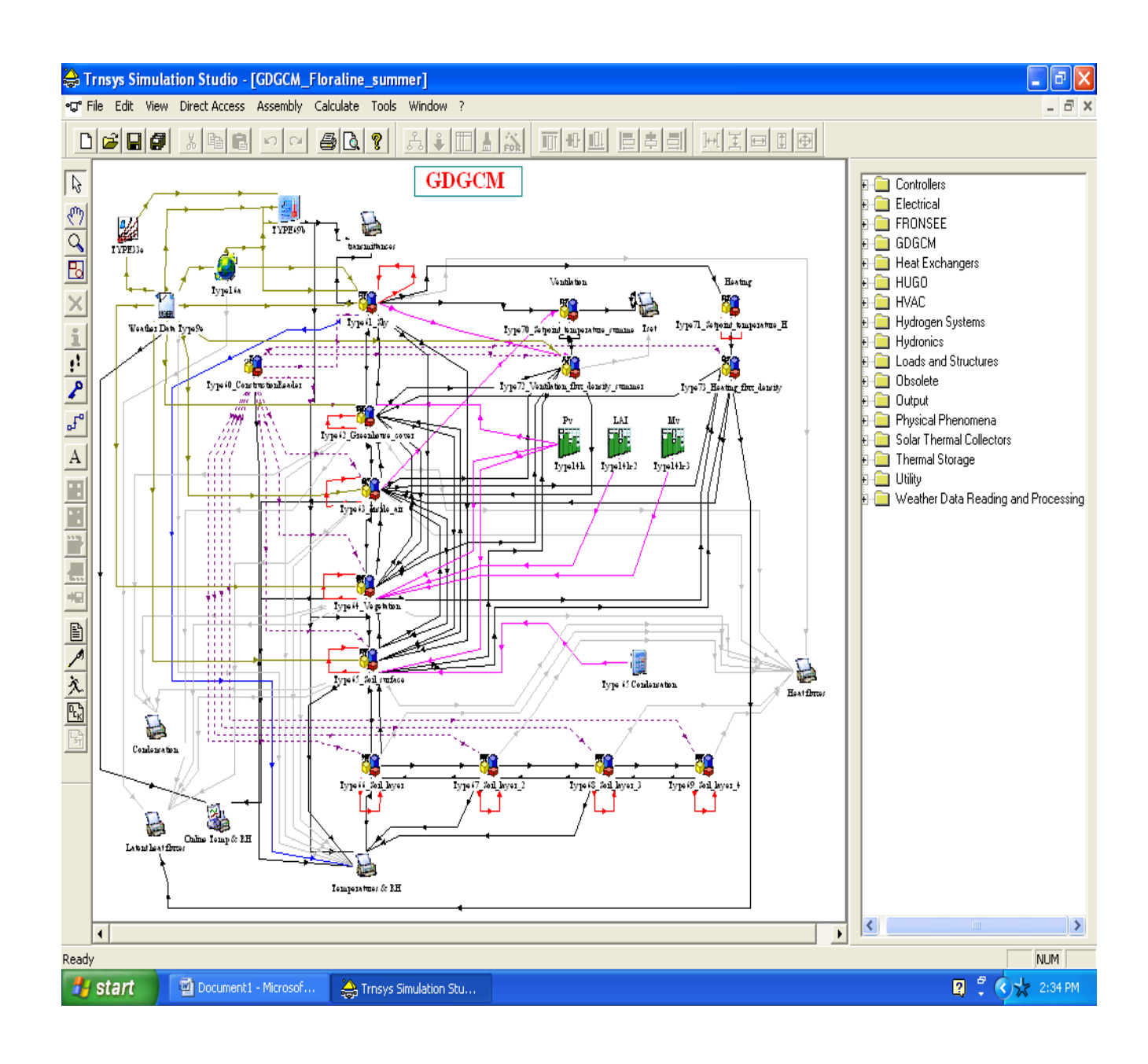


Figure 3.7: The GDGCM running in TRNSYS program

extension. For the modelled ventilation rates the outputs which were selected are the ventilation. out,

Figure 3.7 shows the GDGCM model operating in TRNSYS 16 program, with all 73 sub models. To run the model F8 was pressed and the model simulating microclimate for the whole summer period. The model was run using the outside weather parameters solar radiation, wind speed, air temperature, photo synthetically active radiation (PAR), diffuse radiation, relative humidity, wind speed and direction. The historical data (Mashonjowa et al,2010a) was used to consider the whole summer period from September 2007 – April2008.

3.6.2 Calibration of the ventilation sub model

To calibrate the ventilation sub model the coefficients Cd and Cw were determined statistically using a statistical package Sigma plot by fitting historical data (Mashonjowa et al 2008). The observed ventilation rate obtained from the water vapour balance method was compared with other meteorological parameters from the two automatic weather stations in equation (3.12). The values of Cd and Cw obtained were then used to evaluate the ventilation rate for the different ventilation regimes with the use of an automated climate control system (NETAFIM NETAGROW Version 718.3 Priva, Israel) which controls the positions of roof and side vents.

Table 3.5: Values for the Gembloux Dynamic Greenhouse Climate Model parameters (after Pieters, 1996; Pieters and Deltour, 1997; Pollet and Pieters, 2000)

Soil Characteristics	First Layer	Secon	ıd Layer	Third	Layer	Fourth	h layer
Thermal conductivity [W m	¹ K ⁻¹]	0.70	-	1.95	-	1.9	1.9
Layer thickness [m]	0.05		0.15		0.3	0.7	
Density of soil layer [kg m ⁻³]						1600	1650
Heat capacity of soil layer [k	xJ kg ⁻¹ K ⁻¹]	1.35		1.25		1.25	1.20
Subsoil temperature [°C]				:	18.5		
Thickness of the subsoil layer	er			:	8.8		
Floor							
Floor reflectance for solar ra	diation [-]			:	0.85		
Floor emittance for far infrai	ed radiation [-]		:	0.95		
Characteristic length of gree	nhouse floor [r	n]		:	1001		
Cover Characteristics							
Material: 200µm Diffused P	olyethylene (D	PE)					
Outer cover emittance for far	•			:	0.79		
Inner cover emittance for far	infrared radiat	ion [-]		:	0.79		
Transmittance for far infrare	d radiation [-]			:	0.18		
Cover absorptance for diffus	e radiation [-]			:	0.04		
Dry cover transmittance for	diffuse solar ra	diation	[-]	:	0.69		
Wet cover transmittance for	diffuse solar ra	diation	[-]	:	0.55		
Frame transmittance for sola	r radiation [-]			:	0.95		
Dry cover heat capacity per	unit area [kJm ⁻	${}^{2}K^{-1}$]		:	0.725		
Maximum condensation wat]	:	0.12		
Transmittance and reflectar	nces (beam rad	liation)	at 0, 15,	30,45,	60,75 a	nd 90 ° [[-]
Dry cover transmittance:	0.75	0.74	0.72	0.69	0.63	0.46	0.00
Wet cover transmittance:	0.61	0.61	0.59	0.59	0.57	0.46	0.00
Dry cover reflectance:	0.21	0.22	0.25	0.27	0.33	0.50	1.00
Wet cover reflectance:	0.35	0.35	0.37	0.37	0.39	0.50	1.00
Vegetation Characteristics							
Reflectance for solar radiation	on [-]			:	0.16		
Canopy attenuation coefficie	ent [-]			:	0.61		
Characteristic length of the l	eaves[m]			:	0.06		
Emittance for far infrared rad				:	0.95		
Specific Heat Capacity [kJkg		:	4.18				
Air characteristics							
Humid air density [kgm ⁻³]				:	1.25		
			:	I.256			
Volumetric Heat Capacity [k		1 1			2427		
		K^{-1}		:	2437		
Volumetric Heat Capacity [k		[-1 K-1]		:	0.30		

3.6.3 Validation of the greenhouse Ventilation Sub model

The ventilation determination from both roof and side vents, which were controlled by an automated system (NETAFIM NETAGROW Version 718.3, Priva, Israel) in response to a calculated ventilation temperature (T_{setv}), the temperature above which ventilation is initiated. T_{setv} was calculated as a function of time of day on the basis of set ventilation temperatures and a number of influences, which included the measured inside air relative humidity, outside conditions and the ventilation temperature at the previous time step. The vents were controlled by the ventilation temperature to be realized, the climate control system uses the calculated ventilation temperature to calculate the percentage opening of the vent as function of weather conditions, including the difference between T_{setv} and outside air temperature, wind speed, the radiation flux density and minimum and maximum vent limitations.

To validate the model the observed air renewal rate determined by the water vapour method was compared with the air renewal rate from the model with the parameters from the calibration process.



a)



b)

Figure 3. 8:(a) The AP4 Diffusion porometer for measuring stomatal resistance and (b)the radiation thermometer measuring leaf temperature

Fig 3.6 shows the AP4 diffusion porometer which was used for measuring stomatal resistance on selected days at Floraline Pvt Ltd. The stomatal resistance was used for calibration and validation of stomatal sub model and transpiration determination from Penman- Monteith method.

The stomatal resistance was measured by the dynamic AP4 diffusion porometer (model AP4, Delta T Devices, Cambridge, UK). The stomatal resistance was taken as average of stomatal resistance from 5 different cultivars, the stomatal resistance of two randomly selected leaves of each cultivar were measured every 30minutes. The stomatal resistances will the have to be up scaled to the whole canopy by considering the Leaf Area Index (LAI). This measured stomatal resistance of the canopy was then used to calibrate and validate the stomatal resistance model equation (3.22) by comparing the measured stomatal resistance and measured weather parameters.

3.7 Measurements of Leaf Area Index (LAI)

The leaf area index was determined by two methods which are described in this section.

The sunscan ceptometer (model SS1_TM, Delta T Devices, Cambridge, UK) was used to estimate non destructively the leaf are index which is the ratio of the lead area to the total ground area. A sunscan canopy analysis system is a portable instrument for measuring the light of PAR in plant canopies. It measures the interception of solar radiation by canopy, enabling estimates of canopy leaf area index (LAI). Leaf area index was calculated using Beer's law from measurements of the incident light (I_o) and transmitted light (I) which gives the following relationship with LAI.

$$I = I_o e^{-kLAI} \tag{3.29}$$

Where k is an extinction coefficient depending on the angle of incident and direction of the beam (k=1) for entirely horizontal leaves). The leaf area index (LAI, m^2 leaf m^{-2} ground) was also estimated from leaf length measurements (L, m), using the relationship $S = 0.26L^2$ linking the area S (m^2) of leaflet to L (Katsoulas et al 2001). Measurements were done once a week during

the measurement period. During the period of measurements, the leaf area index LAI referring to the ground area covered by the crop averaged 2.1 for the whole summer period.

The significance of the leaf area index was for scaling up the transpiration rates determined by the Penman- Monteith formula to the whole crop canopy and also was used in the determination of the stomatal model both during calibration and validation.

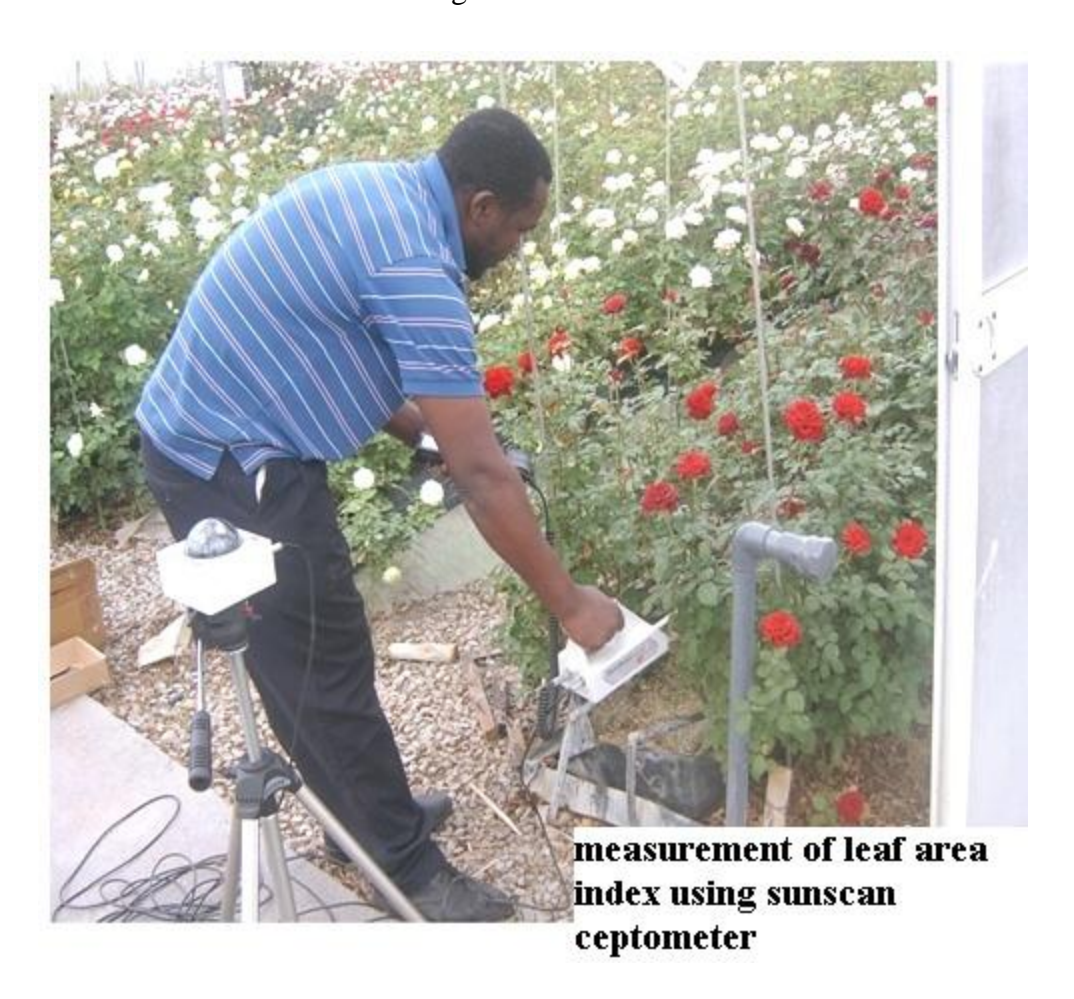


Figure 3. 9: Showing the set up for the sunscan ceptometer for measuring the leaf area index.

Figure 3.9 shows the set up which was used for measuring leaf area index on selected days in summer and the results were compared with the theoretical model by Katsoulas et al, 2001.

CHAPTER 4: RESULTS AND DISCUSSIONS

4.1 Greenhouse microclimate

This section shows the microclimate of the greenhouse measured by the automatic weather station inside the greenhouse at Floraline Pvt Ltd with the ventilation controlled by the automatic climate control systems which responded to set ventilation temperatures, this ventilation incorporated both roof and side vents. Figure 4.1 shows the diurnal variation of relative humidity and air temperature inside the greenhouse on 14 December 2009.

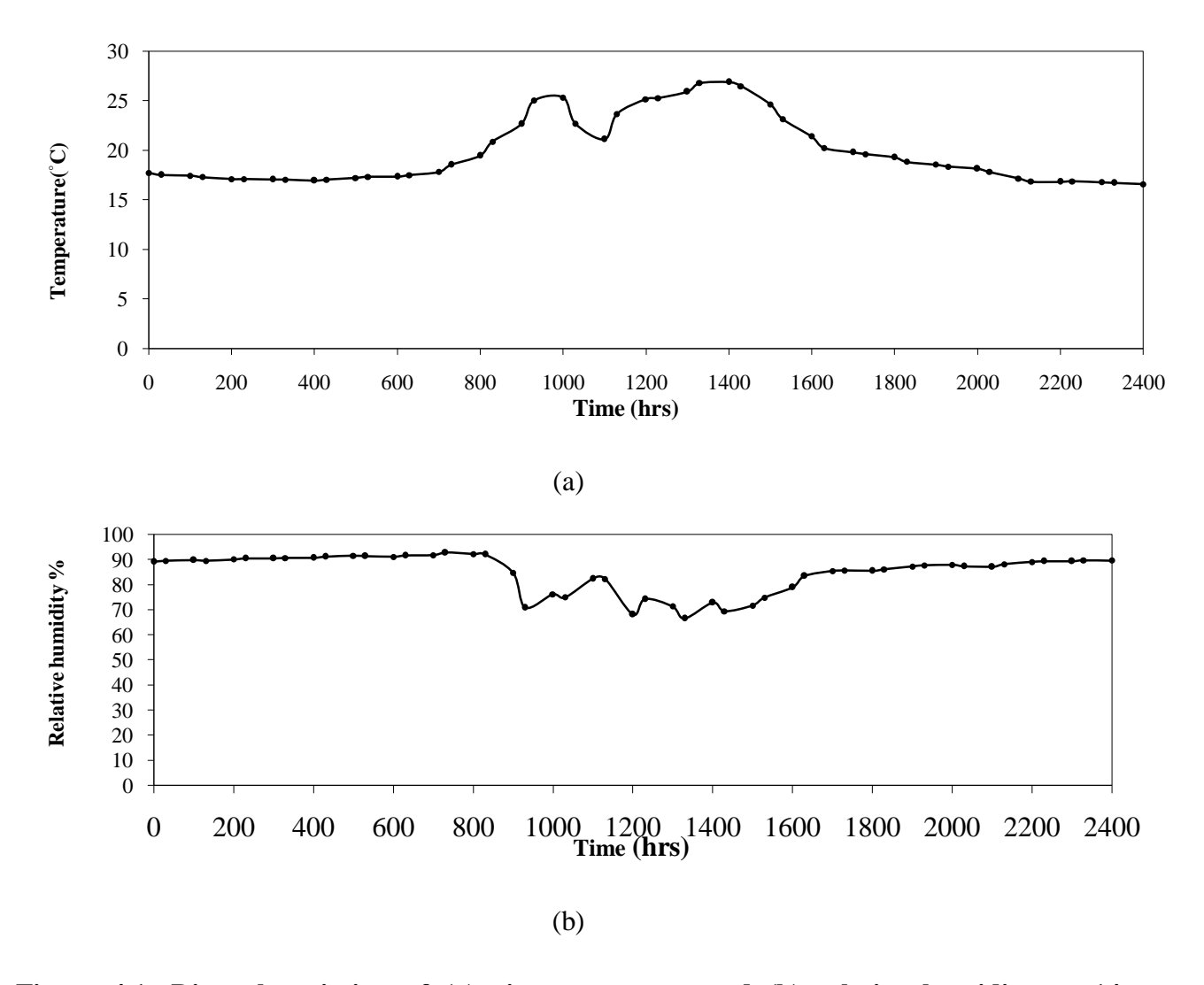


Figure 4.1: Diurnal variation of (a) air temperature and (b) relative humidity on 14 December 2009

Figure 4.1shows that during the night, the greenhouse internal air temperatures were low, and the corresponding relative humidity were high. To prevent condensation the vents should be opened to remove excess humidity. Figure 4.1 (a) shows that during the night, the temperature was almost constant around 17 °C from midnight to 0700 hrs. At 0700 hrs the temperature rose sharply from 17.82 °C to 25.03 °C at 0930 hrs. At 1000 hrs temperature dropped temporarily may be due to partial cloud cover to 21.03 °C at 1100 hrs, before it started rising again until a maximum temperature of 26.9 °C at 1400 hrs. The temperature decreased sharply with time from 1400 hrs until sunset. After sunset the temperature continued to decrease to minimum constant value of 16.85°C. Figure4.1 (b) shows the relative humidity was high during the night above 90 % from midnight to 0700 hrs. The relative humidity dropped sharply as soon as sunrise and was low and oscillates about 70 % for most part of the day. On this particular day the lowest relative temperature was observed to be 66.5% at 1330hrs.

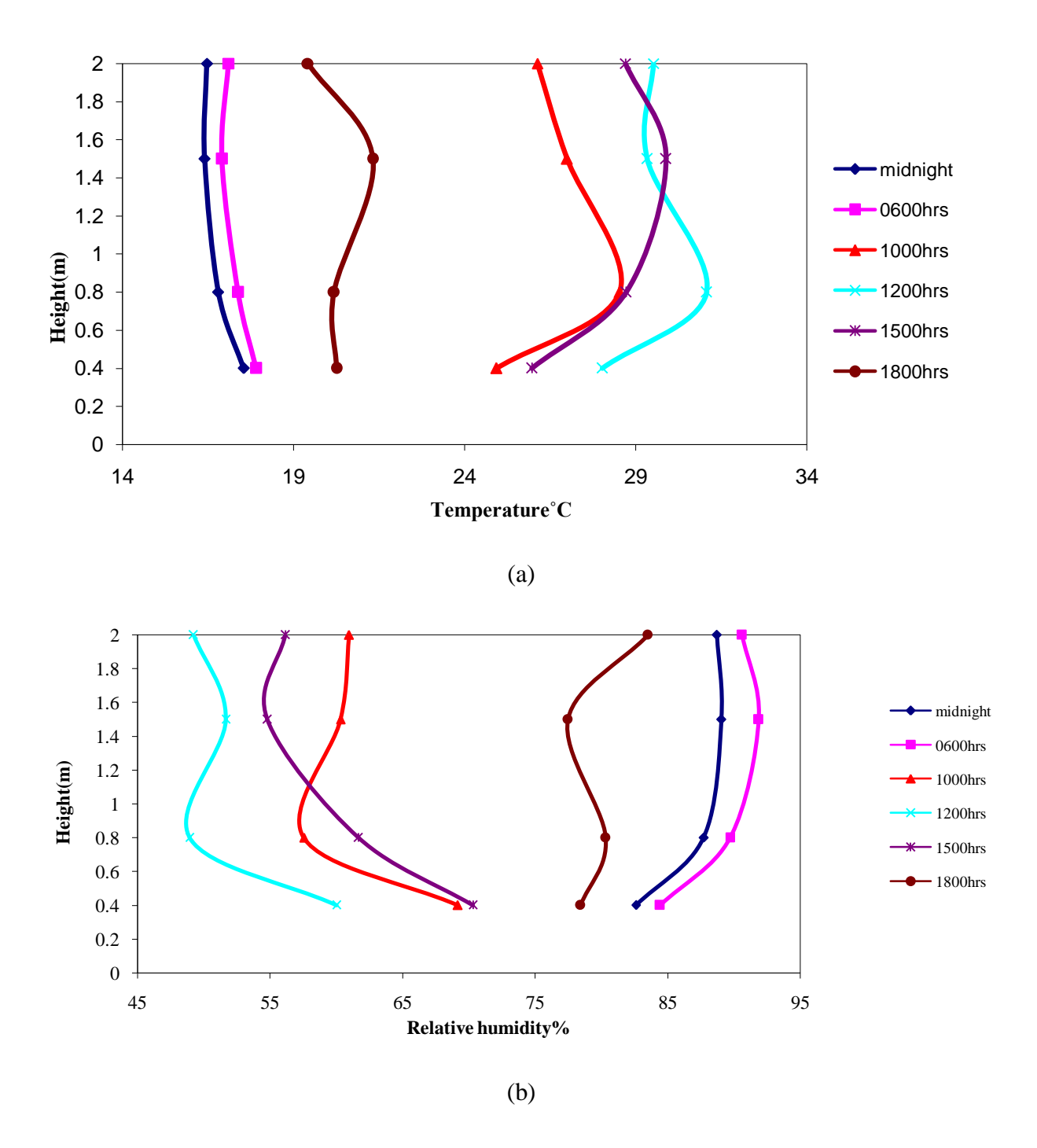


Figure 4.2: The vertical variation of (a) air temperature and (b) relative humidity in the greenhouse on 28 October 2009. The temperature and relative humidity were measured at heights of 0.4 m, 0.8m, 1.5m (crop height) and 2 m at the position of the internal AWS (as shown Figure 3.3).

Figure 4.2 shows the temperature and relative humidity measured at heights of 0.4 m, 0.8 m, 1.5 m and 2 m on the following times: at midnight, 0600 hrs, 1000 hrs, 1200 hrs,1500 hrs and 1800 hrs. Although Figure 4.2 indicates that there are significant differences between the air temperatures and relative humidity within and above the canopy, the absence of significant vertical variations in the air temperature and relative humidity above the canopy suggests that the greenhouse air was well mixed.

Figure 4.3 shows the diurnal variations on 28 October 2009 of the air temperature and air humidity measured at the five positions in the greenhouse (Figure 3.4) and Table 4.1 gives the 4-day average values of the air temperature and relative humidity. Figure 4.4 shows the variation of temperature and relative humidity at 5 measuring during a single day 28 October 2009.

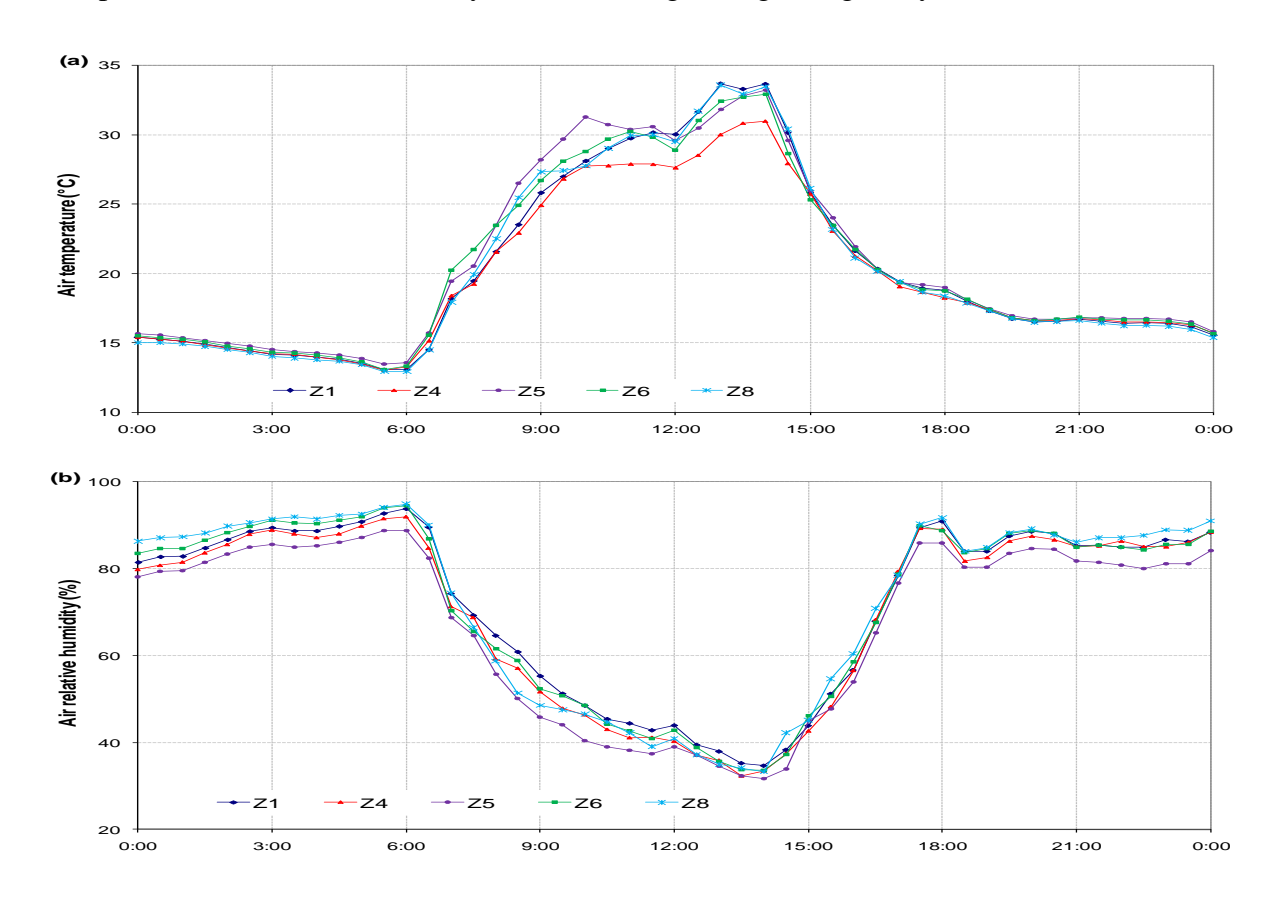


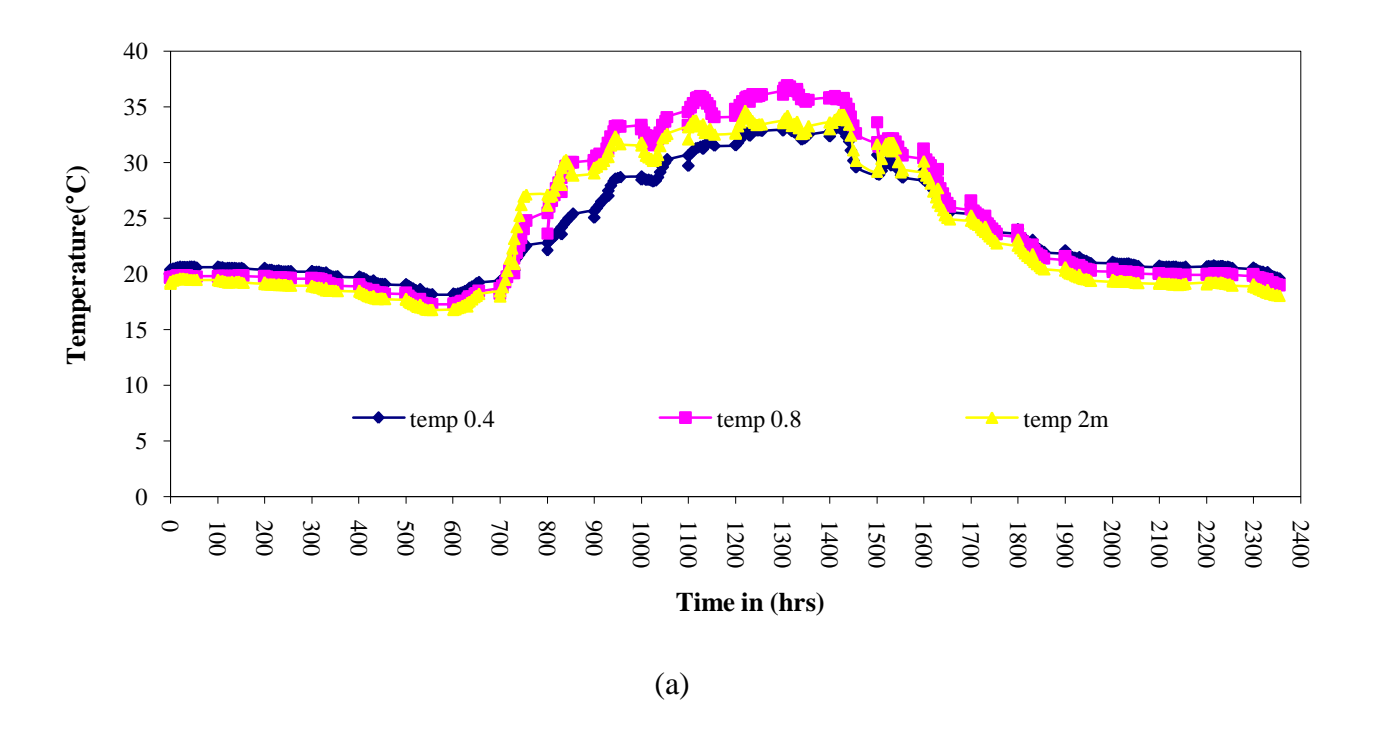
Figure 4.3: Variation of air temperature and relative humidity at five positions in the greenhouse during a single day 28 October 2009.

Table 4.1: Summary of greenhouse air temperature and relative homogeneity test results, measured at five positions during a 4-day period (27-31 October 2009)

Z1	Z 4	Z5	Z6	Z8
23.7	22.8	24.1	23.7	23.8
0.0	-0.8	0.5	0.1	0.2
59.6	57.3	54.9	58.9	58.7
1.7	-0.6	-3.0	1.0	0.9
16.0	16.0	16.4	16.0	15.9
0.0	0.0	0.3	0.0	-0.2
78.6	78.0	75.6	80.2	80.0
0.1	-0.5	-2.8	1.7	1.4
	23.7 0.0 59.6 1.7 16.0 0.0	23.7 22.8 0.0 -0.8 59.6 57.3 1.7 -0.6 16.0 16.0 0.0 0.0 78.6 78.0	23.7 22.8 24.1 0.0 -0.8 0.5 59.6 57.3 54.9 1.7 -0.6 -3.0 16.0 16.4 0.0 0.0 0.3 78.6 78.0 75.6	23.7 22.8 24.1 23.7 0.0 -0.8 0.5 0.1 59.6 57.3 54.9 58.9 1.7 -0.6 -3.0 1.0 16.0 16.4 16.0 0.0 0.0 0.3 0.0 78.6 78.0 75.6 80.2

Table 4.1 show that there was no significant difference between the temperatures at the five positions and hence any point can be used to measure the temperature and relative and those measurements are taken as the representative of the greenhouse microclimate. Sensor Z4 located to the south-west of the greenhouse indicated consistently lower day-time temperatures than the other four sensors. There were no significant differences between the night-time temperatures and the day-time relative humidities measured at the five positions. The night-time humidity measured by sensor Z5 located near the centre of the greenhouse and at the point, at which all climatic measurements were made earlier, was consistently lower than at the other four positions. Since the conditions that are applicable for the use of GDGCM which assumes the eight layers of the be homogeneous and the water vapour balance which requires the greenhouse to be perfectly mixed are met which makes the greenhouse to be suitable for the application of the model and the water vapour method.

Figure 4.4 shows diurnal variation of temperature profiles and relative humidity profiles in the greenhouse at three levels (0.4 m, 0.8 m and 2m above ground). In daytime it is clearly shown that the temperature increases with height. The highest temperature difference between 0.4 m and 0.8 m was about 3 °C. In daytime the lowest value of air relative humidity was observed at the highest level, where the temperature was highest too. During nighttime, the highest value of relative humidity was observed at 0.4 m, while the air temperature was lowest. This demonstrates the cooling effect of transpiring plants. Around 0600 hrs the temperatures started to rise and the temperatures at 0.8 m were higher than at other levels, attaining a maximum value at 1300 hrs similar to the air temperature which is similarly attributable to high solar radiation. The humidity profiles show that during the night, morning and afternoon, the humidity at 0.4 m was lower than other levels. During the day the humidity at all levels decreased attaining minimum values around midday. During the day, the relative humidity at 0.4 m was higher than at other levels. The results shown in Figure 4.4 can be explained by the fact that during the night the greenhouse lose energy by both radiative cooling and convective heat loss than that could be brought in by ventilation, thus the lower ventilations rates associated with night would tend to lower the greenhouse temperature.



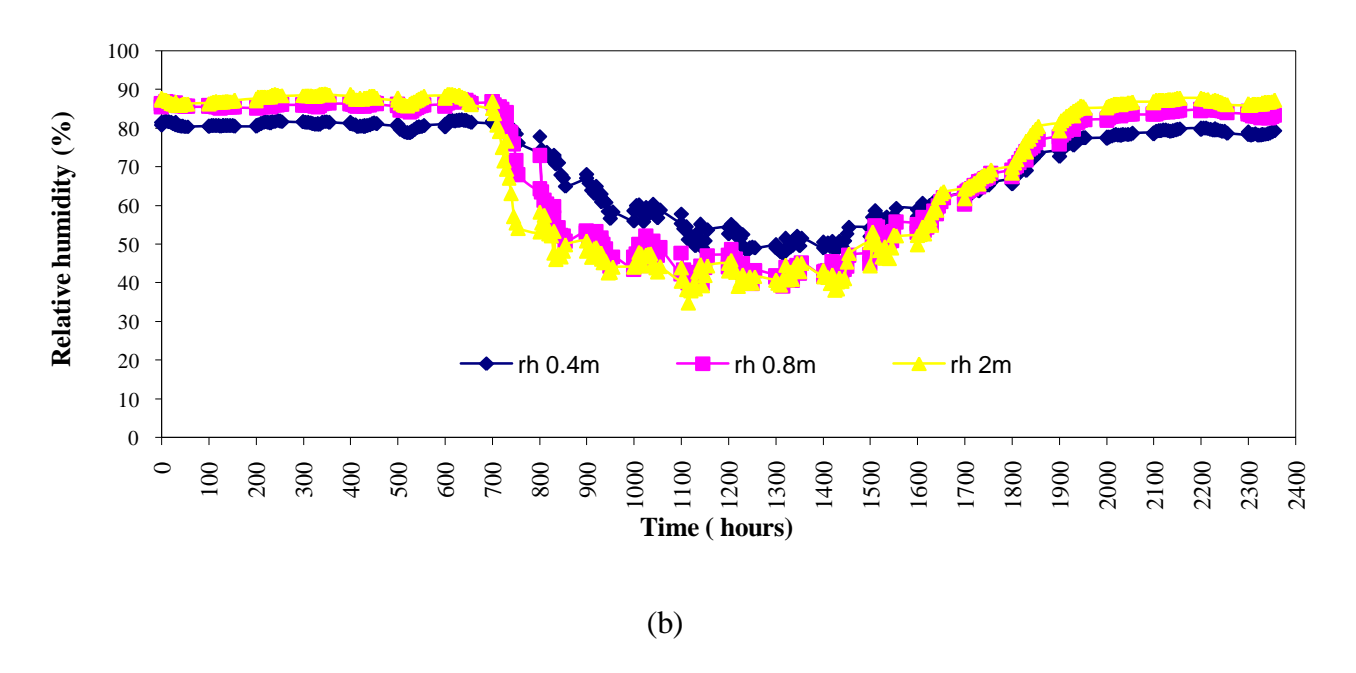
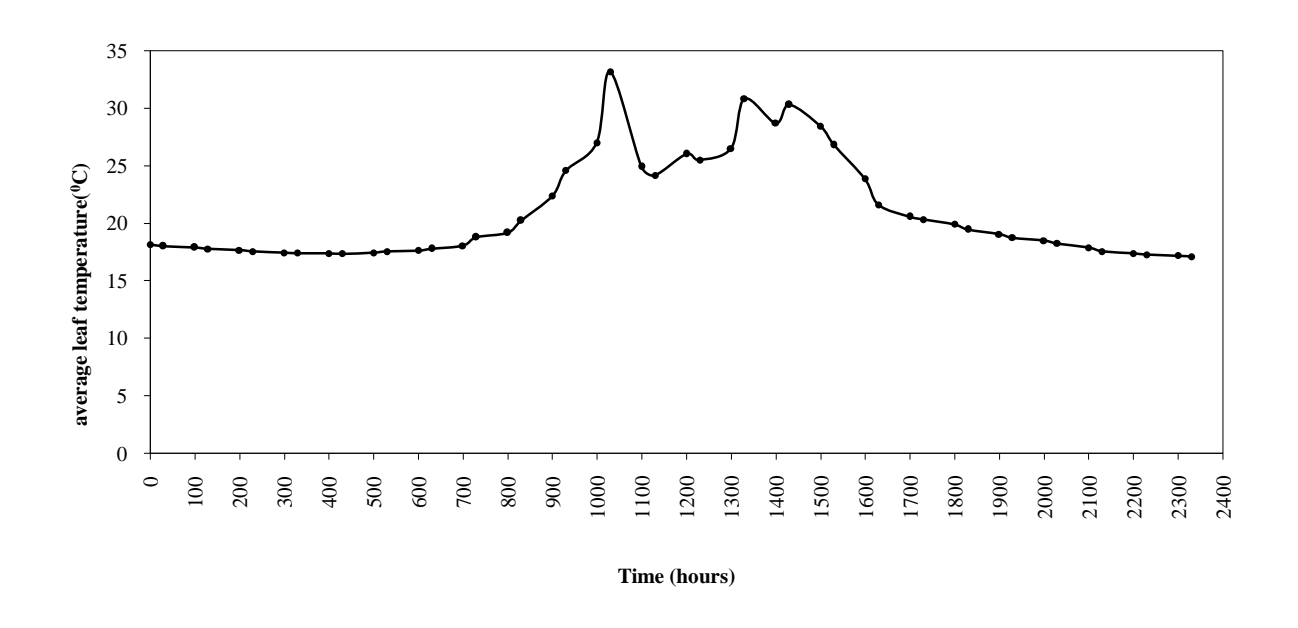


Figure 4.3: Diurnal variation of (a) vertical profile of temperature (b)vertical profiles of relative humidity on 21 January 2010

Temperatures of higher levels were lower than that of 0.4 m due to resistance offered by the canopy to sensible heat loss by convection, the same can also explain the higher humidity also found at 0.4 m thus the water vapour transfer from the crop canopy also experienced some resistance as suggested in theory (Fick's Law). At higher levels where there is free movement of air the transfer of both water vapour and sensible heat experience less resistance and hence they have lower temperatures and higher humidity. However during the day, the greenhouse receives energy from the sun, which causes internal temperature to increase because of heating of the inside air, but due to crop canopy there is high resistance to transfer sensible heat to lower levels of the canopy as well as the attenuation of the intensity of radiation which is transmitted inside the canopy according to Beer's law. Thus the upper levels of the greenhouse receive more radiant energy than lower levels. Thus different heating of levels inside the greenhouse has the effect of causing temperatures at higher levels to be higher than lower levels. The higher humidity at 0.4m might be due to the water vapour content which results from transpiration of the crops and evaporation from the soil is not readily transferred into the atmosphere as the canopy offers some resistance. In summary these findings were similar to what was found by Demrati et al (2007), for the diurnal period, the air temperatures gradient increases with height of greenhouse. It is due to the progressive absorption of solar radiation by the crop canopy, together with limitation to the vertical air exchanges between the regions above and below the crop canopy. As a result air relative humidity at night is higher than below the crop cover than above.



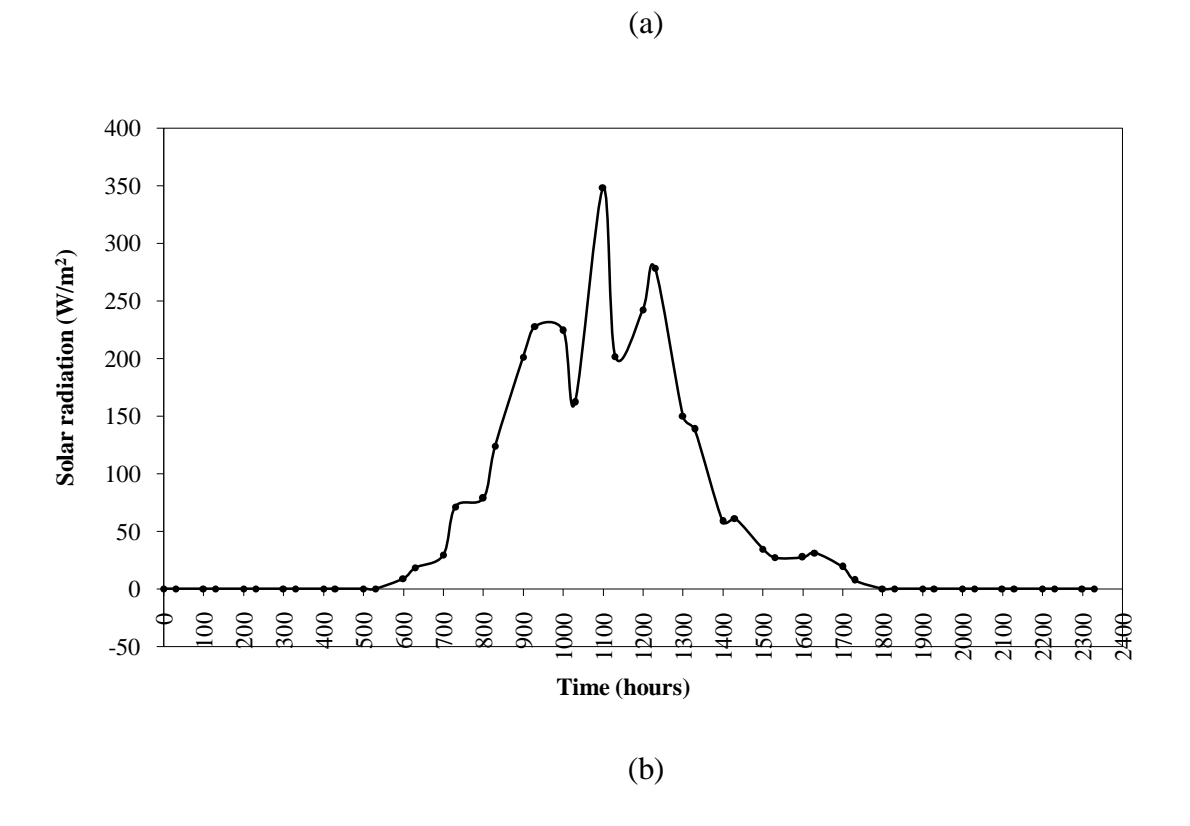


Figure 4. 4: The diurnal variation of (a) of average leaf temperature and solar radiation on 13 December 2009

Figure 4.5 presents the diurnal variation of measured average temperature and solar radiation on 13 December 2009 inside the greenhouse. Figure 4.5(b) shows that at night solar measured was zero and started rising sharply at sunrise attaining a maximum at 1100hrs 0f 348.2 W m⁻². The drop in solar radiation as shown in Figure 4.3 (b) at 1130 hrs to 201.6 W m⁻² may be due to cloud cover. The solar radiation increased to 278.3 W m⁻² at 1230 hrs from which dropped gradual to zero around sunset. Figure 4.5(a) presents the diurnal variation of average leaf temperature which was almost constant at night and also started increasing as solar radiation started increasing attaining a maximum temperature at 1030hrs of 33.2°C. The average leaf temperature also dropped to 24.9 °C at 1130 hrs due to cloud cover as shown in Figure 4.3 (b) for solar radiation. It then rose again to a maximum value of 30.8 °C at 1330 then started decreasing to minimum at sunset of 19.1°C

4.2 Validation of Penman Monteith Method

The ventilation rate was determined using the water vapour balance method in equation (3.14); the transpiration term was evaluated using the Penman-Monteith method as was applied by (Katsoulas et al 2001). To validate the Penman Monteith method it was compared with Sap flow measurements using historical data (Mashonjowa et al 2007). Figure 4.6 shows the correlation between transpiration rates obtained from sap flow and determined by Penman Monteith formula using data from 1 December 2007-31 December 2007.

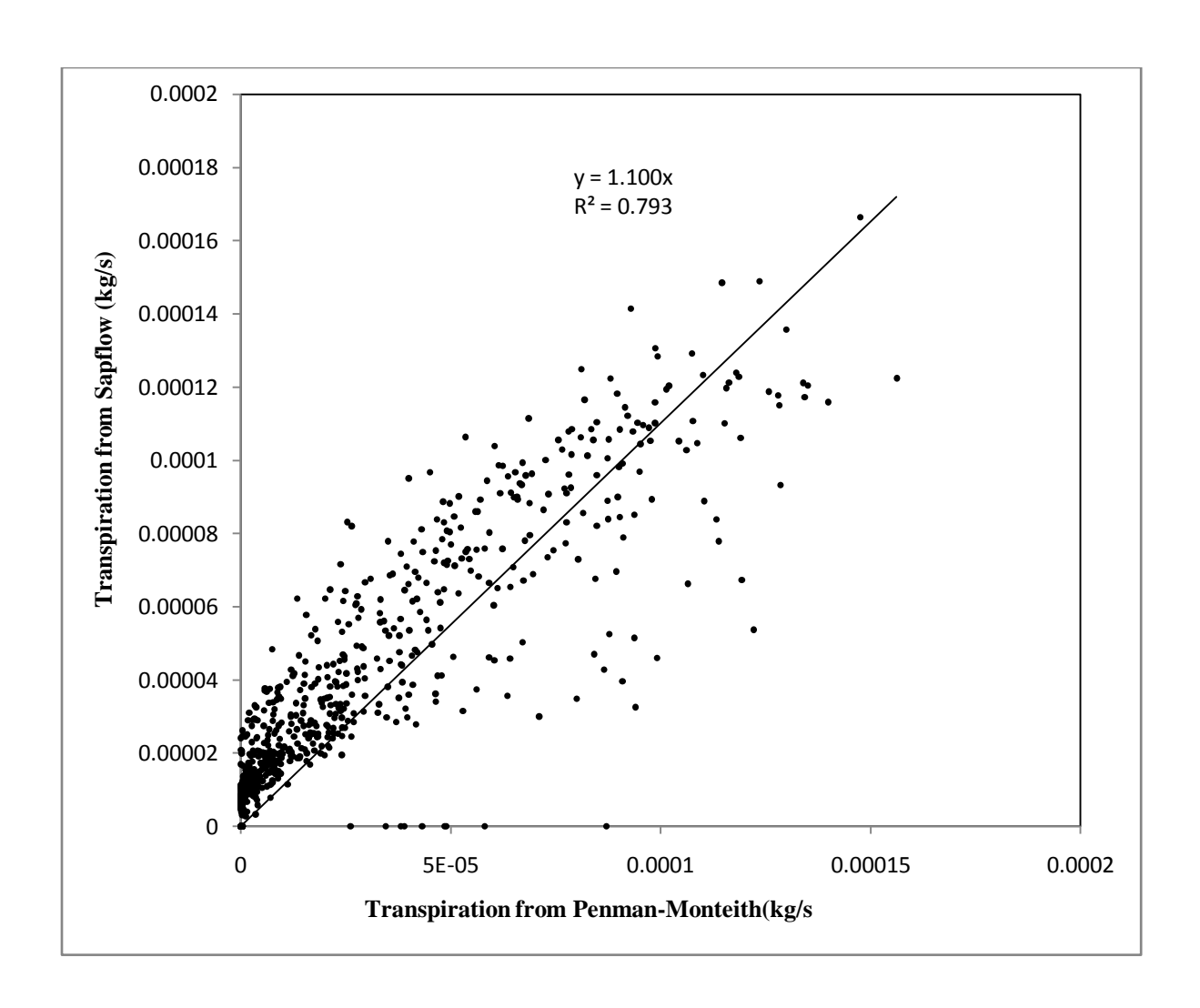


Figure 4.5: correlation between transpiration obtained from sap flow and transpiration obtained from Penman-Monteith method on days 1-31 December 2007

The results showed there is a good fit between the measured transpiration rates from sap flow gauges and the calculated transpiration rates from Penman-Monteith, although the sap flow gauges tends overestimate the crop transpiration in the morning (just after sunrise), and underestimate of crop transpiration in the afternoon (just before sunset) as reported by the following authors (Baker and van Bavel, 1987; Baker and Nieber, 1989 and Grime et al (1995)). This was explained as follows, in the morning when soil temperature exceeds air temperature; there is negative temperature gradient in the sensor as warm sap enters a cooler stem, causing a temporary over-estimation of whole-plant transpiration, if the sensor is near the soil. In the

afternoon, when the ambient air temperature is higher than soil temperature, the sensor registers a higher positive gradient in the sensor, resulting in an underestimation of whole plant transpiration. The errors can also be attributed to up scaling of the leaf transpiration that is based on the assumption the transpiration from the single is uniform throughout the whole canopy.

4.3 Determination of stomatal resistance

The version Penman-Monteith formula which was adopted for determining transpiration rates required the measurements and estimation of aerodynamic resistance and canopy stomatal resistance. The aerodynamic resistance for plants in a greenhouse was assumed to be 200 s m⁻¹. The stomatal resistance in this study was obtained from the stomatal sub-model equation (3.22) in the GDGCM. Before use the stomatal model was calibrated to obtain the equation parameters by experimental data fitting into a statistical package Sigma plot. It was then validated by comparing measured stomatal resistance with predicted stomatal obtained from the model. Figure 4.5 shows the variation of solar radiation and stomatal resistance.

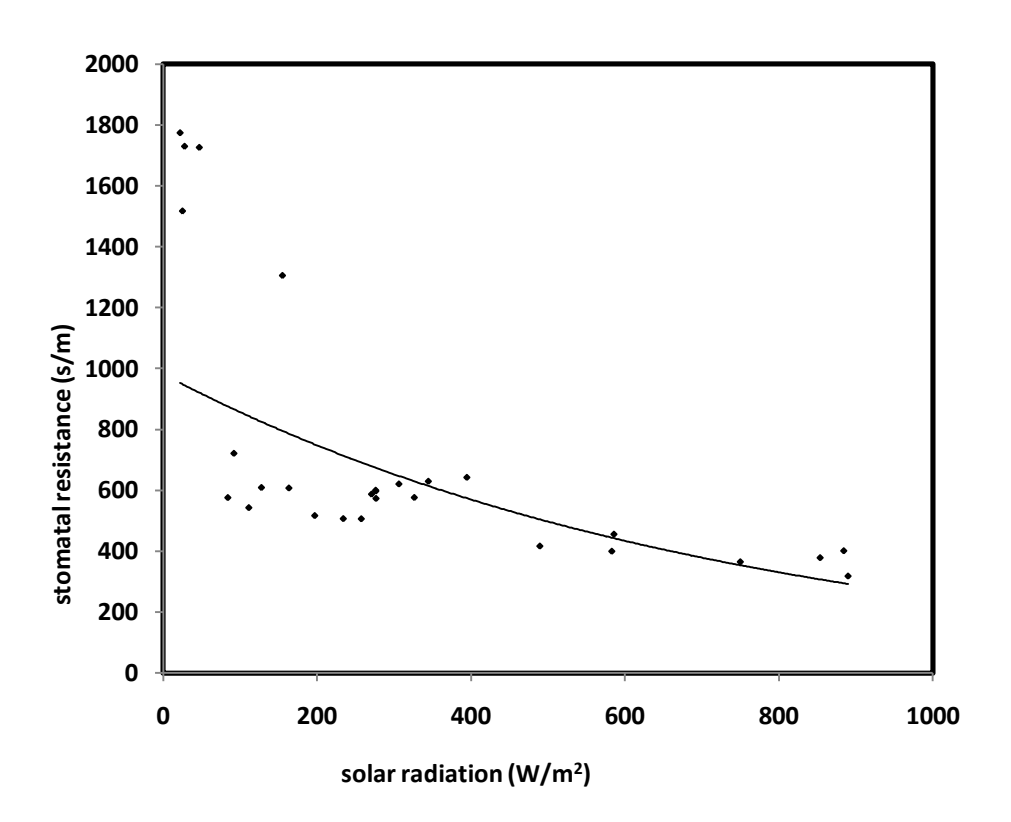


Figure 4.6: Variation of measured stomatal resistance and solar radiation on 28 February 2010 -14 March 2010

Figure 4.7 presents the variation of stomatal resistance and solar radiation. An increase in solar radiation results in a decrease in the stomatal resistance. Figure 4.7 can be used to explain why transpiration is high during the day and almost zero at night. During the day, transpiration is high because the incident solar radiation is high and the canopy stomatal resistance is low. During the night the stomatal resistance is much higher because solar radiation is zero and consequently transpiration is very small because the radiative component in equation (2.29) is almost equal to zero.

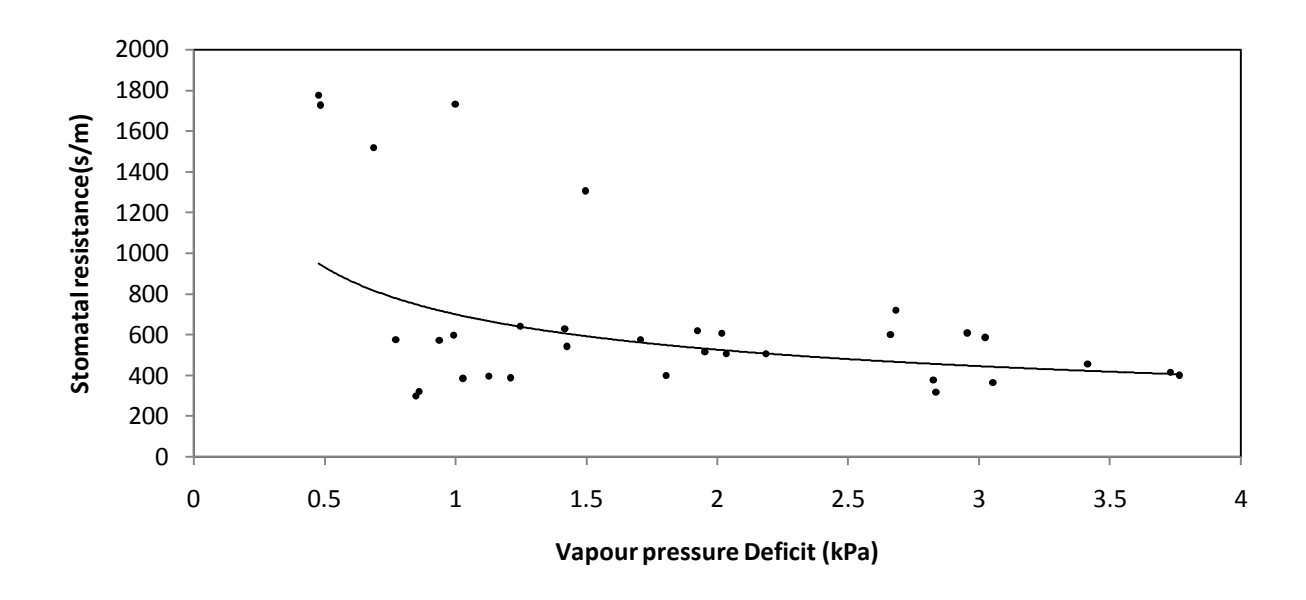


Figure 4. 7: Variation of measured stomatal resistance with vapour pressure deficit (VPD) on 28 February 2010-14 March 2010

Figure 4.8 presents the variation of measured stomatal resistance with vapour pressure deficit. It can be observed that high vapour pressure deficit corresponded to low stomatal resistance, and when the vapour pressure deficit was low, the stomatal was very large. This can be explained as follows: high vapour pressure deficit that occurs when temperature is high and because air can hold more vapour when its temperature rises. The vapour deficit between the leaf and the vapour pressure deficit becomes large and causes stomatal resistance to decrease rapidly. Low temperatures make the air more humid and it also tends to decrease the vapour pressure deficit that tends to increase the stomatal resistance.

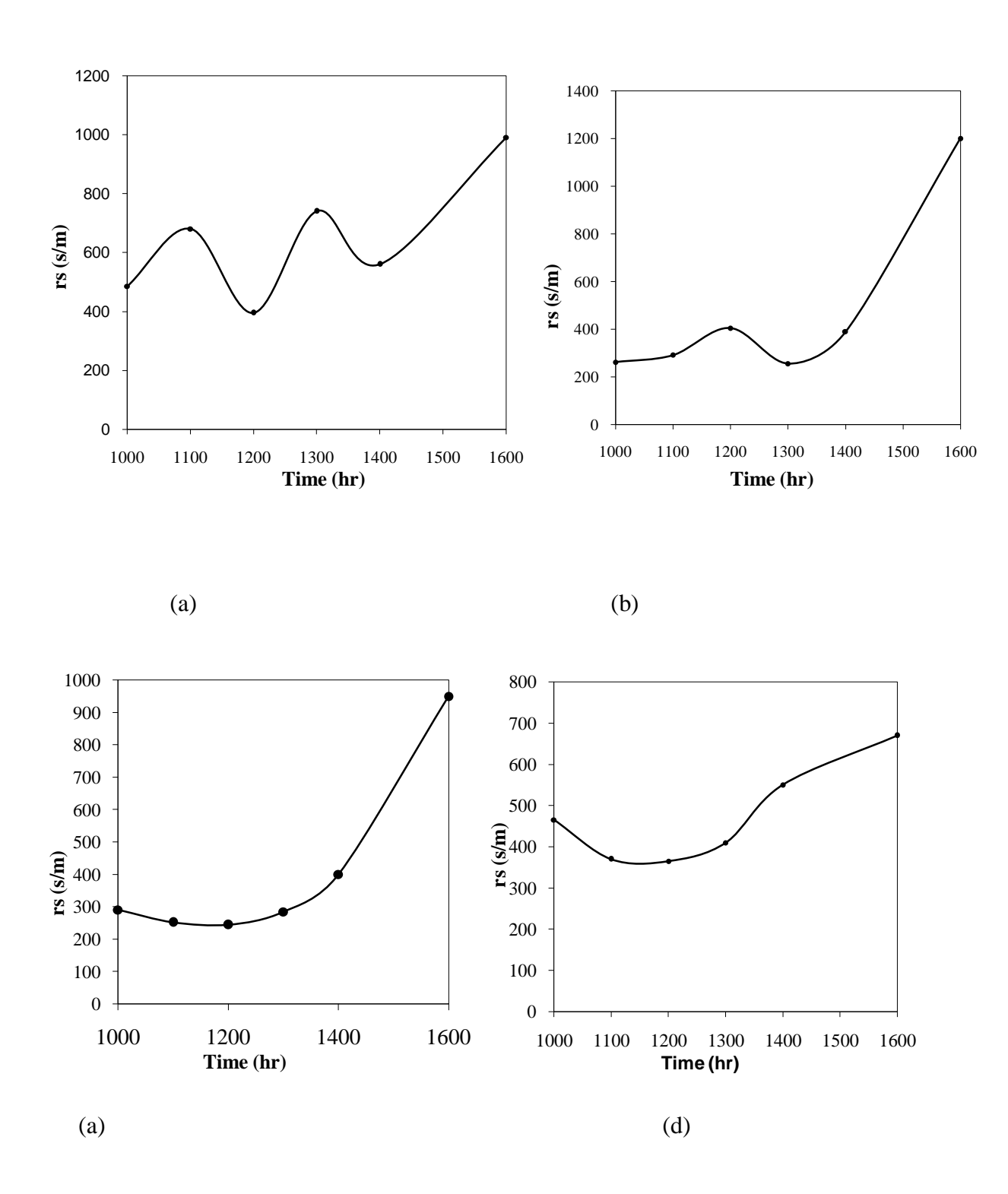


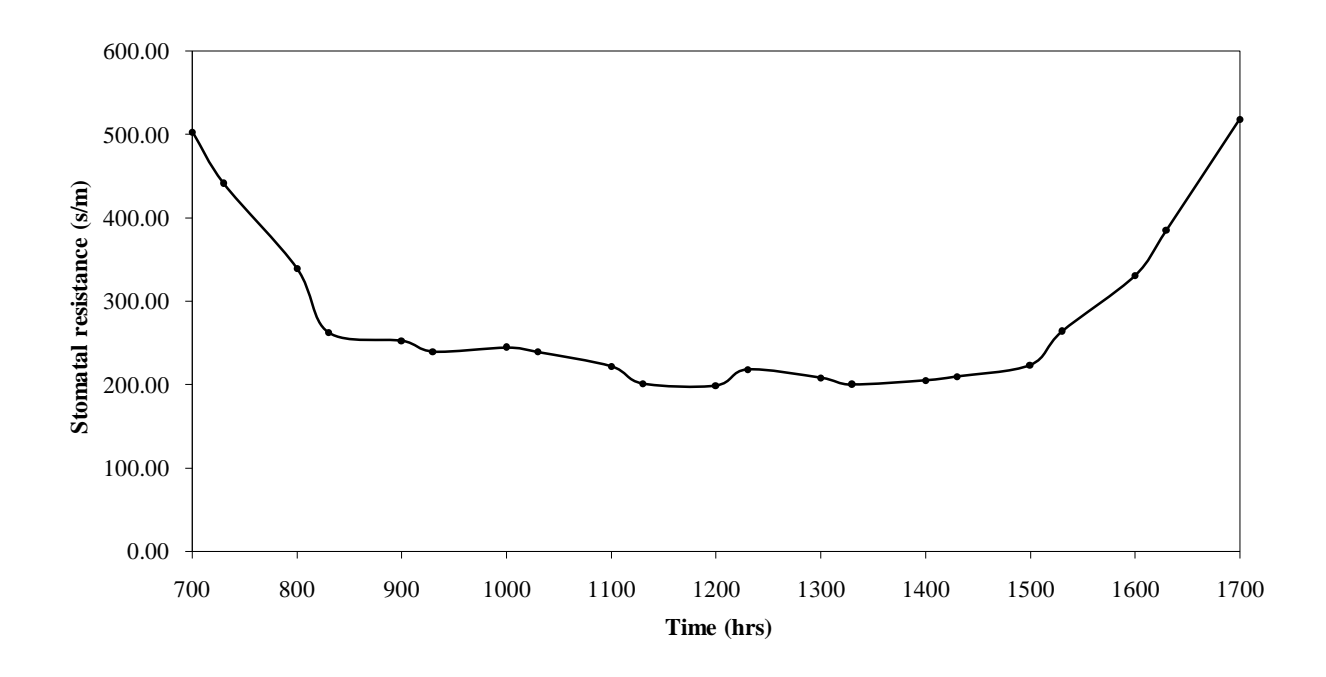
Figure 4.8: stomatal resistance of four different cultivars (a) Upendo, (b) Betsy, (c) Symphonica Rosso and (d)King Arthur on 28 February 2010

Figure 4.8 shows variation of stomatal resistance and vapour pressure deficit (VPD) on 28 February 2010-14 March 2010. Figure 4.8 shows that as vapour pressure deficit increases, the stomatal resistance decreases, and a low vapour pressure deficit 0.48kPa corresponded to a high stomatal resistance of 1775 sm⁻¹. Figure 4.8 shows peaks of the VPD corresponded to high stomatal resistance. The variation of measured stomatal resistance with vapour pressure deficit showed that low stomatal resistance is high solar irradiance, thus high vapour pressure deficit occurred when there was high solar irradiance which corresponded to high internal air temperatures and low internal relative humidity.

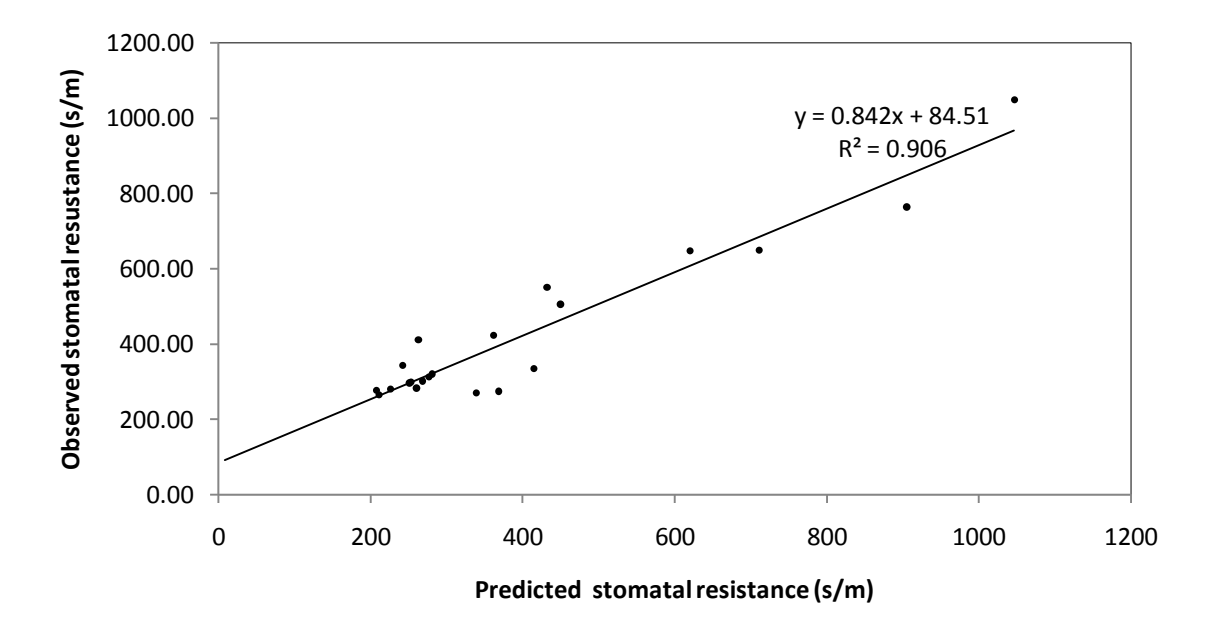
Table 4.2: Model specific parameters obtained in this study compared to those found by Baille et al (1994c) and Kittas et al (1999) for two cultivars of roses (Rosa x Hybrida)

	This study	Baille et al	Kittas et al		
Cultivar	Average of several	cv Sonia in	cv First Red in		
and Substrate	cultivars in vermiculite	rockwool	perlite		
a	546.9752±93.1	349	566		
b	52.3263±17.2	28	90		
c	-0.1299±0.1	1.45	0.276		

Table 4.2 shows the parameters of the stomatal model found by experimental data fitting using a statistical package Sigma plot and what has been found out by other authors; the values obtained in this study was comparable to what has been found out by Kittas et al (1999). However the was great difference to what has been found by Baille et al (1994c), this could be due to different locations, the growing medium of the roses and due to different cultivars. To test the reliability of the stomatal model it was validated by comparing predicted canopy stomatal resistance and measured stomatal resistance.



(a)



(b)

Figure 4.9: Showing (a) the daytime variation of stomatal resistance and (b) the correlation between observed stomatal resistance and predicted stomatal resistance on 16 March 2010

Figure 10(a) shows diurnal variation of stomatal resistance. Stomatal were high in the morning and late afternoon. During the day, the stomatal resistance was low and almost constant, and it was 200 s m⁻¹. There was an increase in stomatal resistance from 1500 hrs to 1700 hrs.

The Figure 4.10 (b) shows there was good fit between the measured canopy stomatal resistance and the simulated canopy stomatal resistance and therefore the stomatal resistance which was required in determination of the transpiration was estimated using the model equation (3.22).

Statistically analysis for stomatal model validation and calibration is shown in Table4.3. The t test was used to carry out the significance to test the null hypothesis H_0 that there is no significant difference between the observed stomatal resistance and predicted stomatal resistance. In both calibration and validation (Table4.3) we accepted H_0 since $|t_{Stat}| < t_{\alpha=0.025}$ and concluded that there was no significant difference between the modeled and the measured stomatal resistance at 5 % level of significance

Table 4.3: Results of significance test using t-test at 5 % level of significance for the observed and predicted stomatal resistance for calibration and validation, including the Root Mean Square Error(RSME)

Process	RSME	Number observations	of t _{Stat}	t _{α=0.025}
Calibration	478.7	33	1.462	2.037
Validation	232	21	-1.357	2.423

The Root Mean Square Error (RSME) is calculated as:

$$RSME = \sqrt{\frac{\sum_{i=1}^{n} (Oi - Mi)^2}{n}}$$
(4.1)

4.4.1 Calibration and Validation of Ventilation Sub-model

This section describes the full scale measurements carried in the greenhouse which were used in the ventilation sub model equation (3.12), which has been derived on the basis of the stack and wind-induced pressure fields.

The ventilation rates G, climate parameters ΔT , the difference between internal and external temperature of the greenhouse, T_e the external temperature of the greenhouse and u_e is the external wind and opening of the vents (A_R and A_S) were used to determine C_D and C_w by fitting experimental data to model using Sigmaplot. The transpiration rates were calculated using Penman Monteith formula equation (2.30). The results obtained are summarized in the Table 4.4; the calibration was done using data 1-31 December 2007 (Mashonjowa et al 2008).

Table 4. 4: Discharge (C_D) and wind effect (C_w) coefficients obtained in this study

coefficient	C_D	C_{w}	\mathbb{R}^2
Value	0.3779±0.0059	0.0374±0.0037	0.702

From Table 4.4 it can be observed that the discharge coefficient, C_D and wind effect coefficient, C_w , obtained are generally of the same order as those found by other researchers for greenhouses with the same circumstances as shown in Table 4.5.

Table 4. 5: Discharge and wind effect coefficients found by other researchers

Discharge	Wind	T _i -T _e	External	Size and type of greenhouse and	Source
Coefficient,	effect	(°C)	wind speed	opening angles of vents	
C_D	coefficient,		speed		
	$C_{\rm w}$		(m/s)		
0.64	0.07-0.10	0.8-	0-2	416m ² 2-span Filclair; roof vents	Boulard and Baille
		12		only;20°	(1995)
0.43	0.07-0.10	0.8- 12	2-4	416m ² 2-span Filclair; roof vents only;20°	Boulard and Baille (1995
0.75	0.07	1-10	0.1-7	416m ² 2-span Filclair; roof vents only;0-30°	Kittas et al. (1997)
0.253	0.075	0.9	4.9	149 m ² , mono-span, screened side vents	Teitel et al.(2008)
0.127	0.038	1-8	2	504m ² , 3-span; screened roof and side vents	Liu et al(2005)
0.363	0.07	1.6	2.2	160m ² ,mono-span arch,screened roof and side vents	Katsoulas et al (2006)

Table 4.5 shows that the parameters C_D and C_w can vary even for similar greenhouses. Boulard and Baille (1995), Roy et al. (2002) and Fatnassi et al, (2003) suggest that the parameters depend on the greenhouse size and design, immediate surroundings of the greenhouse and prevailing weather conditions, particularly wind speed. The values found in this study are inter-mediate

between those for greenhouses with and without screens, further showing that the dependence of these parameters on the circumstances of the greenhouse.

Figure 4.11 shows the regression of measured air renewal rate and modeled air renewal for calibration and validation period.

4.4.2 Calibration and Validation of the Roof vents only model

A statistical package Sigmaplot was used to determine the model parameters C_1 and C_2 by fitting experimental data. The parameters for model are given in Table 4.6

Table 4.6: Coefficients (C_1) and coefficients (C_2) obtained in this study

coefficient	C_1	C_2	R^2
Value	0.0879±0.00304	1.1799±0.4311	0.729

The results in Table 4.6 disagreed with findings by Fernandez and Bailey (1992) shown in Table 4.7

Table 4. 7: Coefficients (C₁) and Coefficients (C₂) obtained by Fernandez and Bailey (1992)

coefficient	C_2	C_2	Author
Value if Alfwin in °C	0.00145	0.00171	Fernandez and Bailey (1992)
Value if Alfwin in rad	0.0831	0.00171	Fernandez and Bailey (1992)

The results show that the parameters obtained in this study were higher than those found by Fernandez and Bailey (1992). This can be attributed to difference the greenhouses location and weather conditions particularly the prevailing wind speed.

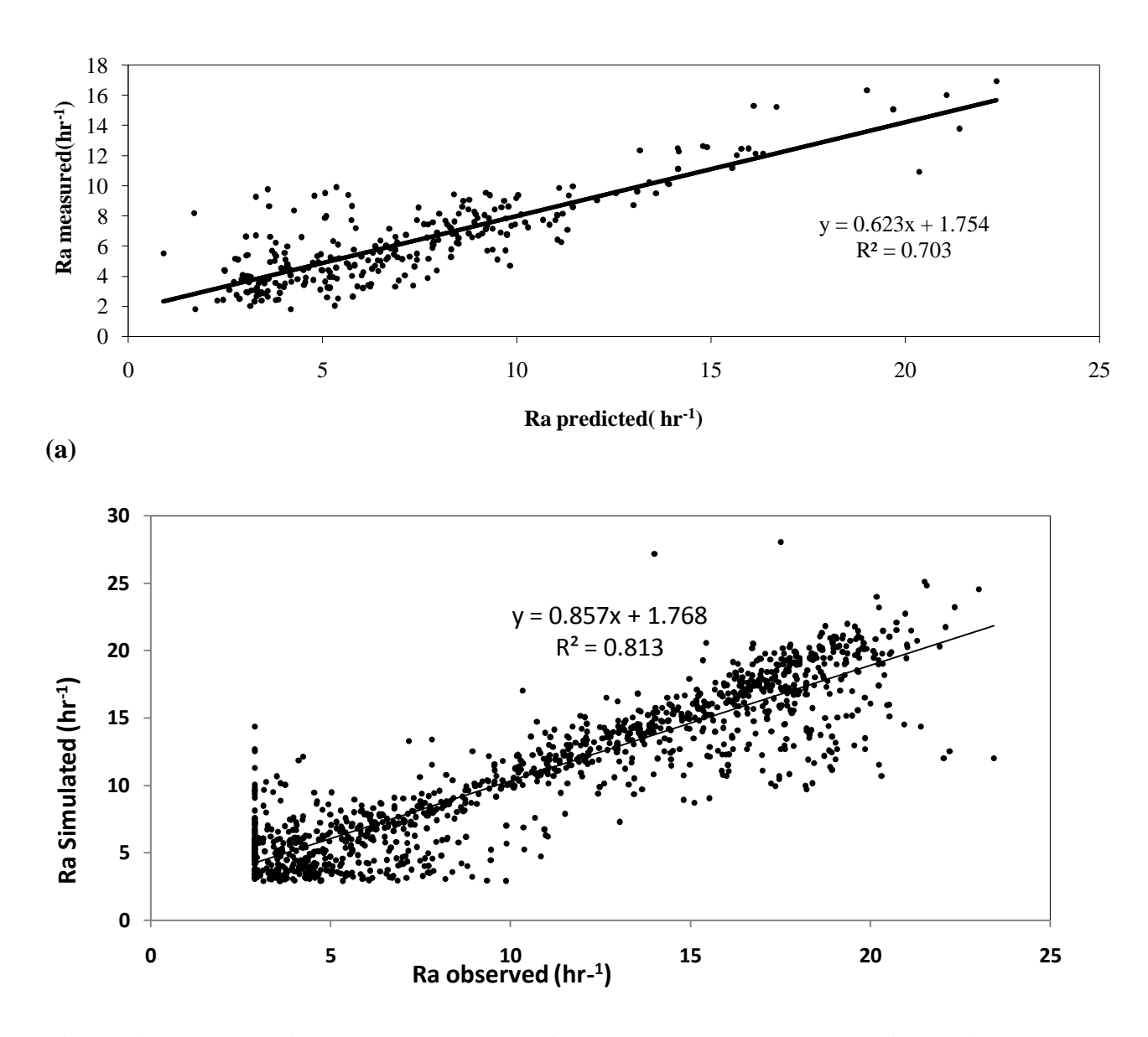


Figure 4.10: Regression between the experimentally observed and predicted air renewal rates for (a) calibration 1-31 December 2007 and (b) validation for the period 1 - 25January and 1-23 February 2008 using model for both roof and side vents

The results show there is a good fit between measured and predicted values, however there is significant differences between measured and predicted air renewal rates of the greenhouse observed during the night, early morning and when it is raining. The differences may be

explained in terms of instrument errors in the measurement of the high relative humidity that occurs at night, early morning and during rain periods. The humidity probes are quoted as having measurement errors of about ± 2 % in the range 10-90 % relative humidity, but above 90 %, and as the sensor ages, the errors increase to about ± 5 % (Delta-T Devices Ltd., 2000; Campbell Scientific Inc., 2007). The ventilation rates in this study heavily relies on the measurement of humidity, thus errors in the air renewal rates at higher humidities (such as at night, early morning and during rain) are likely to be larger than those at other times. Errors in measured air renewal rates may have been introduced by estimation of transpiration rates using Penman-Monteith method, the errors may be due to scaling up from single to whole canopy

Table 4. 8: Results of regression analysis between the predicted and observed air renewal rates, including the 95% confidence intervals and the slope and intercept for the equation $R_{a(obs)} = m R_{a(pred)} + c$

	Number of observations, <i>N</i>	R^2	Slope m	SE	95% confidence interval of slope	Intercept, c (h ⁻¹)	SE	95% confidence interval of intercept
Mode 11								
Calibration 8–31 Dec 07	764	0.859	0.968	0.014	[0.940; 0.995]	0.968	0.179	[0.618; 1.319]
Validation 1–25 Jan 08& 1-23 Feb 08	1189	0.813	0.949	0.013	[0.922; 0.975]	0.367	0.166	[0.042; 0.693]
Mode 5								
Calibration 1– 15 June 07	41	0.654	0.615	0.072	[0.471; 0.760]	1.310	0.248	[0.808; 1.812]
Validation 16-30 June07	35	0.792	0.784	0.07	[0.642; 0.726]	0.784	0.247	[0.642; 1.286]

The results from Table 4.8 show there is good fit between measured and estimated values, particularly during the day. Most significant difference may arise at night, early morning and during rain periods which might be attributable errors in the measurement of relative humidity that occurs at night, early morning and during rain periods when relative humidity is above

90%.other errors arise from estimation of transpiration from Penman Monteith method and the assumption that the soil or medium have negligible evaporation which might not be necessarily true.

4.5 Model Results

4.5.1 Introduction

In this section the results from the simulation of ventilation sub model of the GDGCM are presented for the two ventilation configurations using the same outside weather data and the same greenhouse parameters. The ventilation model allows the simulation of the following parameters inside the greenhouse: air renewal rates, air temperature, relative humidity, canopy temperature and canopy transpiration

4.5.2 Influence of Ventilation Strategy on Air renewal rates

The simulated air renewal rates for the two configurations were found from model outputs. These rates were then compared to find the effects of ventilation on the air renewal rate. The results are displayed in Figure 4.12. The major purpose of ventilation is to reduce the heat load in the greenhouse during period of high solar irradiance. This would prevent crops from overheating; reduce the risk of disease prevalence as excessive humidity will be carried out of the greenhouse, and increase the rate of photosynthesis. During summer, the aim of greenhouse users will be to keep the difference between internal and external air temperature as low as possible.

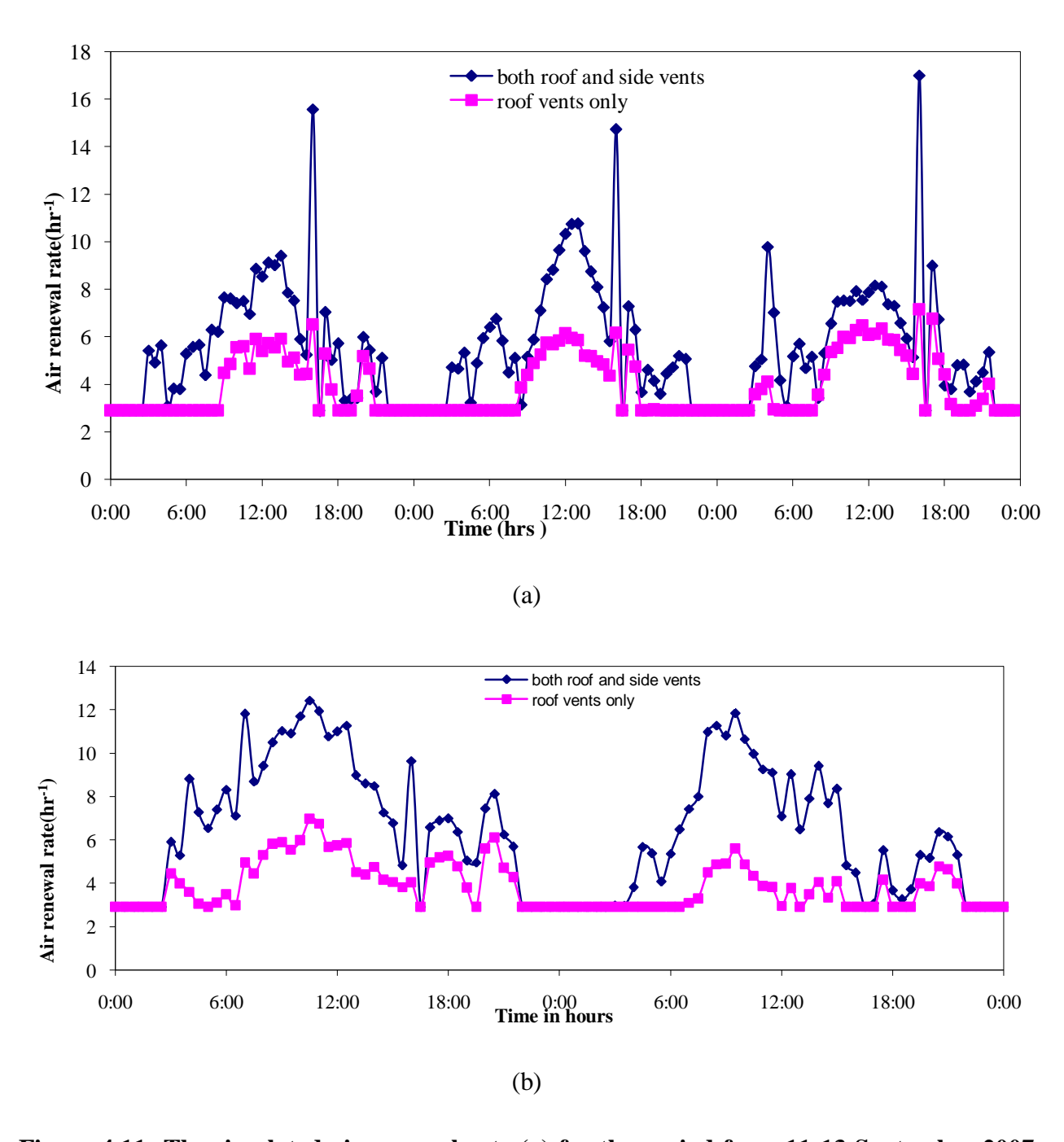


Figure 4.11: The simulated air renewal rate (a) for the period from 11-13 September 2007 and (b) for the period from 16-17 October 2007.

The trends for the air renewal rates for the two ventilation configurations were similar as shown in Fig 4.12(a). Ventilation is vital for cooling the greenhouse in periods of high solar irradiance.

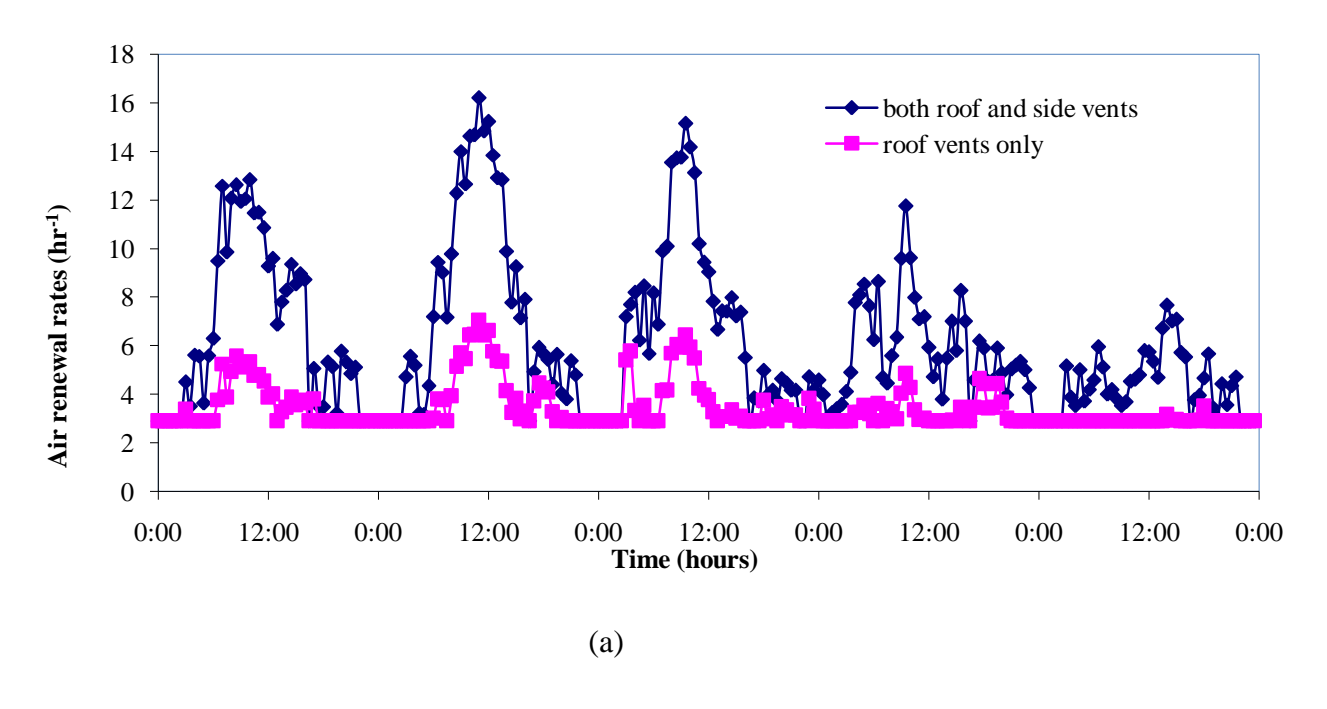
From Fig 4.12 it can be deduced that large difference of air renewal rates occurred during the day. At night, as temperatures are low in the greenhouse, the air renewal rate for the two ventilation regimes were almost equal and corresponded to air exchange rate effected by the leakage of 2.9 hr⁻¹ when the greenhouse vents were completely closed. During the day, the air renewal rates projected were high around midday reaching a maximum value of 15.6 hr⁻¹ for the configuration with both roof and side vents and 6.5 hr⁻¹ for the configuration with roof vents only, on 11 September 2007 at 1600hrs. The air renewal rates were high during the day because the greenhouse receives high solar radiation that consequently heats the interior air, crops and the soil that results in sensible and latent heat. The infrared radiation which is emitted by vegetation and soil trapped within the interior of the greenhouse (greenhouse effect). Sensible, latent heat and infrared radiation in a greenhouse result in increase in temperature increases. Since the greenhouse responds to ventilation set temperature, during the day solar radiation is high and so this explains why there is a maximum air renewal rates around midday and also why there is maximum opening of the vents. With roof vents only, the greenhouse ventilation area is lower than the one with both roof and side vents hence it has lower ventilation rates. . The predicted air renewal rates for the ventilation regime with both roof and side vents were higher than those with only roof vents as expected.

Fig 4.12(a) shows that ventilation rates were higher for the ventilation strategy with both roof and side vents than for the ventilation strategy with roof vents only. As air renewal rate depends on wind speed and internal air temperature, if the opening area is reduced, the wind speed will be reduced hence the reduction in air renewal rate. The greenhouse equipped with roof vents only therefore would have low ventilation as opposed to when greenhouse had both roof and side openings that would have extra opening area of side vents to allow more air movement thereby increasing the ventilation rate. Fig 4.12 (a) shows that during the night, there was no significant difference between the simulated air renewal rates of the two configurations. As both vents were closed at night, there fore the air renewal rates is the leakage rate of 2.9 hr⁻¹. There was a large difference between the simulated air renewal rates for the two ventilation configurations during the day. The modeled results were as follows: on 16 October 2007, the maximum air renewal rate of 12.43 hr⁻¹ for the configuration with both roof and side vents and 6.96 hr⁻¹ for the configuration with roof vents only at 1030 hrs. Fig 12(b) indicates the same trend that is shown

in Figure 4.12(a), there was a maximum air renewal of 12.4 hr⁻¹ for the configuration with roof and side vents and 6.97hr ⁻¹ for the configuration with only roof vents at 1030hrs on the 17 October 2007. The air renewal rates were also high during the day with a maximum of 11.8 hr⁻¹ for the ventilation strategy with both vents and 5.6 hr⁻¹ for the greenhouse with roof vents only. Figure 4.13 shows the variation of simulated air renewal rate with time for the two configurations for selected days of the month for the whole summer period.

The simulated air renewal rates show that air renewal rate for the greenhouse equipped with both roof and side vents were higher than that of the greenhouse with only roof as shown in Figure 4.12 clearly indicating that the transfer of heat and mass transfer are more pronounced in a greenhouse with both roof and side vents.

The difference in air renewal rates for the different day was found to be dependent on the solar radiation incident on the greenhouse and also on the degree of opening of vents. These finding are similar to what have been found by other authors that the combination of roof and side openings increases air velocity hence the air renewal rate (Bartzanas et al., 2005, Fatnassi et al., 2001 and Harmanto et al., 2006)



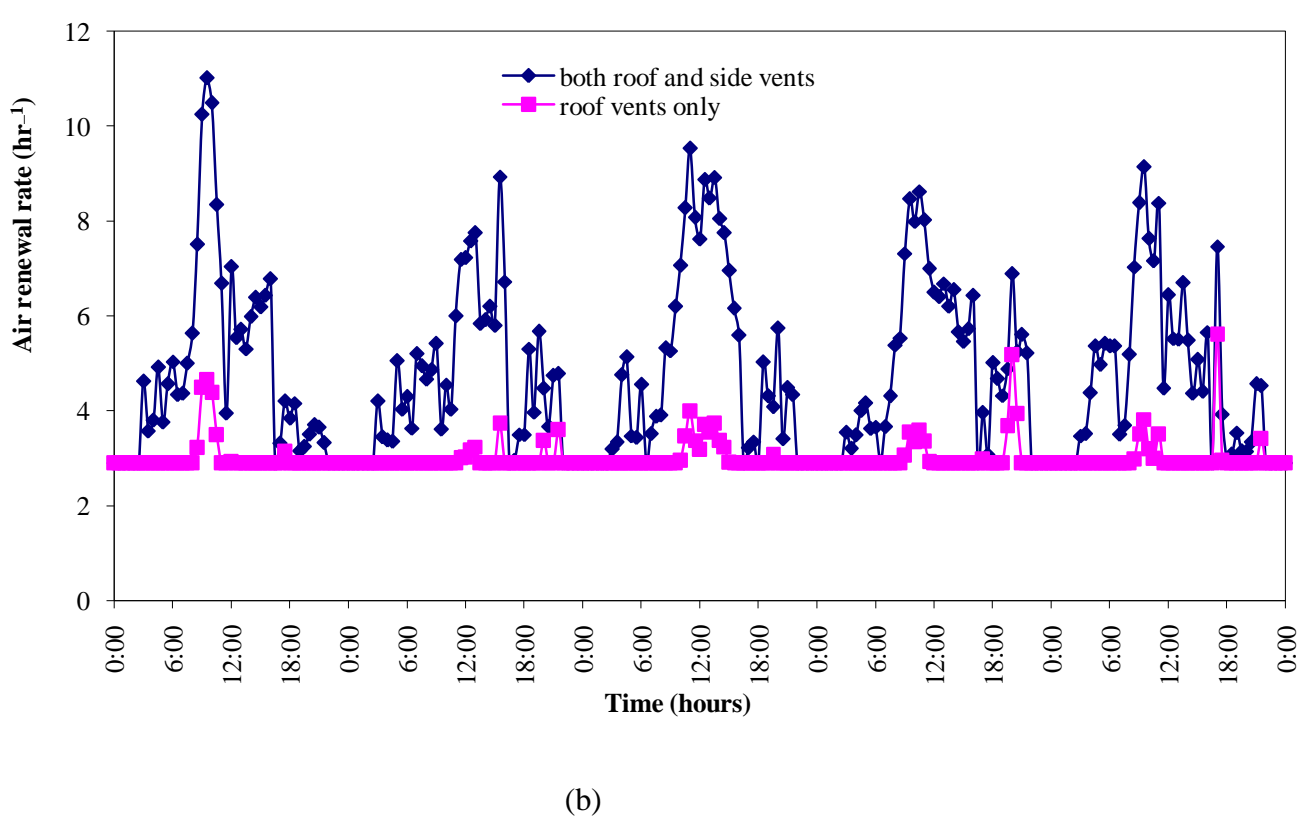


Figure 4.12: Simulated air renewal rate for (a) 1-5 December 2007 and (b) 15-21 January 2008.

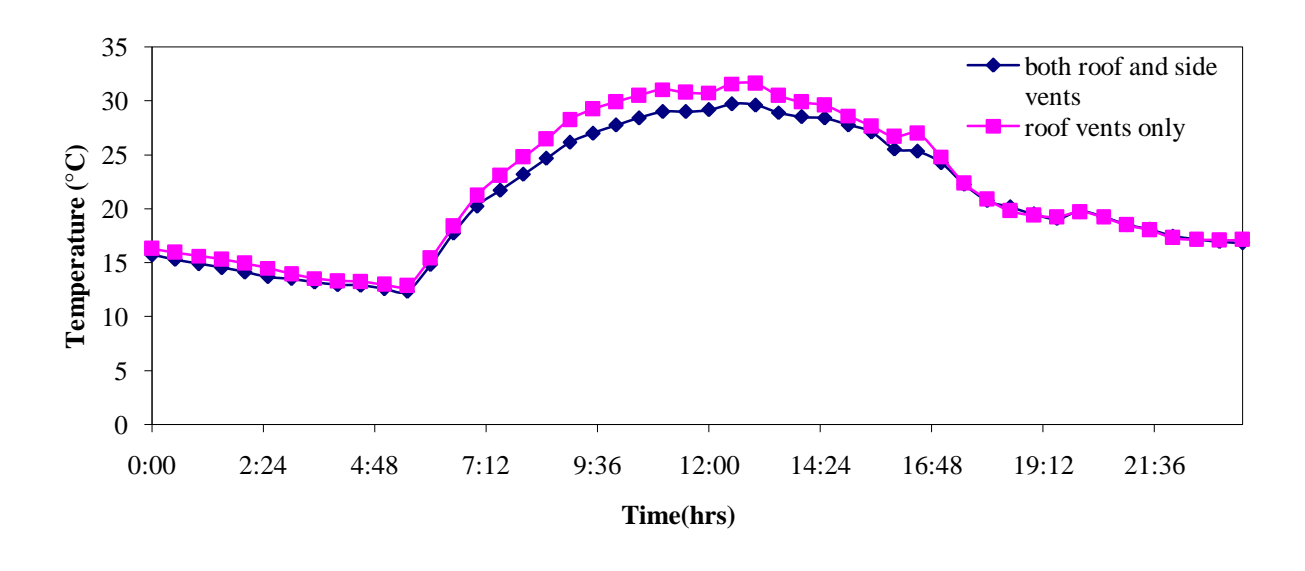
4.5.3 Effects of ventilation on the microclimate of the greenhouse

The purpose of ventilation in a greenhouse is to control temperature, in order to reduce water stress in plants, increase crop growth as most crops grow well in a temperature range. The results from the GDGCM model were used to investigate the effects of the two ventilation regimes using outside weather data and greenhouse parameters.

4.5.3.1 Influence of Ventilation on inside air Temperature

The influence of ventilation strategy on the inside air temperature was shown from the results of predicted inside air temperature from the two models that was done for the greenhouse for the two configurations: one with roof vents only and the other with both roof and side vents using same weather data and conditions but with the only difference in ventilation strategy. The simulated internal air temperature for the two configurations were compared and the results are displayed in Figure 4.14

Temperature is one of the most crucial environmental factors influencing plant growth especially in protected cultivation. The simulated internal air temperature in Figure 4.14 for the two ventilation regimes was compared on selected hottest days of the month for the entire summer period. Figure 4.14 shows that the temperatures for the ventilation strategy with roof vents only were higher than the temperatures for the ventilation strategy with both roof and side vents. The trends shown in Figure 4.14 indicate that there were significant differences during midday.



(a)

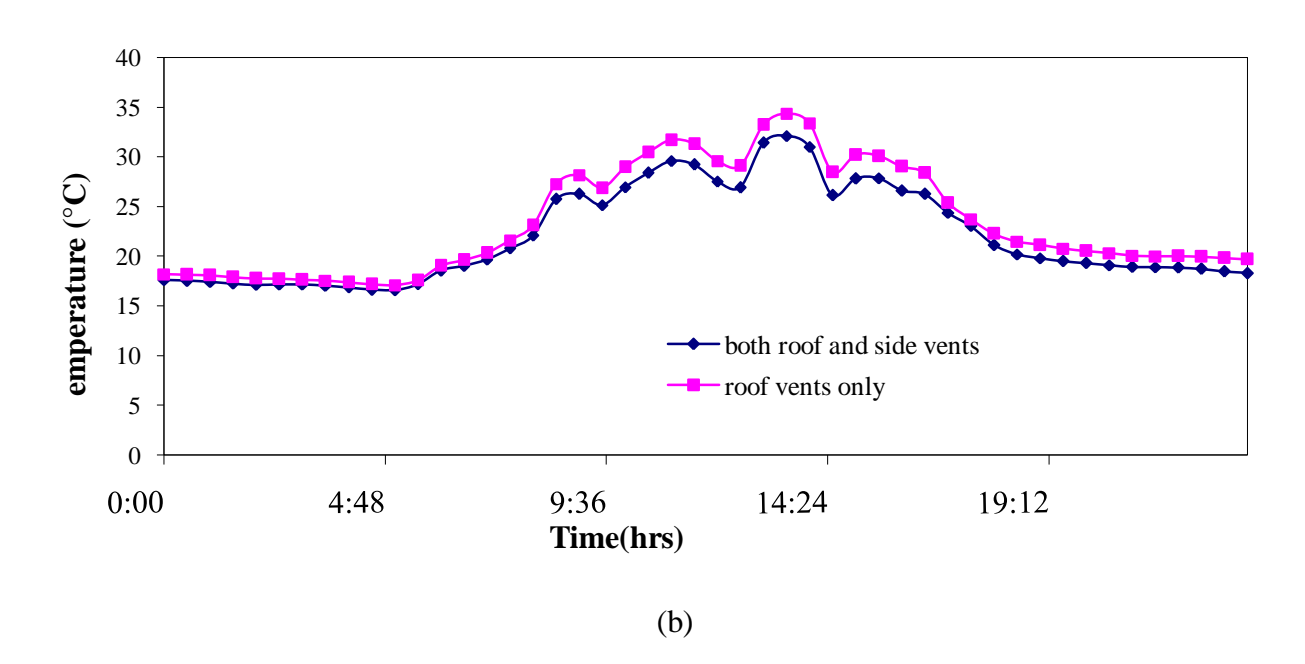
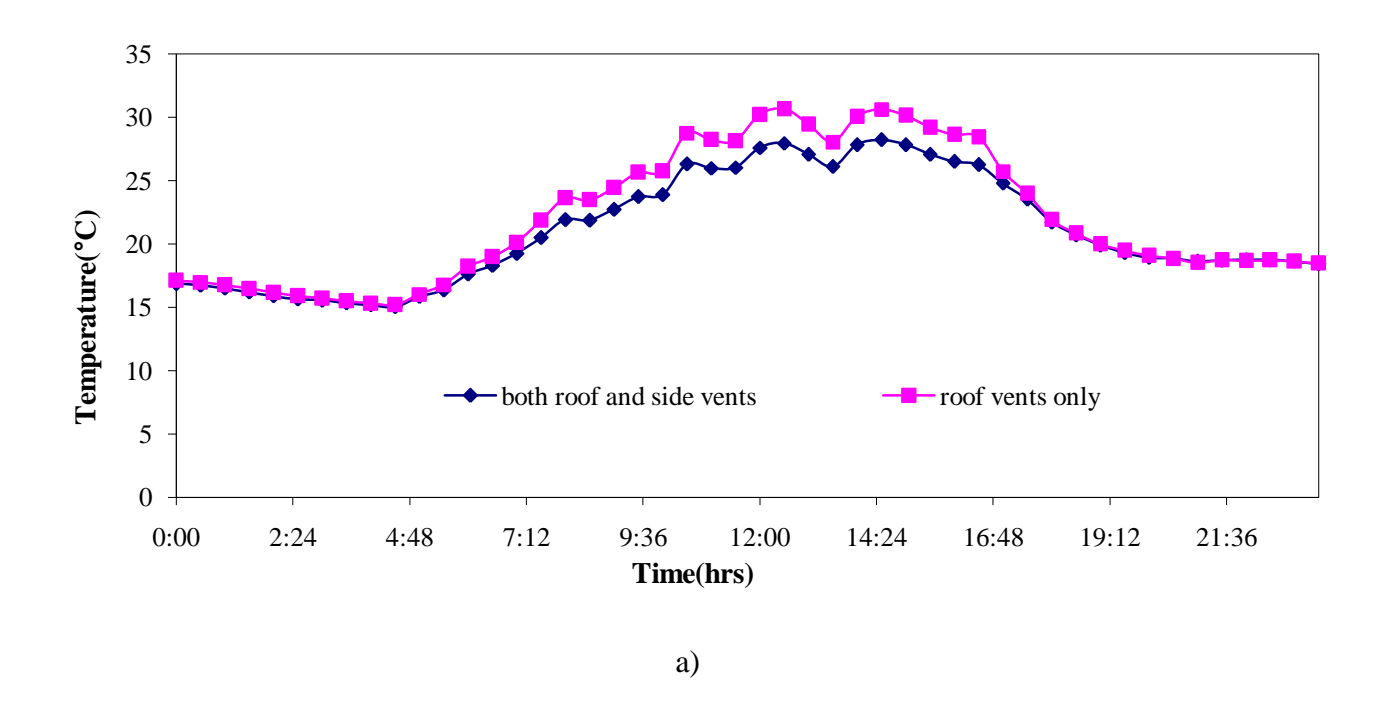


Figure 4.13: The simulated diurnal variation of internal air temperature for the two configurations on (a) 18 October 2007 and (b) on 18 November 2007

During the night, early in the morning and late afternoon, the internal air temperatures from the two models were almost equal. The observed temperature difference between the two ventilation

regimes during the day shows that air temperature is influenced by the ventilation strategy. Thus the temperature of the inside the configuration with both roof and side vents were lower than the corresponding temperatures for roof vents only which had lower air renewal rates. The results from the model show that the ventilation regime affects the cooling of the greenhouse especially in periods of high solar radiation. Temperatures are lower for the configuration with both roof and side vents as compared to configuration with roof vents only. The difference in temperature for the two configurations can be explained as follows since the configuration with roof vents has lower air renewal rates than the configuration with a combination of roof and side vents as shown in Figures 4.12 and 4.13 the temperatures for the configuration with roof vents are therefore higher than for the configuration with roof vents and side vents. This is also similar to what has been reported by Bartzanas et al (2005) that temperature inside the greenhouse follows the air velocity profile and in regions with small air velocity the air was found to be warmer and in regions with high air velocity where found to be cooler.



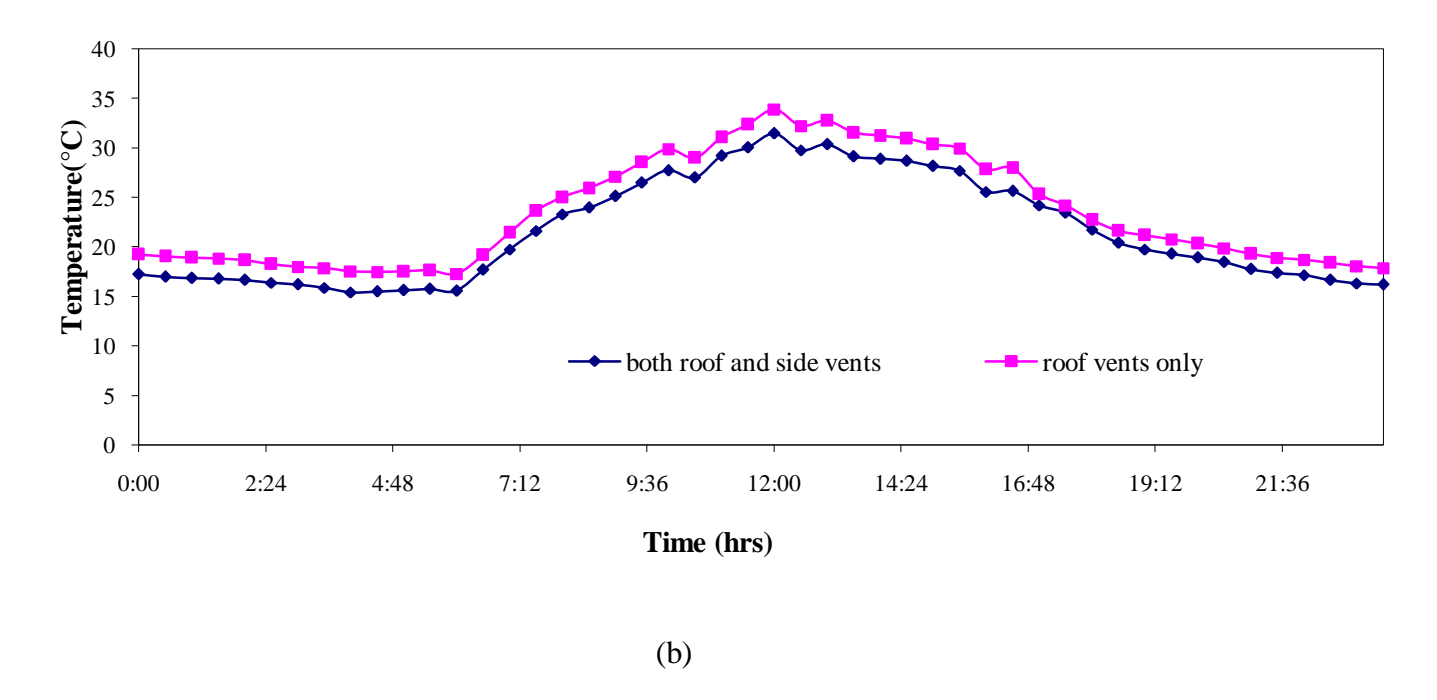
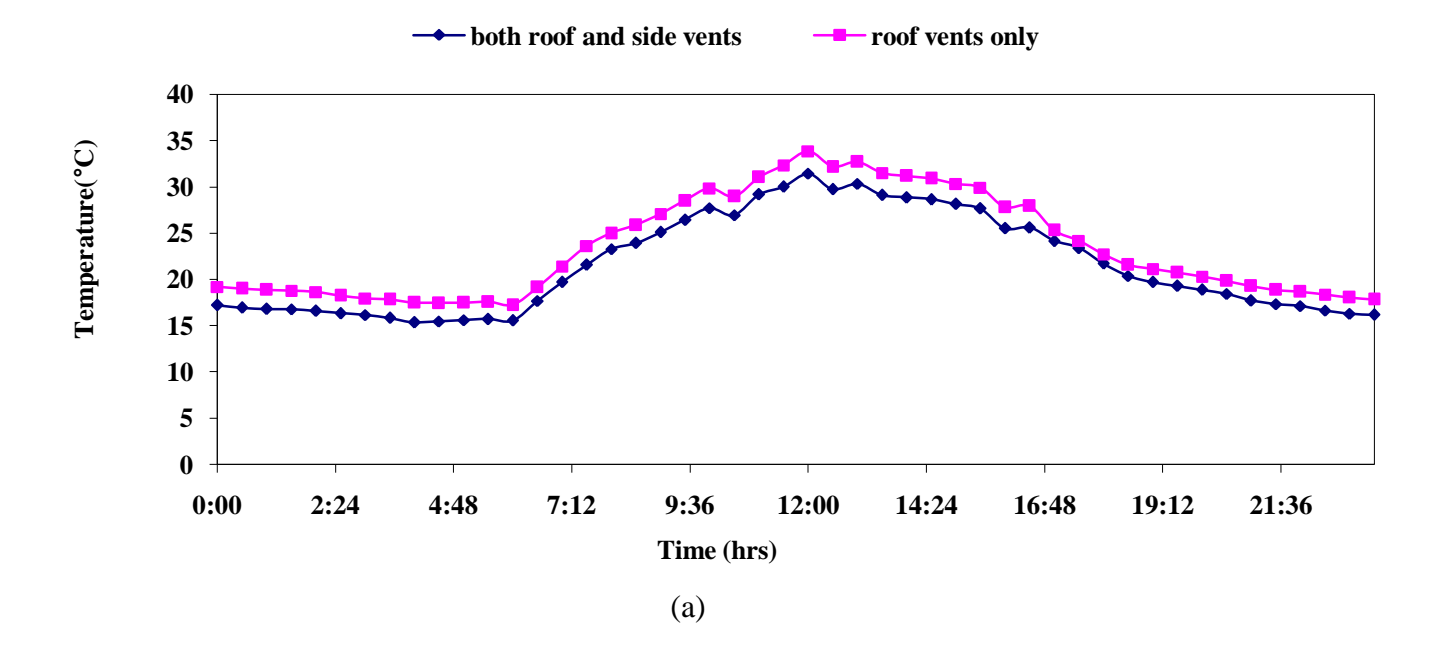


Figure 4.14: Simulated inside air temperature of the greenhouse of the two ventilation regimes on (a) 2 December 2007 and (b) 16 January 2008.



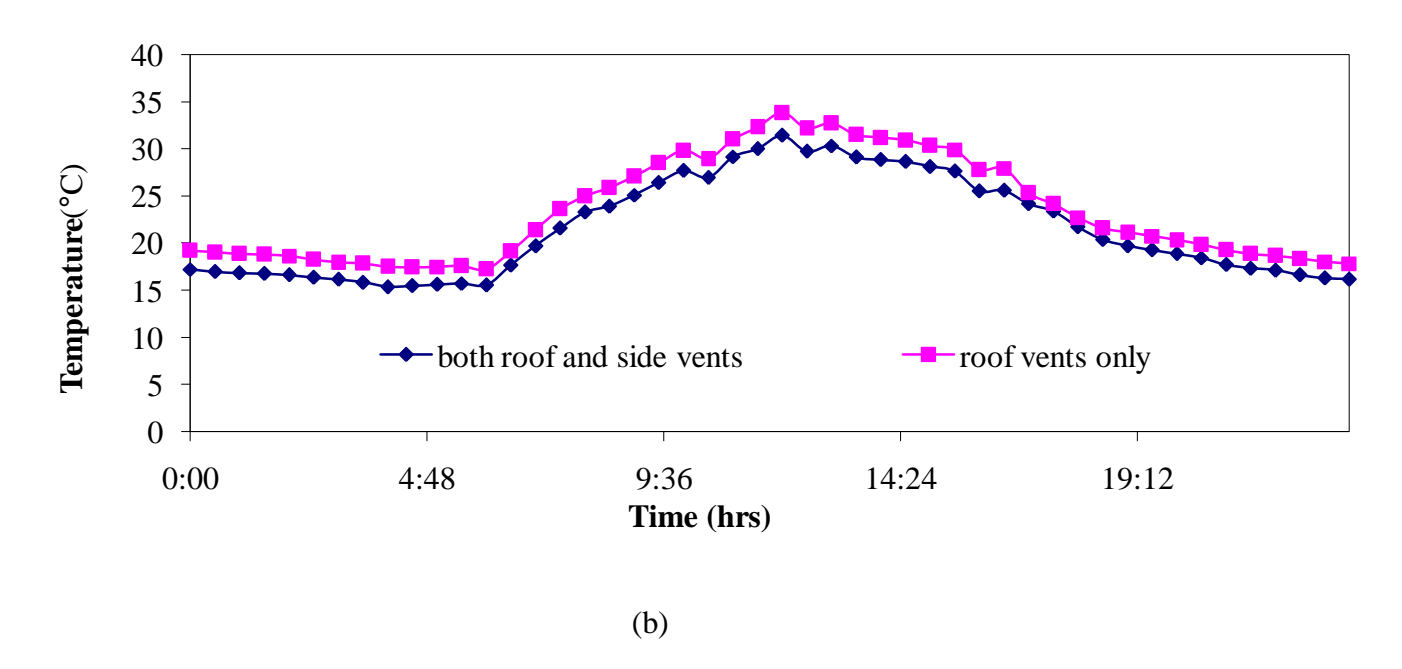


Figure 4.15: Simulated temperature on (a) 1 February 2008 and (b) on 8 March 2008 for the two ventilation regimes

Figure 4.15 and Figure 4.16 shows that the simulated temperatures for both roof and side vents are more effective in cooling the greenhouse than with roof vents only. Table 4.9 shows the predicted maximum temperatures for selected days and average temperature difference for the two ventilation regimes

Table 4.9: Simulated maximum temperatures and average temperature difference for the two ventilation regimes on selected days in summer

Date	- · ·	- '	Average Temp (^O C) difference between the two configurations
18Oct 2007	31.6	29.7	0.84
18Nov2007	30.4	28.2	1.07
2 Dec 2007	30.6	28.2	0.97
16Jan 2008	34.4	32.1	1.3
1Feb 2008	33.9	31.4	1.9
8Mar 2008	31.7	28.8	1.3

Table 4.9 shows that maximum predicted temperatures for the configuration with only roof vents were higher than corresponding temperatures for configuration with both roof and side vents which clearly shows that a greenhouse equipped with both roof vents is most suited for crop production because of its efficiency in cooling the greenhouse during periods of high solar irradiance especially in summer.

4.5.3.2 Effects of ventilation strategy on relative humidity

The water vapour content of the greenhouse is highly influenced by the rate at which the greenhouse is capable of exchanging heat and mass transfer which is dependent upon the ventilation rate. The restriction introduced by incorporating the roof vents only would therefore limit the rate of mass transfer and this was observed in the simulated relative humidity obtained for greenhouse configuration with roof vents only and for the configuration with both roof and side vents. The daily variation of relative humidity for the two configurations are presented as shown in Figure 4.17

The results indicate that inside air humidity was dependent on the vent opening configuration. On 2 December 2007, the simulated relative humidities were similar for both vent configurations and it showed that the inside relative humidities were very high, over 90 % at night until in the morning when humidity for both configurations dropped to 70 % and 60 % for the configuration with roof vents only and for the configuration with both roof and side vents respectively. During the day, the simulated relative humidity for roof vents only was higher than the corresponding relative humidity for both roof and side vents. This can be explained as follows: humidity depends on ventilation rate; the configuration with roof vents only which had lower ventilation rate therefore this configuration had higher humidity than the other configuration that had higher ventilation rates. The observations made from the simulated inside relative humidity are that low ventilation rates tend to make the air more humid because water vapour from transpiring crops will be carried away at a low rate. The results shown in Figure 4.17 are similar to the results in Figure 4.18 and both showed that humidity predicted for roof vents only are also higher than the relative humidity for both roof and side vents.

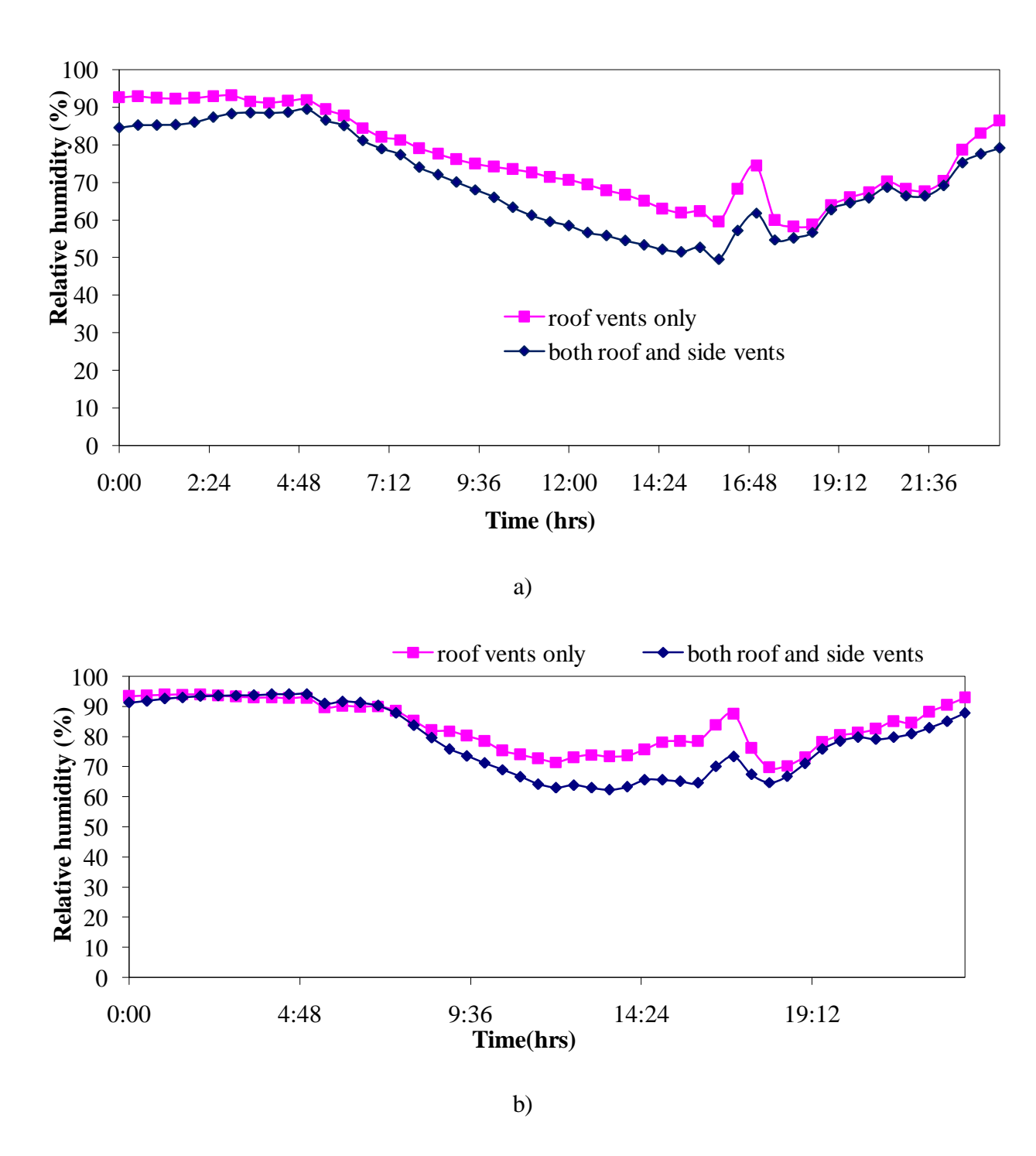


Figure 4.16: The simulated diurnal variation of relative humidity on (a) 18 November 2007 and b) 2 December 2007

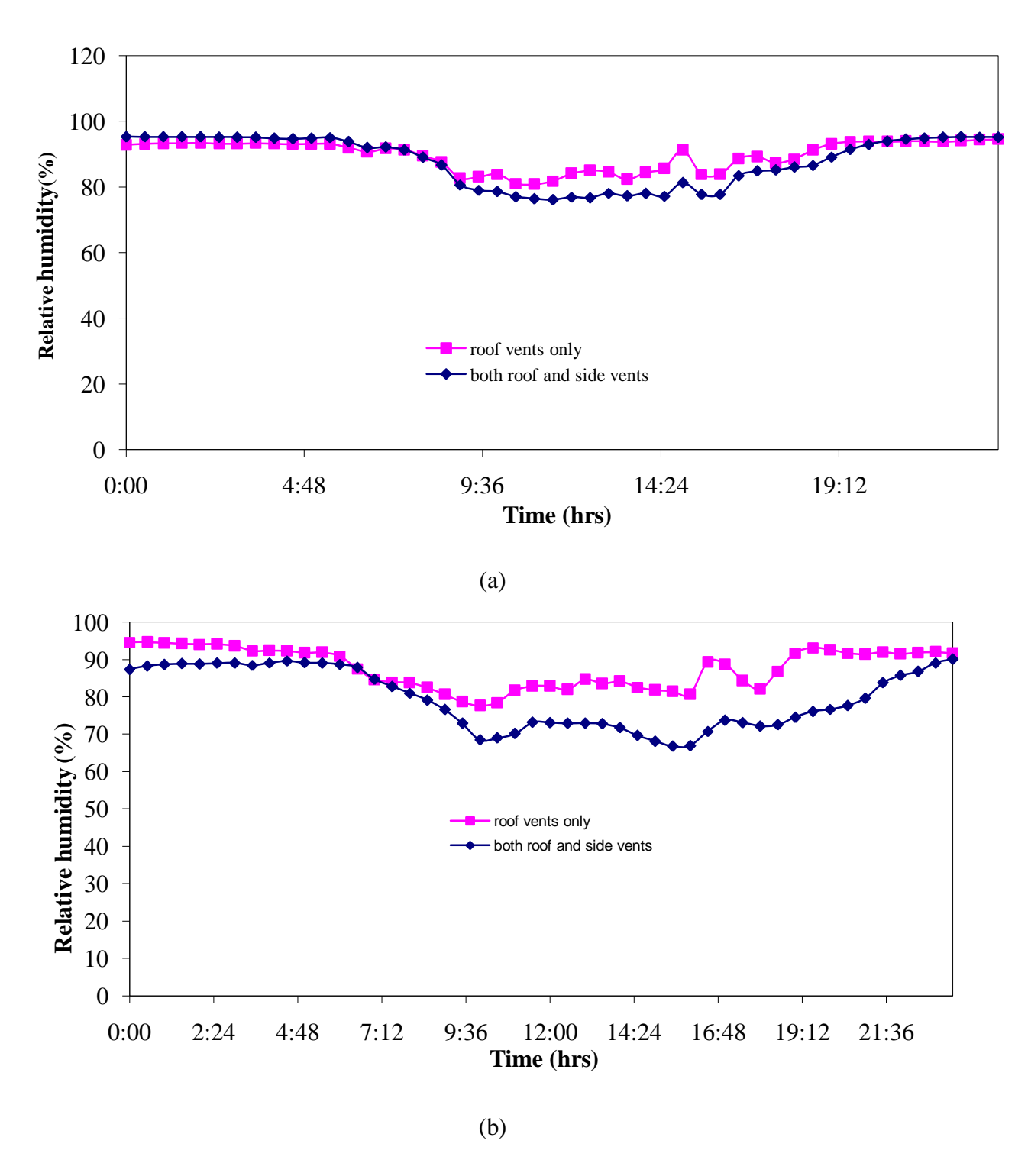


Figure 4.17: The simulated relative humidity on (a) 16 January 2010 and (b) 1 February 2010

The simulated relative humidity from the roof vents only were also similar to Figure 4.17 further giving evidence that low ventilation makes the air more humid, however the relative humidity was higher for the configuration with both roof and side vents during the night and lower during the day as shown in Fig 4.18(a). From the model it can be observed that the two ventilation regimes show much difference during the day for the two configurations. Differences between the relative humidity were found to be high, about 8%. The difference in airflow rates of the two ventilation strategies is responsible for the difference for the observed differences in humidity.

4.5.4 Effects of ventilation regimes on the transpiration

The modelled results showed that transpiration was affected by the ventilation regime. The transpiration from the simulation for the greenhouse equipped with both roof and side vents were higher than the transpiration for the greenhouse with only roof vents. This effect therefore means that crops in the greenhouse with both roof and side vents have higher growth rate than the crops in the greenhouse with only roof vents provided that water is not limiting. Figure 4.19 shows that crop transpiration was high during the day for the two configurations and maximum transpiration occurred at around midday as expected when stomatal resistance is low. This can be explained as follows: the rate of transfer of humidity from the greenhouse is lower in the case of roof vents and higher in the case with both roof and side vents. Lower ventilation rates result in a decrease in vapour pressure deficit that reduces the rate of transpiration. These findings are similar to what has been reported by Baille et al., (2001) and Katsoulas et al., (2001). In their studies they reported that high rates of air exchange between the inside and outside of the greenhouse keep the vapour pressure deficit high and consequently increase the transpiration rate. Figure 4.19 shows that maximum transpiration took place around midday since solar radiation is maximum during midday. This agrees with theory that transpiration is driven by solar irradiance and that the leaves opens their stomata apertures widely in high solar irradiance as a physiological mechanism to cool the leaves (Demratti, 2007). The latent heat from transpiring crops will further reduce the heat load in the greenhouse and thus giving the suitability of employing both roof and side vents for cooling the greenhouse in summer.

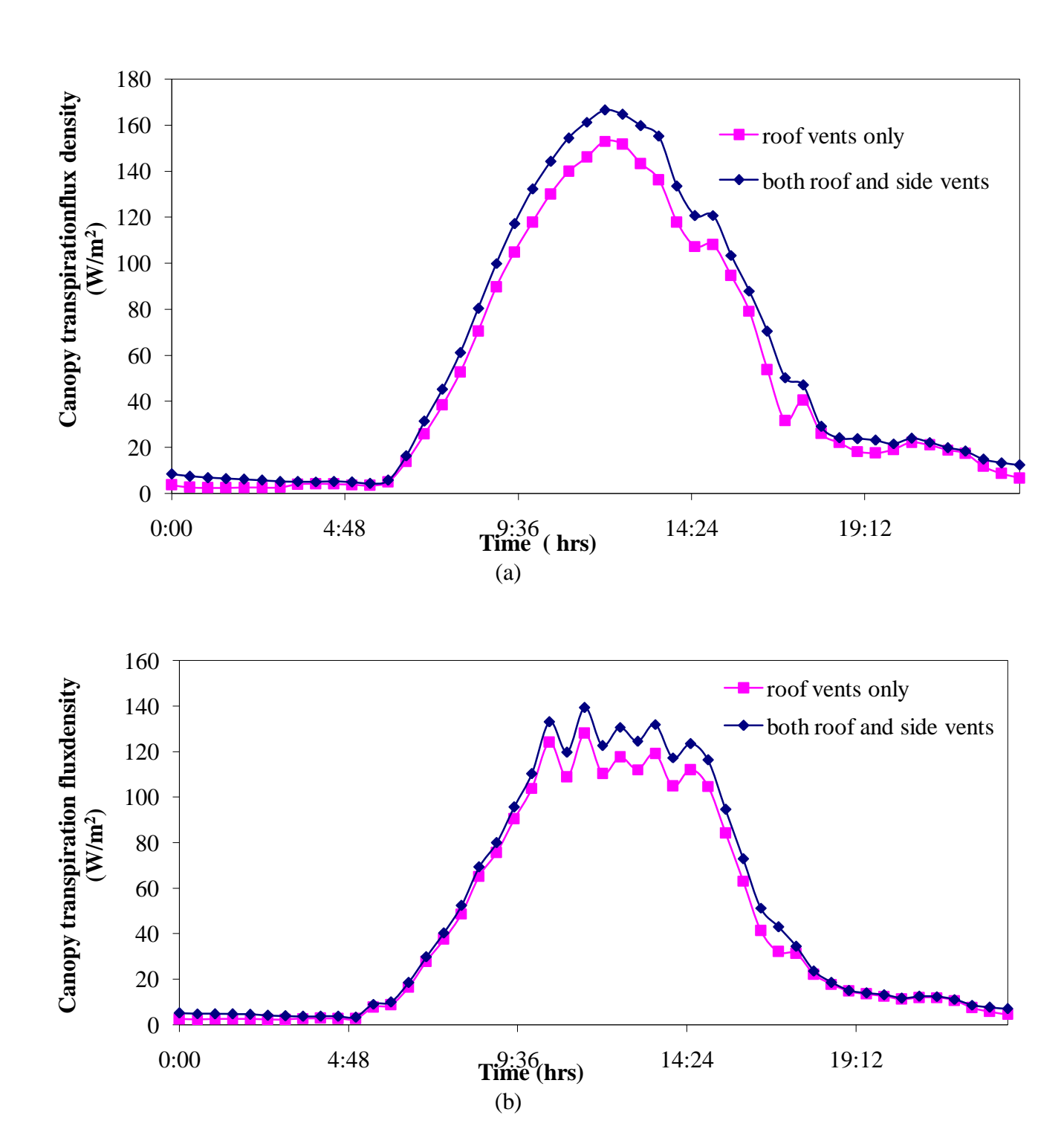


Figure 4.18(i): Simulated canopy transpiration on (a) 18 October 2007 and (b) 18 November 2007 for the two ventilation regimes

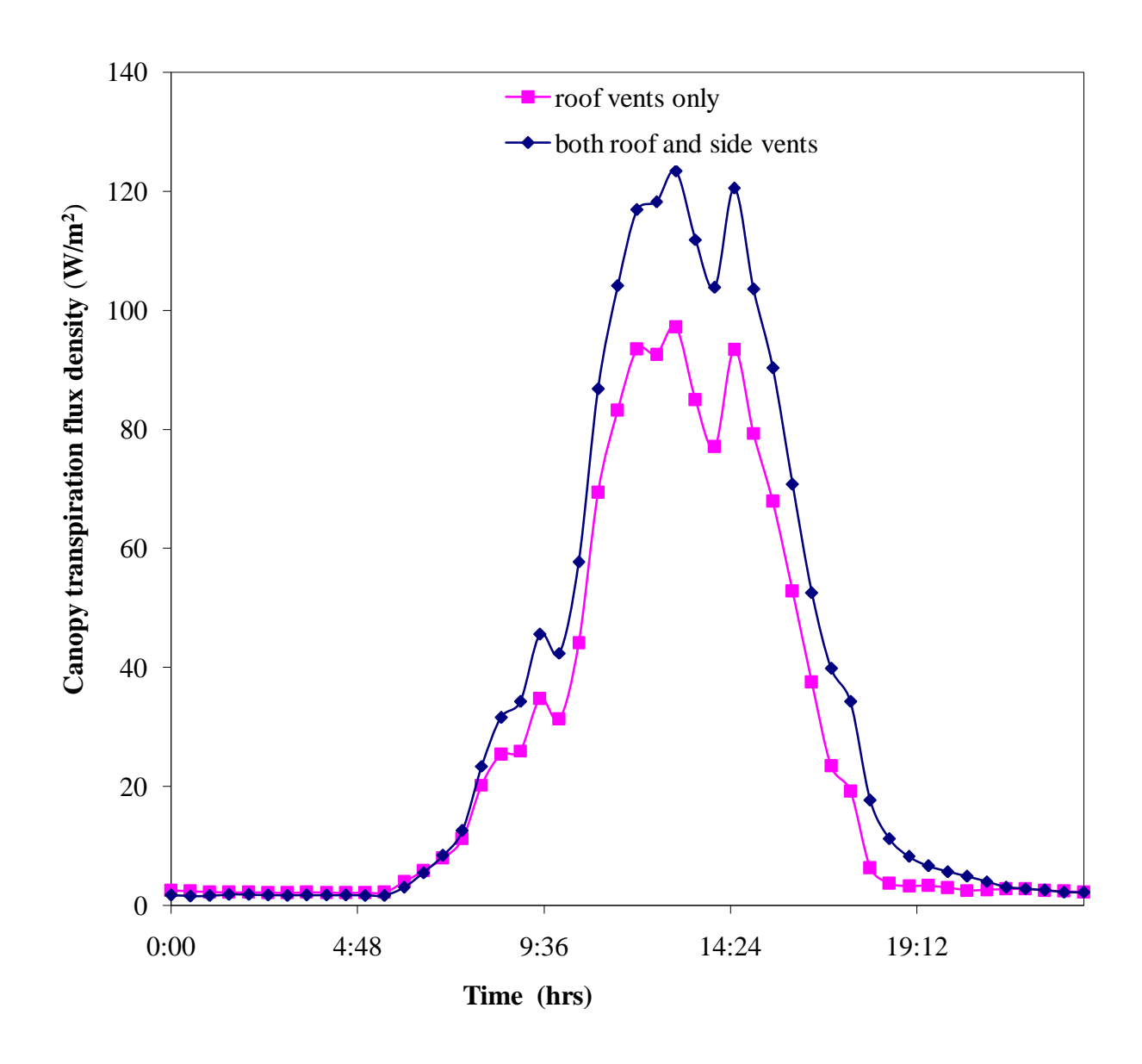


Figure 4.19(ii): Simulated Canopy Transpiration flux density on 21 January 2008 for the two ventilation regimes

The rate of transpiration from simulations shows that it depends highly on the ventilation regime on practice. During the night, the transpiration was slightly above zero showing that there might some nighttime transpiration. The results indicate that the greenhouse with both roof and side vents is well suited for plant growth. Table 4.10summarizes the maximum transpiration of the two ventilation configurations on the selected hot days during summer

Table 4. 10: Maximum transpiration for the two ventilation configurations

Date	Maximum canopy transpiration flux density (W m²) for roof vents only	1.
18 October 2007	153	166.5
18 November 2007	128	139.3
21 January 2008	97.2	123.4
8 March2008	87	95.6

Table 4.10 presents the maximum transpiration for the two configurations and shows that the maximum transpiration on 18 October 2007 was predicted to be 166.5 W m⁻² for the greenhouse with both roof and side vents while it was 153 W m⁻² for the configuration with roof vents only. On 18 November 2007 the predicted maximum transpirations were 139.3 W m⁻² and 128 W m⁻² for the greenhouse with both roof and side vents and for the greenhouse with only roof vents respectively. The transpirations were lower on 21 January 2008 with the modelled maximum transpiration for the greenhouse with both roof and side vents opening being 123.4 W m⁻² and 97.2 W m⁻² for the greenhouse with roof vents only. The lowest predicted maximum transpirations were found on 8 March 2008. The configuration with both roof and side openings had a transpiration rate of 95.6 W m⁻² while the rate was 87 W m⁻² for the other configuration. These findings clearly demonstrate that ventilation strategy affects crop transpiration inside a greenhouse.

4.5.5 Effects of ventilation strategy on canopy temperature

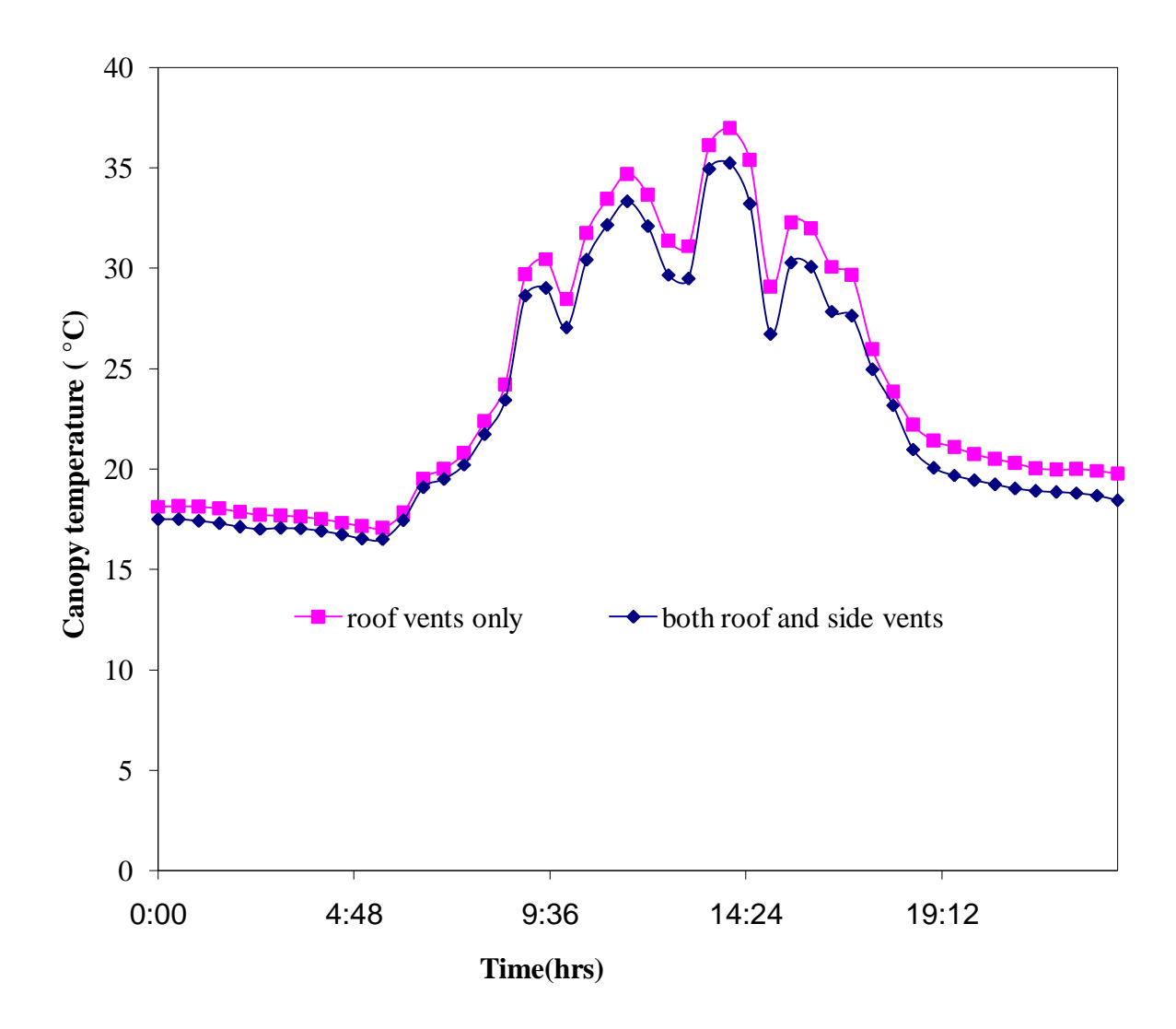


Figure 4. 19: Simulated canopy temperature on 16 January 2008 for roof vents only and for both roof and side vents

The projected canopy temperature for the two configurations had similar trends as illustrated in Figure 4.20. The simulated canopy temperature was found to be higher for the configuration with roof vents only. The reason for that is: the transpiration rate of plants for the ventilation regime with roof vents only was lower than that of plants in a configuration with both roof and side vents. The maximum canopy temperature projected for the greenhouse with roof openings only

is 36.9 °C and 35.2 °C for the configuration that has both roof and side vents. The leaves are cooled more in the greenhouse with both vents opened than when only roof vents are opened. The results illustrated that the ventilation configuration affects the canopy temperature, as has been also been found out by Fuchs et al, 1997 that the air velocity near the crop and the temperature difference between the inside and outside of the greenhouse are important factors influencing crop growth and also spatial heterogeneity of air velocity of air and climate inside the greenhouse interfere with plant activity and influence crop behavior through their effects on crop gas exchanges, particularly transpiration and photosynthesis.

Figure 4.21 and Figure 4.22 show the simulated canopy temperature. The canopy temperature increased with time of day, and from the two Figures, the case of the greenhouse with roof vents only had higher canopy temperature than for the case of the greenhouse with both roof and side vents. This is attributed to the fact that due to high transpiration which was found for the greenhouse with both roof and side vents there is more cooling effect hence higher canopy temperature for the greenhouse roof vents. The difference between the projected canopy temperatures was very significant during the day and high around midday. On 18 October and 18 November 2007, the maximum projected difference of the canopy temperatures between the two ventilation strategies were 2.5 °C and 2.8 °C respectively. The maximum predicted differences between the canopy temperatures were found to be 2.8 °C and 2.6 °C on the 2 December 2007 and 1 February 2008 respectively.

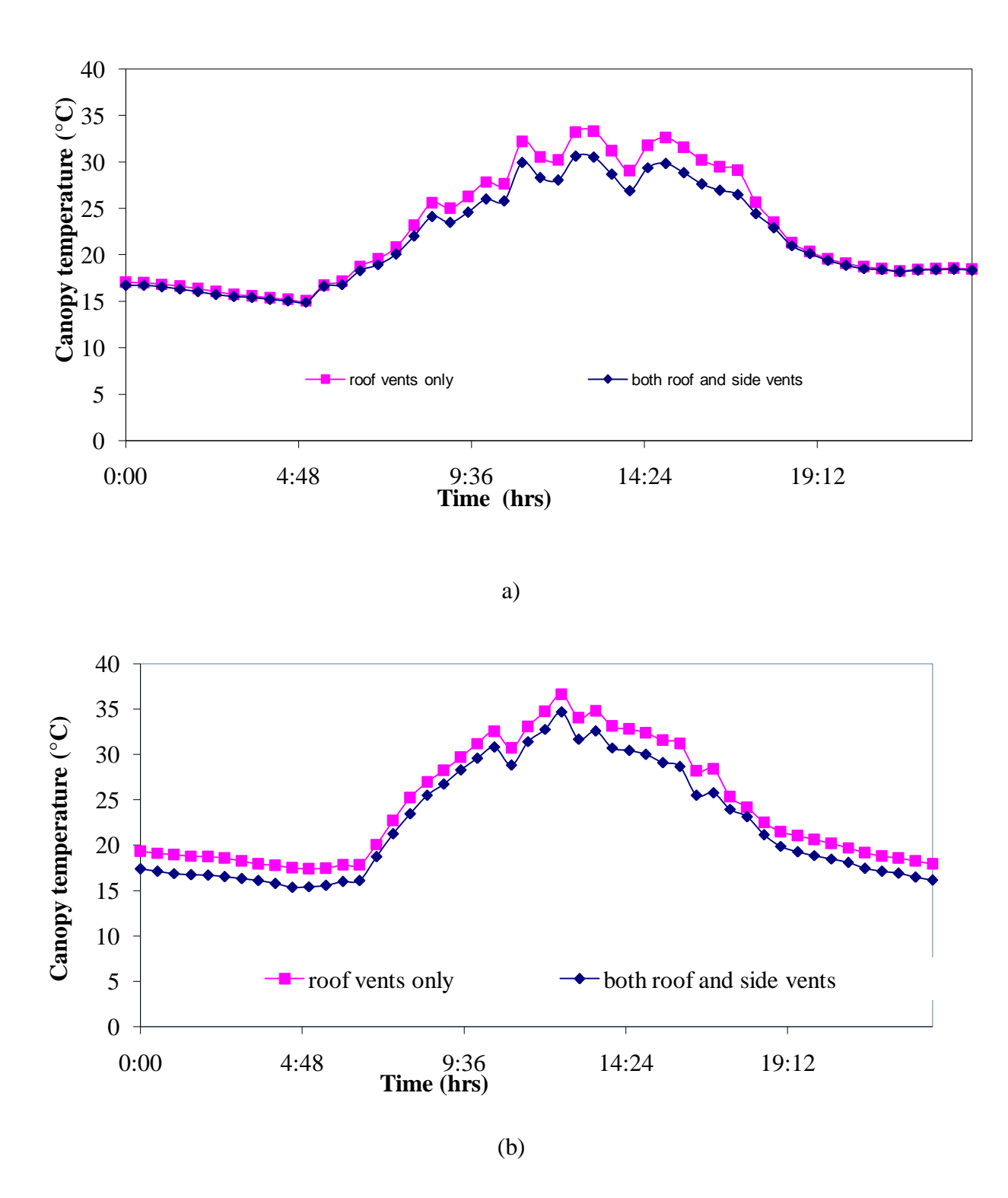
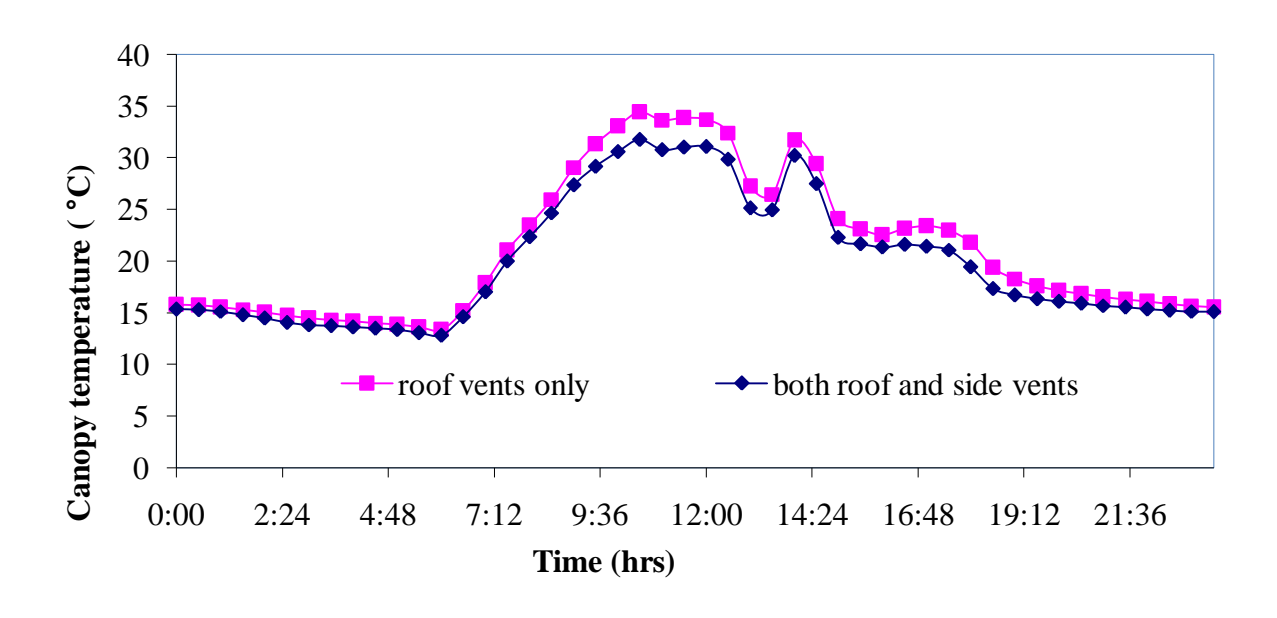


Figure 4.20: The simulated canopy temperature on (a) 2 December 2007 and (b) 1 February 2008



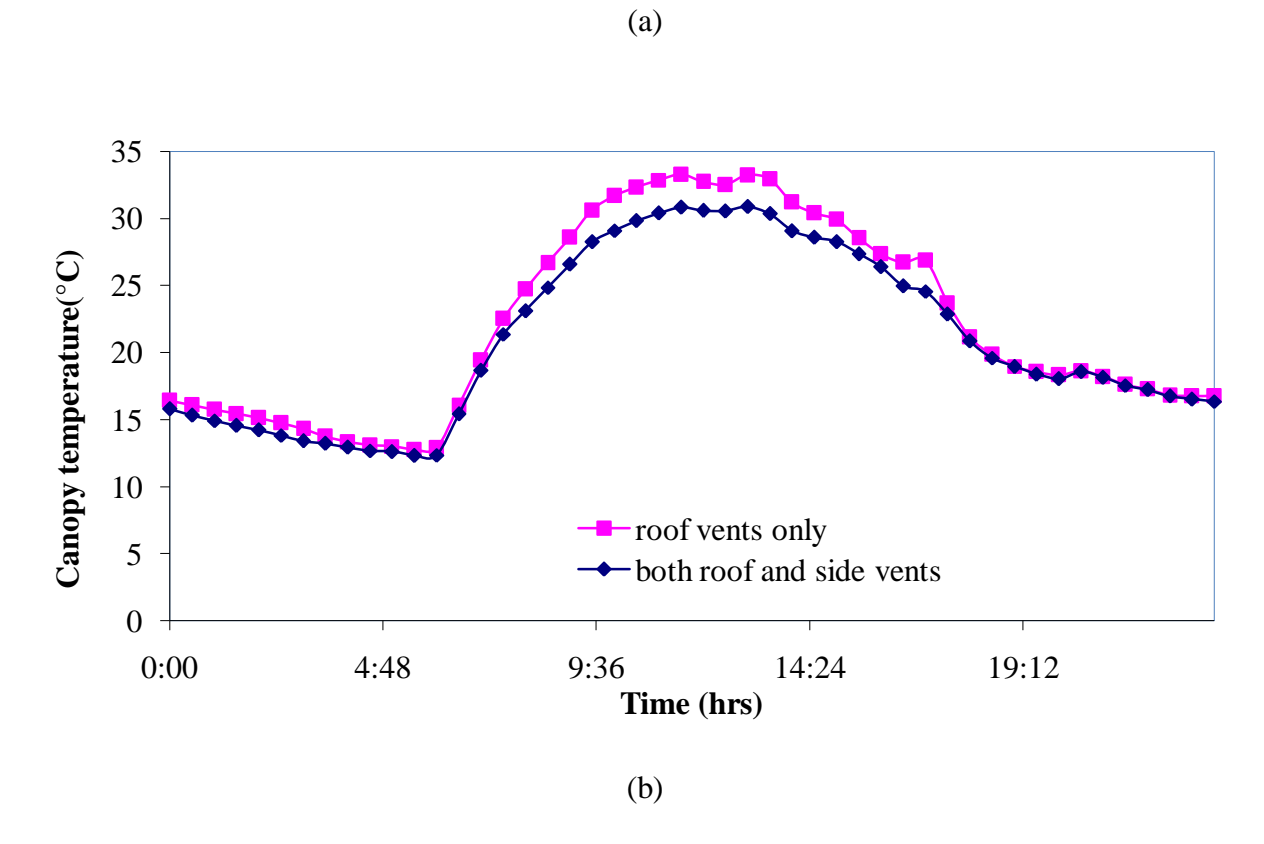


Figure 4. 21: Simulated diurnal variation of canopy temperature on (a) 18 November 2007 and (b) 18 October 2007

CHAPTER5 CONCLUSIONS AND RECOMMENDATIONS

5.1 Conclusions

In this study the influence of the two ventilation configurations was investigated for 3-span Azrom type greenhouse rose crop using the GDGCM climate model. The model was calibrated and validated against experimental data.

It can also be concluded that the GDGCM climate model can be used to simulate the microclimate and the transpiration rate of crops inside the greenhouse in warm climates, and basing on the model results, the ventilation strategy with both roof and side vents was found to provide the suitable microclimate and transpiration for rose crop growth. Thus the GDGCM can be used as designing tool to monitor greenhouse ventilation system using the climatic parameters and greenhouse construction parameters

Field measurements were carried out to predict the ventilation rates and crop microclimate in a commercial greenhouse for rose cultivation. The water vapour method was successfully used to determine the greenhouse ventilation rates which were used for calibration and validation of the GDGCM climate model.

Modeled air exchange rates in a 3-span Azrom type showed that the microclimate and transpiration was adversely affected by the ventilation regime on practice. The results indicates that the configuration with both roof and side vents gave the maximum greenhouse ventilation rates during the day, on selected hot day the predicted air renewal rates were 15.6hr⁻¹ and 6.5hr⁻¹ for the ventilation strategy with roof vents only. These results showed that the configuration with roof vents only gave lower ventilation rates. Basing on these findings it can be concluded that the most effective vent configuration was the combination of roof and side vents.

The simulated temperatures from the model showed that the configuration with both roof and side vents was more effective in reducing the inside air temperature, on selected hot days the average difference between the two ventilation regimes investigated was about 2°C. The

simulated temperatures for roof vents only were found to be higher than the corresponding temperatures for both roof and side vents.

Internal relative humidity was observed to be higher for the configuration with roof vents only than for other configuration. Thus from this study it is recommended that greenhouse users should use greenhouses with both roof and side vents as this would enable them to produce crops of high quality and increase yield. Higher humidity is associated with prevalence of diseases. from the simulated results of ventilation it was observed that the internal relative humidity for the greenhouse with roof vents only is higher than the greenhouse configuration where both roof and side vents were used, it can therefore be concluded that the plants in a greenhouse with roof vents only are more prone to diseases.

The simulated transpiration rate from the model showed that plants in a ventilation regime with both roof and side vents gave more transpiration rates than the plants in a greenhouse with only roof vents. The ventilation regime influenced the transpiration rate and therefore good ventilation provides optimum environment for plant growth. Therefore in order to achieve yield of high quality greenhouse users are encouraged to use ventilation strategy that is viable for plant growth that in the long run empower farmers financially. The leaf temperature which is sign of physiological response to thermal stress indicated that plants in the configuration with roof vents only had higher leaf temperature than those plants in the configuration with both roof and side vents, further strengthening the point that the mode with roof vents only inhibit plant growth. From this study it can be concluded that a greenhouse equipped with both roof and side vents is more efficient in cooling the greenhouse than a green house with only roof vents.

5.2 Recommendations

As ventilation strategy influences the microclimate and transpiration of crops inside the greenhouse, it is recommended that greenhouse growers adopt the use of greenhouses equipped with both roof and side vents for achieving high crop production and reduce operation costs which might arise due to need for cooling the greenhouse in summer. For further studies it is recommended that the degree of opening of the roof should be considered to come up with optimum ventilation that is good for crop growth. As it was beyond the scope of this study to investigate the effects of the greenhouse with side vents only further studies of investigating the effect of closing the roof vents, and also to investigate the effects of the varying the degree of opening of both the roof and side vents. This study should be carried in many locations and other greenhouses with other crops so as to come up with recommendations that are not based on one location and on rose crop.

REFERENCES

- American Society of Heating, Refrigeration and Air-conditioning Engineers (ASHRAE), 2005. ASHRAE Handbook of Fundamentals, **Chapter 27**: Ventilation and Infiltration. Atlanta, GA.
- Baille, A., 1992. Thermique of Energetique des serres, Cours de Diplome d'Agronomie Approfondie, de Génie Agronomique 40, Montpellier, France, E.N.S.A.
- Baille, A., Kittas, C. and Katsoulas, N., 2001. Influencing of whitening on greenhouse microclimate and crop energy portioning.
- Bakker, J.C., Bot, G.P.A., Challa, H., N.J. van de Braak (Editors). 1995. Greenhouse Climate Control: An Integrated Approach. Wageningen, The Netherlands. Wageningen Pers Publisher.
- Baptista, F.J., Bailey, B.J., Randall, J.M. and Meneses, J.F., 1998. Greenhouse Ventilation Rate: Theory and Measurement with Tracer Gas Techniques. Journal Agricultural Engineering Res (1999)**72**: 363-374
- Bartzanas, T., Katsoulas, N., Kittas, C., Boulard, T., Mermier, M., 2005. Effect of vent configuration and insect screen on greenhouse microclimate. International Conference "Passive and Low Energy Cooling for the Built Environment", Santorini, Greece.
- Bot, G.P.A., 1983. Greenhouse Climate from physical processes to a dynamic model. Ph.D. Thesis, University of Wageningen, Wageningen, The Netherlands.
- Boulard, T., 1993. Experimental and modeling study on greenhouse natural ventilation; recapitulative of the 1988-1992 experiments. Note interne I.N.R.A. **93-1**, Station de ^ Bioclimatologie de Montfavet, France.
- Boulard, T., Baille, A., 1995. Modeling of air exchange rate in a greenhouse equipped with continuous roof vents. Journal Agricultural Engineering, Research **61**: 37-48.
- Boulard, T., Wang, S. 2000. Greenhouse crop transpiration simulation from external climate conditions. Agricultural and Forestry Meteorology **100**: 25-34.
- Bruce, J.M., 1982. Ventilation of a model livestock building by thermal buoyancy. Transactions of the ASAE, **25161**: 1724-1726.
- Chou, S.K., Chua*, K.J., Ho, J.C., Ooi, C.L., 2004. On the study of an energy-efficient greenhouse for heating, cooling and humidification applications. Applied Energy 77: 355-373

- De Jong, T., 1990. Natural ventilation of large multi-span greenhouses. Ph.D. Thesis, University of Wageningen, Wageningen, The Netherlands.
- Demrati, H., Boulard, T., Bekkaoui, A. and Bouirden, L., 2001. Natural ventilation and microclimatic performance of a large-scale banana greenhouse. J.agric.Engng Res., **80(3)**: 261- 271
- Demrati, H., Boulard, T., Bekkaoui, A., Fatnassi, H., Majdoubi, H., Elattir and Bouirden, L., 2007. Microclimate and transpiration of a greenhouse. Biosystems Engineering 98: 66-78)
- Dynamax Inc. (2005) Dynagage Sapflow sensor user manual. Dynamax Inc., 10808 Fallstone Rd. Houston TX77099, USA (http://www.dynamax.com)
- Fatnassi, H., Boulard, T. and Bouirden, L., 2003. Simulation of climatic conditions in full-scale greenhouse fitted with insect-proof screens. Agric. For.Meteorol., 118: 97-111
- Fatnassi, H., Boulard, T., Demrati, H., Bouirden, L., Seppe, G., 2001. Ventilation Performance of a large Canarian-Type Greenhouse equipped with insect- proof nets. Biosystems Engineering, **82(1)**: 97-105.
- Fernandez, J.E., Bailey, B.J., 1992. Measurement and Prediction of greenhouse ventilation rates. Agricultural and Forestry **58**: 229-245.
- Fuchs, M., Dayan, E., Shmuel, D., Zipori, I., 1997. Effects of ventilation on the energy balance of a greenhouse with bare soil. Agricultural and Forestry Meteorology (86):273-282.
- Fuchs, M., Segal. Dayan, E., Jordan, K., 1996. Improving greenhouse microclimate control with help of plant temperature measurements. BARD project No IS- 1816-90R. Final report 2.
- Gandemer, J. and Bietry, J.1989, Cours d'aërodynamique.REEF, vol2, Sciences du Batiment CTBS Nantes
- Hanan, J.J., 1998. Greenhouses: Advanced technology for protected horticulture. CRC Press. London. 684pp
- Harmanto, Tantau, H.J and Salonke, V.M., 2006. Microclimate and air exchange rates in greenhouses covered with different nets in the humid tropics. Biosystems Engineering, **94(2)**: 239-253
- Jarvis, P.G., 1985. Coupling of transpiration to the atmosphere of horticultural crops. Acta Horticulturae, 171: 187-205
- Jones, H.G., 1992. Plants and microclimate. Cambridge University Press, UK
- Katsoulas, N., Bartzanas, T., Boulard, T., Mermier, M. and Kittas, C., 2006. Effect of vent openings and insect screens on greenhouse ventilation. Biosystems Engineering, **93(4)**: 427 436

- Kittas, C. Katsoulas, N., and Baille, A., 1999. Transpiration and Canopy Resistance of Greenhouse Soilless Roses: Measurements and Modelling. Acta. Hort. **507**: 61-68
- Kittas, C., Boulard, T. and Papadakis, G., 1997. Natural ventilation of a greenhouse with ridge and side openings: Sensitivity to temperature and wind effects. Transactions of the ASAE, **45**(4): 415-425
- Klein,S.A., Beckham, W.A., Cooper, P.I., Dufie, N.A., Freeman, T.L., Mitchel, J.C., Beekman, D.M., Oonk, R.L., Hughes, P.J., Eberlein, M.E., Karman, V.D., Pawelski, M.J., Utzinger, D.M., Duffie, J.A., Brandemuehl, M.J., Arny, M.D., Theilacker, J.C., Morrison, G.L., Clark, D.A., Braun, J.E., Evans, B.L.& J.P. Kummer. 1988.

 TRNSYS: A transient system simulation program. Engineering experiment station report 38-12:Solar Energy Laboratory, University of Wisconsin-Madison, USA.
- Mashonjowa, E., Ronse F., Milford, J.R, Lemeur, R., J.G., 2010b. Measurement and simulation of the ventilation rates in a naturally greenhouse in Zimbabwe. Applied Engineering in Agriculture, in press
- Mashonjowa, E., Ronse, F., Milford, J.R., Lemeur, Pieters, J.G., 2010a. Calibration and validation of a dynamic model in Zimbabwe. Submitted to Agricultural and Forestry Meteorology
- Mashonjowa, E., Ronse, F., Pieters, J.G., Lemeur, R., 2007b. Modelling heat and mass transfer in naturally ventilated greenhouse in Zimbabwe. Applied Engineering in Agriculture, in press
- Monteith, J.L., 1973. Principles of Environmental Physics, Arnold, Paris
- Monteith, J.L., Unsworth. 1990 Principles of Environmental Physics, Edward and Arnold, UK
- Papadakis, G., Frangoudakis, A. and Kyritsis, S., 1994. Experimental investigation and modeling of heat and mass transfer between a tomato crop and the greenhouse environment. J. Agriculture Engineering. Res., **57**: 217-227
- Pasian, C.C. and Lieth, J.H., 1989. Analysis of response of net photosynthesis of rose leaves of varying ages to photosynthetic active radiation and temperature. Journal American Society Horticulture Science **114(4)**, 581-586
- Pieters, J.G., and Deltour, J.M., 1997. Performances of greenhouses with the presence of condensation on cladding materials. J.Agriculture Engineering. Res., **68(2)**: 125-137.
- Rosenberg, N.J., Blad, B.L. and Verma, S.B., 1983. Microclimate: Biological environment. Second Edition. John Wiley &Sons, New York
- Roy, J.C., Boulard, T., Kittas, C. and Wang, S., 2002. Convective and ventilation transfers in greenhouses, part 1: the greenhouse considered as a perfectly stirred tank. Biosystems Engineering, **83(1)**: 1 20

- Seginer, L., 1984.Transpirational cooling of a greenhouse crop with partial ground cover. Agricultural and Forestry Meteorology **100**: 265-281.
- Stanghellini, C., 1987. Transpiration of greenhouse crops; An aid to climate management. Ph.D. Thesis, University of Wageningen, Wageningen, The Netherlands.

APPENDIX A

Characteristics and parameters of the ventilation model used in GDGCM Type 72

Characteristics

At Agr total greenhouse floor area [m²]

BETc β'c roof slope [°]

CVa ρ'hacha volumetric heat capacity air [kJ/(m³.K)

VOL V greenhouse volume [m³]

Parameters

1 Myent- Ventilation simulation mode

0-constant air renewal

1-Ventilation flux demand

2-P-controlled ventilation system

3- Ventilation function of BOT (1983)

4-Ventilation function of DE JONG (1990)

5-Linear ventilation function

6-Ventilation function of KITTAS et al.(1995)

For ventilation mode 0

2 Ramin Ra, min constant minimum air renewal rate [hr⁻¹]

For ventilation mode

2 tvent Δ tvent temperature restore time step for ventilation

For ventilation mode2

2 Ra, min Ra, min minimum air renewal rate [hr⁻¹]

3	Ra, max	Ra, max	maximum air renewal rate [hr ⁻¹]
4	DTvmin	Δ Tvent, min	difference between the inside air temperature and the ventilation set point temperature, below which the ventilation is used at its minimum capacity [°C]
5	DTmax	ΔTvent, min	difference between the inside air temperature and the ventilation setpoint temperature, above which the ventilation system is used at its maximum capacity [°C]

For ventilation modes $\mathbf{3}, \mathbf{4}, \mathbf{5}$ and $\mathbf{6}$

2 Pwir	1	pwd	area of the ventilation windows, expressed as the fraction of the total cover area [-]
NPCT			indicator for the units in which the opening of the ventilation windows is expressed 0-for opening angles [°C]
			1-for opening percentages i.e. the opening of the ventilation window is expressed as the ratio of 100 opening angle. Normally the maximum opening angle for which the ventilation the window lays in the plane of the opposite roof (at other side of the ridge).
4	COEF1	C1	first constant in the ventilation function
5	COEF2	C2	second constant in the ventilation function
6	COEF3	C3	third constant in the ventilation function (only for simulation mode 6)

Inputs

For ventilation mode 0

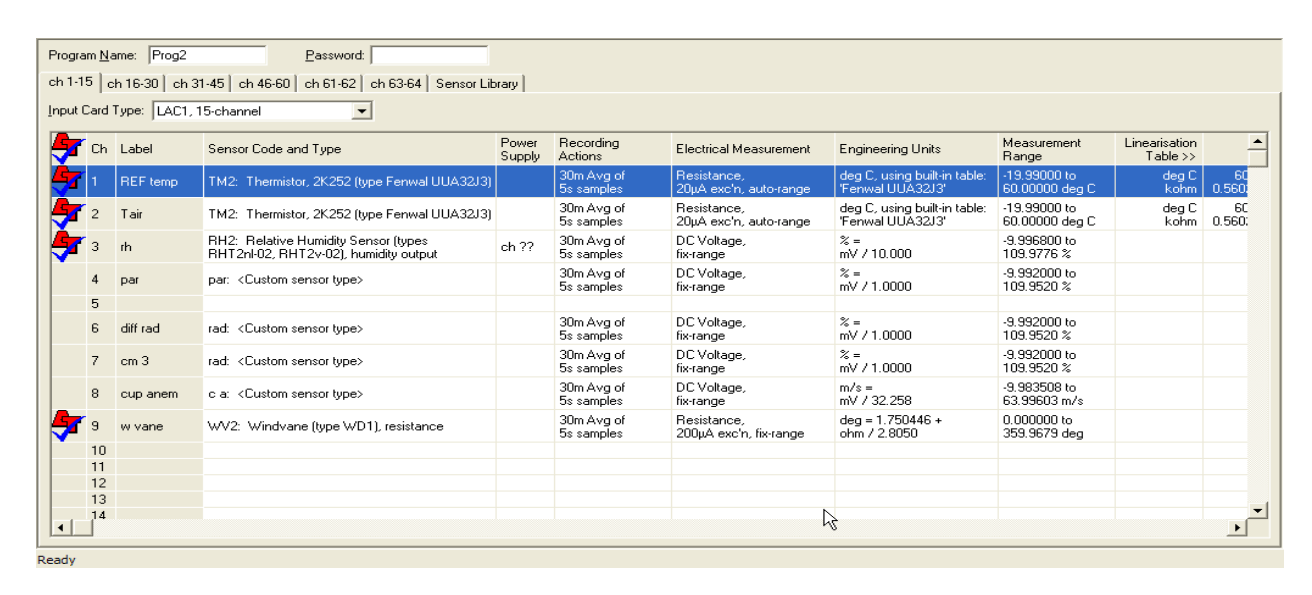
No inputs are required

For ventilation mode 1

1	Te	Te	outside air temperature [°C]
2	TcI	Tc $(t-\Delta t)$	initial cover temperature [°C]
3	Til	Ti (t-Δt)	initial inside air temperature [°C]

4	TvI	Tv $(t-\Delta t)$	initial vegetation temperature [°C]
5	TsI	$Ts(t-\Delta t)$	initial soil surface temperature[°C]
6	HVic	$h(i\rightarrow c)$	coefficient of convective heat transfer from the inside air to the cover [kJ/(m².hr.K)]
7	HVi	$h_V(v{ ightarrow}i)$	coefficient of convective heat transfer from the vegetation to the inside air [kJ/(m².hr.K)
8	HVsi	$h_{V(S \rightarrow i)}$	coefficient of convective heat transfer from the soil surface to the inside air [kJ/(m².hr.K)]
9	TSETv	Tset,vent(t)	ventilation set point temperature for the current time step [°C]
For ve	entilation mode	es 3, 4, 5 and 6	
1	Ue	ue	wind speed [m/s]
2	win		opening of the leeside ventilation windows [° or %]
Outpu	ıts		
1	Ra	Ra(t)	actual air renewal rate [hr ⁻¹]
Intern	al variables		
Alfwi	n	α'	ventilation window opening [°]
DTv			actual difference between the inside air temperature and the ventilation set point temperature [°C]
QVic		$q_V(i\rightarrow c)$	convective heat flux density from the inside air to cover $[kJ/(m^2.hr)]$
QVie		$q_V(i \rightarrow e)$	convective ventilation heat flux density from the inside to the outside air [kJ/ (m².hr)]
QVsi		$q_V(s \rightarrow i)$	convective heat flux density from the soil surface to the inside air $[kJ/(m^2.hr)]$
QVvi		$q_V(v{ ightarrow}i)$	convective heat flux density from the vegetation to the inside air $\left[kJ/\left(m^2.hr\right)\right]$

APPENDIX B



(a)

		Type: LAC1,	15-channel ▼							
7	Ch	Label	Sensor Code and Type	Power Supply	Recording Actions	Electrical Measurement	Engineering Units	Measurement Range	Linearisation Table >>	
•	1	ref temp	TM1: Thermistor, 2K (type Fenwal UUA32J2)		30m Avg of 5s samples	Resistance, 20µA exc'n, auto-range	deg C, using built-in table: 'Fenwal UUA32J2'	-19,99000 to 60,00000 deg C	deg C kohm	60 0.497
7	2	Tair 636	TM1: Thermistor, 2K (type Fenwal UUA32J2)		30m Avg of 5s samples	Resistance, 20µA exc'n, auto-range	deg C, using built-in table: 'Fenwal UUA32J2'	-19.99000 to 60.00000 deg C	deg C kohm	6 0.497
7	3	RH 636	RH2: Relative Humidity Sensor (types RHT2nI-02, RHT2v-02), humidity output	ch ??	30m Avg of 5s samples	DC Voltage, fix-range	% = mV / 10.000	-9.996800 to 109.9776 %		
	4	TSL 29	TSL: <custom sensor="" type=""></custom>		30m Avg of 5s samples	DC Voltage, fix-range	mV = mV / 1.0000	-9.992000 to 109.9520 mV		
	5									
	6	PAR	PAR: <custom sensor="" type=""></custom>		30m Avg of 5s samples	DC Voltage, fix-range	mV = mV / 1.0000	-9.992000 to 109.9520 mV		
	7	Rnet	NRL: <custom sensor="" type=""></custom>		30m Avg of 5s samples	DC Voltage, fix-range	mV = mV / 1.0000	-9.992000 to 109.9520 mV		
•	8	sltemp1	TM1: Thermistor, 2K (type Fenwal UUA32J2)		30m Avg of 5s samples	Resistance, 20µA exc'n, auto-range	deg C, using built-in table: 'Fenwal UUA32J2'	-19.99000 to 60.00000 deg C	deg C kohm	0.49°
7	9	sltemp2	TM1: Thermistor, 2K (type Fenwal UUA32J2)		30m Avg of 5s samples	Resistance, 20µA exc'n, auto-range	deg C, using built-in table: 'Fenwal UUA32J2'	-19.99000 to 60.00000 deg C	deg C kohm	0.49°
	10									
	11									
	12									

(b)

Figure B- 1: (a) Program for outside automatic weather station Delta-T datalogger and (b) the program for inside weather Delta-T dalogger

APPENDIX C

The parameters of the greenhouse construction characteristics used by the model

❖ GRLAT	φ	Latitude of the greenhouse [°]
❖ GRLEN		Length of the greenhouse [m]
❖ GRWID		width of the greenhouse
❖ NRSP		number of spans[-]
EAVES		height of the eaves[m]
❖ RIDGE		height of the ridge[m]
❖ EPSc1	ϵ_{c1}	far infrared radiation emittance of the outer cover
		surface
❖ EPSc2	ϵ_{c2}	far infrared radiation emittance of the inner cover
❖ TAURc	τ	cover transmittance for far infrared [-]
♦ AAT(I)	$\tau_S(V)$	cover transmittance for solar radiation as function if
		Incidence angle [-]
		The values of the solar radiation transmittance at 0,
		15,30,45,60, and 90° are stored in the array
♦ AAR(I)	$\rho_S(V)$	cover reflectance for solar radiation as function of
		the incidence angle [-]
		The values of the solar radiation reflectance at 0,
		15,45,60,75 and 90° are stored in the array AAR
❖ ALFSdc	$lpha_{Sc,dif}$	cover absorptance for diffuse solar radiation [-]
❖ TAUSdc	$ au_{ m Sc,dif}$	cover transmittance for solar radiation [-]

*	TAUSfr	$ au_{\mathrm{Sfr}}$	frame transmittance for solar radiation [-]
*	Cc	c'dc	dry cover heat capacity per unit area [kJ/(m².K)]
*	WFT cmax	$l_{cf,max}$	maximum condensation water film thickness [mm]
*	RHOc2	$ ho_{c2}$	far infrared radiation reflectance of the inner cover
			surface [-]
*	At	$A_{ m gr}$	total greenhouse floor area [m ²]
*	VOL	V	greenhouse volume [m ³]
*	dc	d_c	characteristic length of the cover[m]
*	ВЕТс	β΄c	slope of the cover[°]
*	Ac	A_c	total greenhouse cover area [m]